A Genome-Wide Survey of Sexually Dimorphic Expression of *Drosophila* miRNAs Identifies the Steroid Hormone-Induced miRNA let-7 as a Regulator of Sexual Identity

Delphine Fagegaltier,*,†,1 Annekatrin König,‡ Assaf Gordon,* Eric C. Lai,§ Thomas R. Gingeras,† Gregory J. Hannon,*,† and Halyna R. Shcherbata‡,1

*Howard Hughes Medical Institute, Watson School of Biological Sciences, Cold Spring Harbor Laboratory, Cold Spring Harbor, New York 11724, ‡Max Planck Research Group of Gene Expression and Signaling, Max Planck Institute for Biophysical Chemistry, Göttingen 37077, Germany, §Department of Developmental Biology, Sloan-Kettering Institute, New York, New York 10065, and †Watson School of Biological Sciences, Cold Spring Harbor Laboratory, Cold Spring Harbor, New York 11724

ABSTRACT MiRNAs bear an increasing number of functions throughout development and in the aging adult. Here we address their role in establishing sexually dimorphic traits and sexual identity in male and female *Drosophila*. Our survey of miRNA populations in each sex identifies sets of miRNAs differentially expressed in male and female tissues across various stages of development. The pervasive sex-biased expression of miRNAs generally increases with the complexity and sexual dimorphism of tissues, gonads revealing the most striking biases. We find that the male-specific regulation of the X chromosome is relevant to miRNA expression on two levels. First, in the male gonad, testis-biased miRNAs tend to reside on the X chromosome. Second, in the soma, X-linked miRNAs do not systematically rely on dosage compensation. We set out to address the importance of a sex-biased expression of miRNAs in establishing sexually dimorphic traits. Our study of the conserved let-7-C miRNA cluster controlled by the sex-biased hormone ecdysone places let-7 as a primary modulator of the sex-determination hierarchy. Flies with modified let-7 levels present doublesex-related phenotypes and express sex-determination genes normally restricted to the opposite sex. In testes and ovaries, alterations of the ecdysone-induced let-7 result in aberrant gonadal somatic cell behavior and non-cell-autonomous defects in early germline differentiation. Gonadal defects as well as aberrant expression of sex-determination genes persist in aging adults under hormonal control. Together, our findings place ecdysone and let-7 as modulators of a somatic systemic signal that helps establish and sustain sexual identity in males and females and differentiation in gonads. This work establishes the foundation for a role of miRNAs in sexual dimorphism and demonstrates that similar to vertebrate hormonal control of cellular sexual identity exists in *Drosophila*.

SEXUAL dimorphism is pervasive throughout the animal kingdom. From insects, fishes, reptiles, and birds to mammals, hormones and genes shape the morphological, behavioral, and reproductive potential of each sex throughout development and adult life. *Drosophila* is no exception, with males and females differing in many ways: anatomical differences include the number of abdominal segments and their pigmentation, the proboscis, labial parts, dimorphic reproductive organs, the formation of sex combs exclusively in males, and 25% larger size in females. Differences that affect male and female behavior exist also in the nervous system and the brain. Y chromosome aside, male and female cells possess a strictly identical genomic content. Most of the differences between the sexes arise and persist via the regulation of sets of genes in a sex-specific manner.

The question of how hundreds if not thousands of genes are differentially expressed in males and females to produce

doi: 10.1534/genetics.114.169268
Manuscript received May 20, 2014; accepted for publication July 14, 2014; published Early Online July 31, 2014.
Supporting information is available online at http://www.genetics.org/lookup/suppl/doi:10.1534/genetics.114.169268/-/DC1.
Available freely online through the author-supported open access option.
miRNA libraries from male and female tissues have been submitted to the GEO database at NCBI as series GSE57029.
[1]Corresponding authors: Cold Spring Harbor Laboratory, McClintock Bldg., 1 Bungtown Road, Cold Spring Harbor, NY 11724. E-mail: fagegalt@cshl.edu; Max Planck Institute for Biophysical Chemistry, Am Fassberg 11, Göttingen 37077, Germany. E-mail: halyna.shcherbata@mpibpc.mpg.de

sexually dimorphic individuals is extensively studied. Refined genomic and genetic studies have converged toward a model of differential expression that requires that both spatial and temporal programs be established throughout development (Arbeitman *et al.* 2002; Parisi *et al.* 2004; Lebo *et al.* 2009; Chatterjee *et al.* 2011). Probably the most important of these programs in flies is the sex-determination hierarchy (Baker *et al.* 1989; Christiansen *et al.* 2002; Camara *et al.* 2008; Clough and Oliver 2012). The primary determinant of *Drosophila* sex is the X chromosome to autosome (X:A) ratio (Bridges 1921), which determines the production of alternative splice variants of Sex lethal (*Sxl*) to generate an active SXL protein in females and a nonfunctional truncation in males (Cline 1978). *Sxl* activity is sufficient to direct the entire developmental programs of both somatic and germline sex determination (Christiansen *et al.* 2002; Robinett *et al.* 2010; Salz 2011; Whitworth *et al.* 2012). *Sxl* serves two essential functions: it restricts dosage compensation to males and controls the sex-determination hierarchy in each sex.

Dosage compensation is the process by which males double the transcription of genes on their single X chromosome to match the levels found in diplo-X females. This process requires a ribonucleoprotein complex, the compensasome, composed of two noncoding RNAs (*roX1* and *roX2*) and six proteins (male-specific lethals MSL-1, -2, -3, the helicase/ATPase MLE, histone acetyltransferase MOF, and histone kinase JIL1). In females, SXL represses the production of MSL-2 at both the transcriptional and translational level, therefore preventing dosage compensation. In males, lack of SXL function allows the male-specific expression of MSL-2 and its assembly into compensasomes to initiate dosage compensation (Bashaw and Baker 1997; see Duncan *et al.* 2006 for review).

At the top of the sex-determination hierarchy, SXL controls which sex-specific isoform is being processed from the doublesex (*dsx*) transcripts (reviewed in Christiansen *et al.* 2002). If the X:A ratio is 1, *Sxl* produces a female-specific splicing factor that causes female-specific splicing of the transformer (*tra*) transcript. TRA interacts with the transformer-2 (TRA2) splicing factor to produce a female-specific splice variant of *dsx* (Belote *et al.* 1989; Sosnowski *et al.* 1989; Ryner and Baker 1991). The female-specific DSX^F protein then activates female and inhibits male development. Because males lack SXL and subsequently TRA, a "default" male-specific splicing of *dsx* transcript generates the DSX^M protein, which inhibits female and promotes male traits. Loss-of-function mutations in *Sxl*, *tra*, and *tra2* transform XX individuals into males, but have no effect in XY males. In contrast, the *dsx* gene is important for the sexual differentiation of both sexes—in the absence of *dsx*, both XX and XY flies are anatomically and behaviorally intersex (Baker and Ridge 1980; Belote *et al.* 1985).

Only a few transcriptional targets through which DSX ultimately functions are known (Luo *et al.* 2011). DSX regulates sex-specific pigmentation patterns with abdominal-B (*Abd-B*) and bric-a-brac1 (*bab1*), resulting in males' darker abdomen (Williams *et al.* 2008). DSX^M controls the development of male-specific bristles or sex combs on the forelegs with sex-comb reduced (*Scr*) (Tanaka *et al.* 2011). In each sex, DSX orchestrates the differentiation of larval genital discs into mature dimorphic reproductive organs, external genitalia, and analia (Hildreth 1965; Chatterjee *et al.* 2011). DSX^F directly upregulates the expression of yolk proteins (Yp1, Yp2) (Burtis *et al.* 1991), and DSX^M downregulates their transcription.

The thorough dissection of *dsx* expression reveals that DSX presents two main characteristics (Lee *et al.* 2002; Hempel and Oliver 2007; Rideout *et al.* 2010; Robinett *et al.* 2010). First, the levels of DSX protein vary greatly throughout development within cells and tissues, implying a tight regulation of its steady states. Second, DSX is not present in all cells in a given tissue, so only some cells know their sex while others remain asexual.

MicroRNAs (miRNAs) appear as critical regulators of development and are themselves highly regulated (Ambros and Chen 2007; Bartel 2009; Smibert and Lai 2010; Dai *et al.* 2012). The interaction of microRNAs with the 3′-UTRs of transcribed mRNAs affects both a transcript's stability and its translation. Each miRNA can target several different mRNAs and each mRNA can be targeted by multiple miRNAs, generating an intricate network of gene expression regulation. As miRNAs could provide a rapid and tissue-specific means to alter gene expression, they represent ideal candidates for the regulation of spatial and temporal expression patterns of sex-determination genes, their cofactors, and downstream targets. Ultimately, the sex-biased expression of miRNAs could control directly the differential expression of many genes contributing to sexually dimorphic traits at a given time and place during development.

Sexually dimorphic miRNA profiles have been reported in mouse and chicken gonads, and in whole adult *Caenorhabditis elegans* (Mishima *et al.* 2008; Kato *et al.* 2009; Baley and Li 2012). In *Drosophila*, probing miRNA populations in whole animals during development has revealed widespread developmental regulation (Aravin *et al.* 2003; Ruby *et al.* 2007). However, the small RNA libraries generated in these studies came from either mixed-sex samples or single-sex but non-homogenous tissues, which may mask important sex- and tissue-specific variability in miRNA expression and function. To date, *Drosophila* lacks a critical examination of miRNA expression in two important contexts: sex-biased expression that may lead to sexually dimorphic function or spatial and temporal heterogeneity in expression that may drive tissue-specific functions. Both are critical to understanding the role of miRNAs across development.

To investigate these issues, we first established the profiles of miRNAs in several male and female adult parts and organs, larval dissected tissues, and embryonic cells. Their comparison reveals, in each tissue, sets of male- and female-biased miRNAs, increasing in number and extent with the complexity and sexual dimorphism of each tissue. We further address two aspects of miRNA functions in the

context of sexual identity: first, we test whether X-linked miRNAs are regulated by dosage compensation in males and, second, we explore the role of the steroid-induced miRNA let-7 in regulating sexually dimorphic traits and how its male-biased expression in the gonads affects germline differentiation programs.

Materials and Methods

Fly strains and genetics

Oregon-R flies were used for miRNA profiling. *Msl3^{p}*, *mle^{1}*, and *pr mle$^{12.17}$* mutants are described in Fagegaltier and Baker (2004). All chromosomes but the mutant-bearing allele were exchanged to create isogenized lines by back crossing to a *w^{1118}*; *MKRS/TM6B* stock for >10 generations. Wandering non-*Tb*- mutant male and female larvae were identified by their gonads. Overexpression of miRNAs was performed using a *dsx–GAL4* driver (Robinett *et al.* 2010). *UAS–NLS–GFP* flies are from Bloomington (BL4776); *UAS–let-7*, *UAS-mir-100*, *UAS–mir-125*, and *UAS–let-7-C* constructs are described in Bejarano *et al.* (2012). In *let-7-C* and *ecd* mutant studies, flies were raised on standard cornmeal–yeast–agar-medium at 25° and fattened on wet yeast paste 1 day before dissection unless otherwise stated. The two knockout alleles *let-7-C^{GK1}* and *let-7-C^{KO1}* lack the whole let-7-C cluster; *let-7-C^{GK1}* contains the transcriptional activator GAL4 under the control of the *let-7-C* promoter; *let-7-C^{GK1}/let-7-C^{KO1}* are referred to as *Δlet-7-C* (Sokol *et al.* 2008). Flies with a transgene rescuing the let-7-C cluster *(P{W8, let-7-C}; let-7-C^{GK1}/let-7-C^{KO1})* are referred to as *let-7-C* Rescue. The *P{W8, let-7-C Δlet-7}* construct restores all let-7-C miRNA members except for *let-7*. For miRNA loss of function, *let-7-C^{GK1}/let-7-C^{KO1}*; P{*W8, let-7-C Δlet-7*}/+ flies referred to as *Δlet-7* were used. The following additional fly stocks were used: *FRT40A let-7 mir-125/CyO and UAS–let-7-C*; *Sco/CyO* (Caygill and Johnston 2008), *UAS–let-7/TM6* (Sokol *et al.* 2008), *Ubi–GFP FRT40A/CyO*; *bab1–Gal4:UAS–Flp/TM2* (a gift from A. González-Reyes), *UAS–CD8GFP:UAS–nuc lacZ* (a gift from F. Hirth), *Oregon-R*, *w^{1118}*, and *ecd^{1ts}* (BL4210).

Sample collections for miRNA–Seq and validation

To ensure that miRNA–Seq samples are not contaminated by other tissues, ~120 Oregon-R heads were individually separated with a scalpel from the rest of the body of ~24-hr-old males and females, collected on ice and quickly frozen. Salivary glands were dissected from ~130 wandering late L3 larvae of each sex identified by their gonads. For qPCR validations of miRNA–Seq data sets, at least two additional independent collections were performed as above. We also collected ovaries and testes from 0- to 2- and 2- to 4-day-old Oregon-R individuals, S2 (Invitrogen), and Kc-167 cells (DGRC) washed in 1× PBS. All dissected tissues and cells were quickly snap frozen in liquid nitrogen and RNA preparations enriched for small RNAs using an adapted Trizol protocol.

miRNA–Seq

30-100μg of total RNAs were subject to *2S* rRNA depletion and DNAse treated. Size selected 18-29nt sRNAs were cloned according to (Malone *et al.* 2012). Libraries were clustered and sequenced on the Illumina GAIIx platform.

Cuticle preparations

Three- to 4-day-old flies were placed in ethanol and incubated in 10% NaOH for 1 hr at 70°. Adult abdominal cuticles were mounted and flattened in 30% glycerol. Pictures were taken at the same magnification using a Nikon SMZ150 microscope and Nikon DS-RiI camera.

Perturbation of ecdysone levels

The *ecd^{1ts}* temperature-sensitive mutation is known to reduce ecdysone levels at the nonpermissive temperature (Garen *et al.* 1977). Oregon-R and *ecd^{1ts}* flies were kept at the permissive temperature (18°) and 2- to 4-day-old adults were shifted to the restrictive temperature (29°) for 5–11 days to block ecdysone synthesis. Control Oregon-R and *ecd^{1ts}* flies were kept at 18° for the same time.

Clonal analysis

Somatic cell clones in CpCs and ECs were induced using mitotic recombination as described previously (König *et al.* 2011). *FRT40A let-7 mir-125/CyO*; *P{W8, let-7-C Δlet-7}* flies were crossed to *Ubi–GFP FRT40A/CyO*; *bab1–Gal4:UAS–Flp/TM2*. Third-instar larvae were heat shocked for 2 hr on 2 consecutive days in a 37° water bath and returned to 25°. Mutant clones were identified by the absence of GFP in 5-day-old adult ovaries.

Immunofluorescence and antibodies

Ovaries and testes were fixed in 5% formaldehyde (Polysciences, Inc.) for 10 min and stained as described in König and Shcherbata (2013). We used the following mouse monoclonal antibodies: anti-adducin (1:50), anti-lamin C (1:50), anti-arm (1:50), anti-FasIII (1:50), rat monoclonal antibody anti-DE-cadherin (Developmental Studies Hybridoma Bank), guinea pig anti-Tj (1:3000, D. Godt), rabbit anti-vasa (1:5000, gift from R. Pflanz), anti-β-Gal (1:3000, Cappel), and anti-GFP-directly conjugated with AF488 (1:3000, Invitrogen), Alexa 488, 568, or 633 goat anti-mouse, anti-rabbit (1:500, Molecular Probes), goat anti-rat Cy5 (1:250, Jackson Immunoresearch). Images were obtained with a confocal laser-scanning microscope (Zeiss LSM700) and processed with Adobe Photoshop.

Testis analysis and statistics

To determine the frequency of somatic cell differentiation defects in testis, the percentage of testis with somatic cell clusters (<5, ≥5, and >10) and epithelium appearance at the apex or at the lateral side of the anterior region of testicular tube were quantified. Statistics were calculated using two-way tables and chi-square test.

Determination of let-7 expression

To analyze the expression pattern of *let-7-C*, *let-7-C^{GK1}/CyO* flies were crossed to *UAS–mCD8–GFP:UAS–nuc–lacZ*. To analyze *let-7-C* levels upon stress, 3- to 5-day-old *let-7-C^{GK1}/UAS–mCD8GFP:UAS–nuc–lacZ* flies were heat shocked for 1 hr at 37° and their gonads were dissected and assayed for immunohistological analysis.

Quantitative PCR Assays (RT–qPCR)

For qPCR validation of the miRNA–Seq data sets and X-linked miRNA expression studies, 100 ng/μl RNA samples were spiked after DNAse digestion with a synthetic primer at 6.10e9 copies/μl, polyadenylated and reverse transcribed according to the miScript reverse transcriptase kit instructions (Qiagen). Each miRNA was quantified with a specific primer (Supporting Information, Table S1) following the miScript SYBR green PCR kit instructions. All miRNAs were tested in triplicates on two independent biological replicates with the appropriate controls. Ct values were normalized to *U6* snRNA levels in miRNA–Seq validation experiments using the $\Delta\Delta C_T$ method and $2^{-\Delta\Delta CT}$ values calculations and to *Dspt4* mRNA levels in the dosage compensation mutant studies (see Table S11, Table S12, Table S13, Table S14, Table S15, and Table S16).

For let-7 quantification, reverse transcription and qPCR were performed following the manufacturers' protocol using TaqMan MicroRNA assay, with *2S* rRNA as an endogenous control. Let-7 levels were determined in gonads and carcasses from Oregon-R males and females. To eliminate effects that could possibly arise because ovaries contain different amounts of eggs and late egg chambers, late-stage egg chambers and eggs were removed from the dissected ovaries, leaving only the anterior part of the ovary containing the germaria. To measure let-7 levels upon perturbation of ecdysone, ovaries and testes of Oregon-R and *ecd^{1ts}* mutants raised at 18° and shifted to 29° for 5 or 11 days (or kept at 18° for control for the same amount of time) were dissected. RNA was extracted in Trizol according to the manufacturer's instructions before proceeding with RT–qPCR.

Sex-specific mRNA transcript levels were assessed in 5- to 7-day-old *Δlet-7* and *let-7-C* Rescue control whole flies that were raised at 25° and shifted to 33° for 4 days or in Oregon-R and *ecd^{1ts}* mutants raised at 18° and shifted 1–3 days after hatching to 29° (or kept at 18° for control) for 5 or 11 days. cDNA was generated using the cDNA reverse transcription kit (Applied Biosystems) according to the manufacturer's instructions and qPCR performed using the fast SYBR Green Master Mix (Applied Biosystems). A Step One Plus 96 well system (Applied Biosystems) was used for all analyses. All reactions were run in triplicates with appropriate blanks. The reactions were incubated at 95° for 10 min followed by 40 cycles at 95° for 15 sec and 60° for 60 sec (TaqMan MicroRNA). The ΔC_T value was determined by subtracting the C_T value of the endogenous control from the experimental C_T value. $\Delta\Delta C_T$ was calculated by subtracting the ΔC_T of the control sample from the suspect ΔC_T value. The relative RNA levels were calculated using $2^{-\Delta\Delta CT}$. Primers are described in Table S1.

Bioinformatics

The libraries produced in this study (NCBI GEO series record GSE57029) were complemented with existing libraries from lymphoid cells (GSM272653, Kc cells; GSM272652, S2 cells) (Chung *et al.* 2008) and from 2- to 4-day-old Oregon-R adult testis (GSM280085) and ovary (GSM280082) (Czech *et al.* 2008). Reads were clipped of the adapter sequences, filtered for sequences mapping to viruses and simple repeats, and aligned to the *Drosophila melanogaster* genome (BDGP R5/dm3) with no mismatches using NexAlign (program available from the OSC: Data & Resource website). Uniquely mapped reads were annotated using a priority pipeline as in (Czech *et al.* 2008) and FlyBase r5.26, miRbase r.15 and in-house miRNA annotations. Reads corresponding to 184 annotated miRNAs were extracted and counts reported to estimate expression levels (Table S9). For each library, miRNA reads are normalized using the trimmed median ratio used to calculate a correction factor applied to all miRNA counts in a given library. Normalized counts (Table S10) were then input to calculate the relative expression and fold change in expression in pairwise comparisons between male and female samples. The contribution of each miRNA to a library was calculated as the normalized read counts over the total number of miRNA reads in the library (Table S22). The relative abundance of a miRNA across tissues was calculated by dividing the normalized count by the total of normalized counts across all libraries. Heatmaps were generated in R using the hclust() function to perform hierarchical cluster analysis.

Results and Discussion

MiRNA profiling in male and female tissues

We adopted a genomic approach and surveyed the populations of miRNAs in several *Drosophila* male and female tissues selected at various stages of development. Sexed miRNA–Seq data sets include late-embryo-derived lymphoid cells, larval salivary glands, and ~1-day-old adult head and body, as well as germline-enriched tissues (ovary and testis) from mature adults (2- to 4-day-old).

Libraries prepared in different ways have been shown to result in variable sequencing efficiencies for individual miRNAs, so that differences in miRNA read counts between libraries may be caused by differential cloning efficiencies rather than reflect differences in their expression. To assess potential biases between sexes as accurately as possible, we prepared libraries and integrated carefully selected existing data sets (see *Materials and Methods*). All provide sufficient depth and breadth and were prepared with the Rnl2 truncated ligase, identical 5′ and 3′ cloning adaptors, and PCR conditions.

Several methods are available to analyze high-throughput miRNA profiling; however, none has reached a consensus.

The choice of a processing and normalization method can affect greatly the estimates of differentially expressed miRNAs between tissues, especially when comparing tissues that differ substantially in their miRNA content (Dillies *et al.* 2013). We find the trimmed median method most suitable to normalize our data sets, which cover a wide range of tissues (see *Materials and Methods*). Normalized counts were then input to get empirical estimates of the relative abundance of a given miRNA in a library, in pairwise comparisons between male and female tissues, and across all samples. To assess the accuracy of our analyses, we assayed the expression of miRNAs across these samples using an independent method (qPCR; Figure S1). Of the 22 miRNAs tested for validation, 16 miRNAs show similar trends by qPCR and deep sequencing consistently across all samples. For five additional miRNAs, the enrichment trend and/or sex biases could not be confirmed in one or more tissues, while consistent in others. One miRNA showed systematically different profiles by qPCR and deep sequencing due to the presence of miRNAs with very close sequences that qPCR could not distinguish. Although cloning artifacts that may alter miRNA expression profiles in some libraries cannot be excluded, the highly overlapping trends of our qPCR validation set with those of normalized miRNA-Seq data suggest that our analysis reflects miRNA populations in each tissue and supports our main conclusions.

Samples included in our data set were selected to allow a detailed examination of the biases in miRNA content between male and female in tissues of increasing complexity with regard to the nature and number of different cells they contain and in tissues ranging from poorly to highly sexually dimorphic. We assess sex biases of miRNAs at the level of single cells in culture (lymphoid cells), in a very simple tissue with functions in both sexes (salivary glands), and in several fly parts of variable complexity and sexual dimorphism (head, body, ovary, and testis).

Each tissue is enriched for specific miRNAs, highlighted in clusters in Figure 1A, many of which are enriched in both sexes. Ubiquitous and evolutionary conserved miRNAs (mir-14, bantam, mir-8, mir-1) are highly expressed in most tissues (Table 1). However, even for such prevalent miRNAs, their relative abundance varies greatly depending on the tissue and stage studied (Table 1 and Figure 1A), denoting a high degree of variation in miRNA populations between tissues and the compartmentalization of their functions in a dynamic fashion.

In addition to a temporal and spatial regulation of miRNAs during development (Ruby *et al.* 2007), a novel layer of complexity arises as we compare miRNA populations between males and females. Regardless of its heterogeneity, each tissue examined reveals miRNAs differentially or even exclusively expressed in one sex (Figure 1, B–H). The example of mir-8 illustrates how a miRNA classically regarded as abundant presents unexpected differences at the cellular level: mir-8 ranks within the top two most abundant miRNAs in heads and salivary glands (10–15% of reads), but fourth in lymphoid Kc cells (4%), and only 17th in S2 cells (<1%; Table 1). Following from this example, we systematically analyzed the miRNAs families present in each tissue and estimate their sex-biased expression.

MiRNAs in lymphoid embryonic-derived cells

We examined miRNAs populations in two embryonic hemocyte-derived cell lines commonly considered as male (S2) and female (Kc-167) based on the status of dosage compensation (Alekseyenko *et al.* 2012). In S2 cells, the X chromosome is upregulated by compensasomes recruited along the X chromosome at sites identical to those seen in embryos, male salivary glands, and whole larvae (Alekseyenko *et al.* 2006; Legube *et al.* 2006; Straub *et al.* 2008). In Kc cells, dosage compensation does not occur.

In our assays, most miRNAs are common to both Kc and S2 cell lines (Figure 1B). Overall, mir-14, mir-184, and bantam are most abundant and account for about half of all miRNA reads (Table 1) in both cell lines. Our miRNA profiles agree with the medium levels of mir-2 (mir-2a/-2b mainly) and high levels of mir-34 described in S2 cells (Sempere *et al.* 2003). High expression of mir-14 in these immortalized cell lines is consistent with its role as a cell-death suppressor (Xu *et al.* 2003). In addition, we do not detect miRNAs from the let-7-C cluster (let-7, mir-100, mir-125) in either cell type. This is consistent with previous reports in which the let-7-C miRNAs are detected only upon addition of the steroid hormone ecdysone, which has the opposite repressive effect on mir-34 (Sempere *et al.* 2003; Chawla and Sokol 2012).

For sexually dimorphic expression, we identify sex biases for several miRNAs: mir-12, mir-304, mir-92a, and mir-278 are more abundant in female Kc cells, whereas mir-252, mir-307, mir-282, and mir-980 are more prominent in male S2 cells (full lists in Table S2). Simple male and female embryonic cell lines express comparable miRNAs, yet differ in the level at which they express them.

MiRNAs in larval salivary glands

We examined miRNAs in larval salivary glands, organs that secrete the "glue" allowing the larva to attach to a substrate before pupariation. Salivary glands consist of two simple cell types (Kerman *et al.* 2006): secretory cells and duct cells that connect them to the larval mouth. Each type originates from ~100 cells in the embryonic ectoderm. The secretory cells initiate multiple rounds of DNA replication and differentiate without subsequent division (endoreplication) to create the giant polytene chromosomes needed to meet the increased metabolic requirements of these cells to produce secretory proteins.

Among all samples, miRNAs with a strong preference for expression in salivary glands are, in descending expression levels, mir-263a, mir-375, mir-304, mir-275, mir-283, mir-308, mir-286, mir-5, and mir-307-as (Figure 1A). Many of these highly expressed miRNAs (*e.g.*, mir-8, mir-263a, mir-275, mir-12, and mir-304) match those whose expression peaks during the larval stages (Ruby *et al.* 2007). In contrast, others (bantam, mir-13b, mir-11 or mir-14, mir-2b) are expressed more ubiquitously during development.

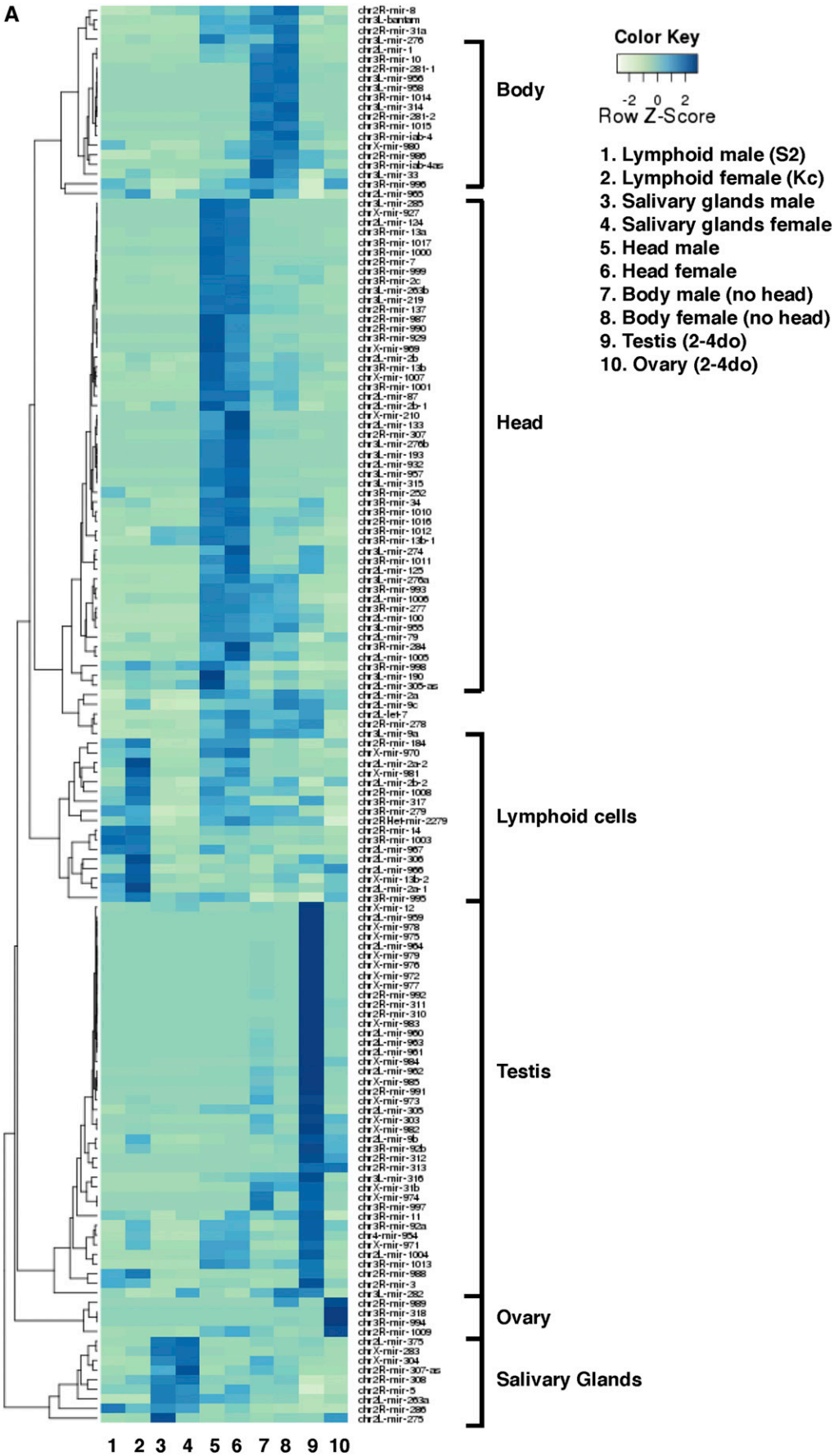

Figure 1 Expression of miRNAs in various male and female tissues. (A) Expression of miRNAs across 10 sexed libraries. Blue color intensity ranging from light to dark indicates an increasing abundance of normalized counts estimates for a given miRNA relative to all miRNAs in that library and to all libraries. Clusters of miRNAs enriched in a given tissue are highlighted. The 147 miRNAs with >30 normalized reads across all libraries were retained. 2–4 do: 2- to 4-day-old flies. The biased expression of miRNAs and their expression levels are shown in pairwise comparisons in each tissue in (B) embryonic hemocyte-derived S2 (male) and Kc-167 (female) cells. (C) Late larvae L3 Salivary Glands. (D) Adult Head. (E) Adult body (head removed). (F) Testis compared to male Body. (G) Ovary compared to female Body. (H) Testis compared to ovary. For each miRNA, the ratio of normalized reads (M/M+F or F/M+F) (*x*-axis) is plotted against its normalized expression level (%, log scale). Each dot represents a miRNA; miRNA's present in one sexed tissue have a ratio of 0 or 1. Pearson correlations between male and female samples: 0.95 in lymphoid cells; 0.98 in salivary glands; 0.96 in heads; 0.99 in body; 0.25 in testis/ovary. M, Male; F, Female.

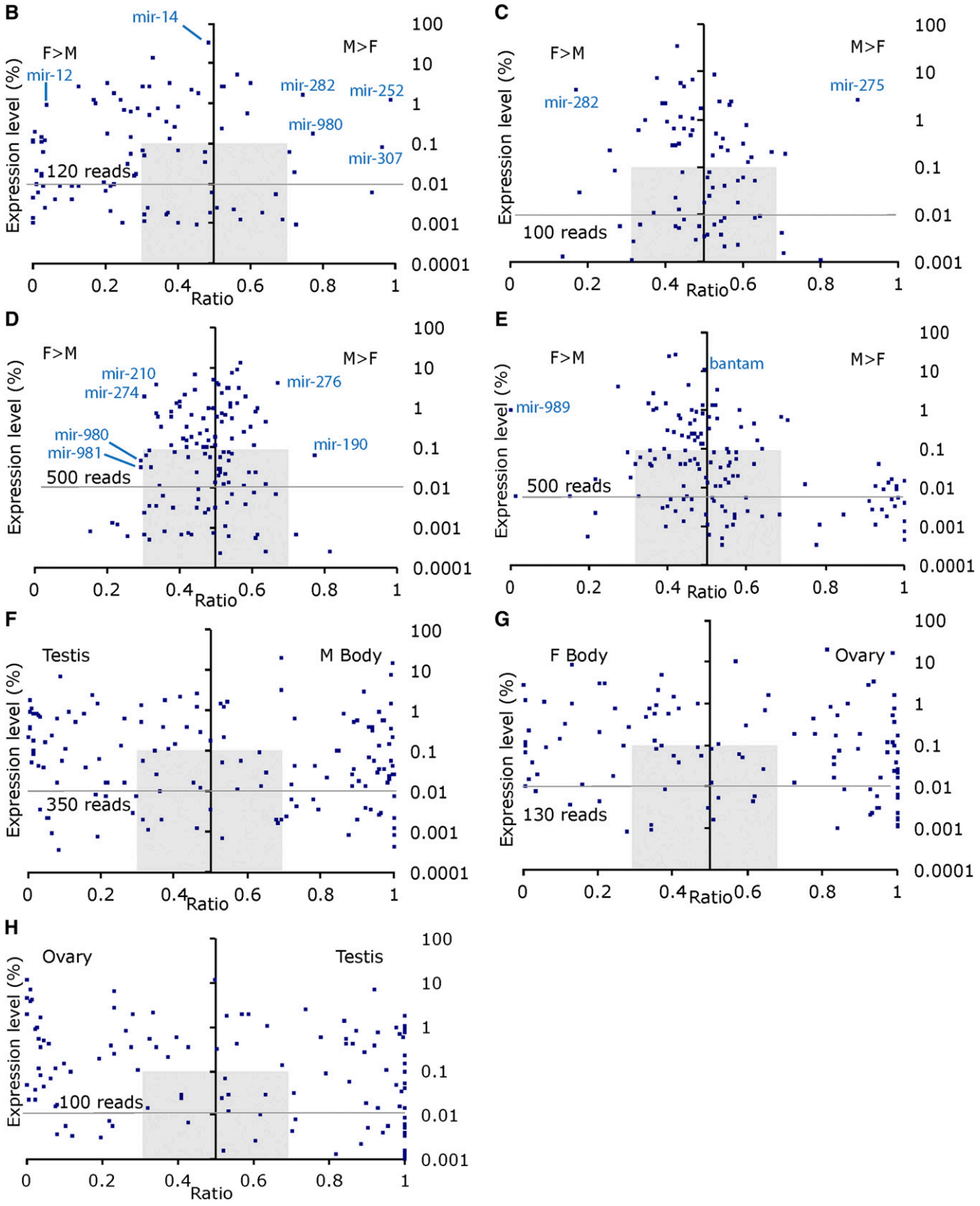

Figure 1 (*Continued*)

As expected from a tissue of low complexity with functions essential to both sexes, miRNAs are found in most instances at levels comparable in male and female salivary glands (Figure 1C). This overwhelming similarity is not without exceptions. Salivary glands present a limited number of miRNAs whose expression is biased toward

Table 1 Twenty-five most abundant miRNAs in male and female libraries from embryonic lymphoid cells (S2, male; Kc, female), third-instar larval salivary glands, 1-day-old adult head and body, and 2- to 4-day-old adult gonads

Embryonic lymphoid cells				Larval salivary glands				Adult heads				Adult body				Adult gonads			
S2	%	Kc	%	Male	%	Female	%	Male	%	Female	%	Male	%	Female	%	Testis	%	Ovary	%
mir-14	38.35	mir-14	29.10	mir-8	32.42	mir-8	35.67	mir-8	14.57	mir-8	11.44	mir-1	25.56	mir-1	26.75	mir-12	16.87	mir-989	18.37
mir-184	11.35	mir-184	16.38	mir-263a	10.45	mir-12	8.49	mir-1	10.00	mir-1	8.18	mir-8	23.01	mir-8	25.64	mir-8	15.35	bantam	11.43
bantam	7.44	mir-2a	4.44	mir-375	7.15	mir-263a	7.75	bantam	8.19	mir-276a	7.63	bantam	12.56	bantam	9.79	mir-305	5.04	mir-8	9.30
mir-996	4.85	mir-8	4.15	mir-12	6.25	mir-375	6.72	mir-276a	5.81	bantam	7.14	mir-276a	4.66	mir-276	5.02	mir-959	4.68	mir-2a	7.73
mir-279	3.47	bantam	4.08	mir-304	5.73	mir-282	6.30	mir-276	5.39	mir-210	5.00	mir-277	3.91	mir-276a	4.27	mir-2a	3.85	mir-318	7.25
mir-11	3.29	mir-34	3.40	mir-275	5.19	mir-304	6.01	mir-277	4.66	mir-277	4.90	mir-276	2.47	mir-2a	2.93	let-7	3.13	mir-184	6.40
mir-34	2.93	mir-988	3.37	bantam	4.71	bantam	4.82	mir-184	4.06	mir-184	4.17	mir-2a	2.20	mir-277	2.68	mir-34	3.11	mir-996	5.92
mir-988	2.90	mir-317	3.15	mir-2a	3.04	mir-11	2.46	mir-34	3.58	mir-34	3.61	mir-996	1.54	mir-989	1.76	mir-282	3.00	mir-2b	3.30
mir-282	2.84	mir-2b	3.11	mir-305	2.73	mir-13b	2.45	mir-2b	3.42	mir-14	3.20	let-7	1.49	mir-282	1.68	mir-964	2.74	mir-994	3.01
mir-252	2.79	mir-276	2.30	mir-2b	2.43	mir-305	1.93	mir-2a	3.23	mir-285	2.95	mir-9a	1.48	mir-31a	1.48	mir-277	2.59	mir-275	2.62
mir-13b	2.43	mir-996	2.30	mir-13b	1.99	mir-2a	1.91	mir-285	3.22	mir-2a	2.92	mir-14	1.34	mir-2b	1.21	mir-11	2.51	mir-13b	2.20
mir-2b	2.09	mir-279	2.26	mir-11	1.91	mir-2b	1.55	mir-14	2.46	mir-2b	2.73	mir-31a	1.28	mir-9a	1.18	mir-978	2.29	mir-9b	2.20
mir-317	1.92	mir-13b	2.20	mir-283	1.79	mir-283	1.54	mir-210	2.44	mir-276	2.72	mir-282	1.20	mir-996	1.08	mir-977	2.20	mir-263a	1.46
mir-276a	1.92	mir-11	2.09	mir-282	1.58	mir-996	1.20	mir-124	2.35	mir-274	2.60	mir-12	1.10	let-7	1.08	mir-274	2.15	mir-79	1.40
mir-2a	1.65	mir-9b	1.77	mir-996	1.14	mir-276	1.15	mir-13b	2.20	let-7	2.39	mir-13b	1.08	mir-184	1.06	mir-976	2.04	mir-282	1.38
mir-276	0.95	mir-276a	1.62	mir-308	1.06	mir-308	1.00	let-7	1.62	mir-124	2.28	mir-10	0.98	mir-13b	0.96	mir-9a	1.86	mir-11	1.34
mir-8	0.84	mir-12	1.58	mir-14	0.99	mir-998	0.99	mir-1000	1.47	mir-252	1.76	mir-2b	0.94	mir-10	0.84	mir-983	1.83	mir-34	1.32
mir-995	0.79	mir-305	1.54	mir-998	0.81	mir-276a	0.74	mir-263a	1.37	mir-13b	1.63	mir-281-1	0.91	mir-11	0.75	mir-9b	1.82	mir-305	1.08
mir-277	0.78	mir-2a-2	1.45	mir-276	0.74	mir-79	0.69	mir-987	1.16	mir-9a	1.53	mir-304	0.88	mir-14	0.74	mir-14	1.82	mir-9c	0.94
mir-305	0.70	mir-306	0.91	mir-34	0.63	mir-995	0.64	mir-252	1.14	mir-996	1.28	mir-184	0.79	mir-281-1	0.72	mir-988	1.79	mir-12	0.92
mir-998	0.65	mir-998	0.89	mir-995	0.62	mir-34	0.59	mir-274	1.09	mir-263a	1.21	mir-279	0.75	mir-314	0.60	mir-2b	1.64	mir-33	0.84
mir-306	0.52	mir-9c	0.84	mir-79	0.61	mir-14	0.52	mir-7	1.09	mir-1000	1.20	mir-11	0.74	mir-279	0.56	mir-960	1.47	mir-995	0.76
mir-9b	0.52	mir-995	0.84	mir-9a	0.59	mir-275	0.51	mir-9a	0.95	mir-31a	1.03	mir-305	0.72	mir-263a	0.52	mir-13b	1.41	mir-14	0.63
mir-79	0.43	mir-79	0.81	mir-9b	0.48	mir-33	0.45	mir-929	0.95	mir-11	1.00	mir-79	0.62	mir-305	0.50	mir-317	1.22	mir-1	0.62
mir-2a-2	0.42	mir-282	0.69	mir-33	0.47	mir-9a	0.43	mir-31a	0.91	mir-7	0.97	mir-263a	0.61	mir-34	0.44	mir-316	1.20	mir-312	0.58

miRNAs are ranked in decreasing order and their contribution to the library given as a percentage of all miRNA reads in the library. The full list and percentages are provided in Table S22.

male (mir-275) and female cells (miR-279, mir-282) (Table S3).

For several miRNAs, including mir-304, mir-12, mir-283, mir-314, and mir-981, the relative abundance in male and female salivary glands is matched in whole larvae, suggesting widespread or general functions (D. Fagegaltier, data not shown). Others vary, suggesting more discrete roles—these include miR-210, mir-13b, mir-100, mir-1013, and miR-979 (note that the latter has low reproducibility in salivary glands in our assay). Supporting this view, we detect by qPCR higher amounts of mir-979, mir-210, and mir-314 in whole larvae compared to salivary glands, and mir-979 and mir-314 are expressed in mixed L1-L3 larval imaginal discs (Ruby *et al.* 2007).

Surprisingly, although let-7 is undetectable by Northern blot on unsexed whole L3 larvae (Sempere *et al.* 2002), we find let-7 in salivary glands of both males (48 normalized reads) and females (219 reads) (Table S3). The function of let-7 in salivary glands is unknown, but sex-biased expression could reveal interesting differences and asynchrony in tissue homeostasis during male and female transition from larval to pupal stages.

MiRNAs in adult heads

In adult heads from 1-day-old flies, the most prominent miRNAs are mir-8, mir-1, mir-276a, and bantam (Table 1). All were shown to act on neural target genes, genes controlling circadian rhythms, eye development, and growth (see Smibert and Lai 2010 for review; Marrone *et al.* 2012; Li *et al.* 2013). Interestingly, whole heads do not differ dramatically in their miRNA profiles between males and females (Figure 1, A–D). Mir-2a, mir-2b, mir-277, mir-278, and, importantly, let-7, mir-34, and mir-124 are expressed at comparable levels in both sexes, in agreement with their general role in specifying neuronal cell fate, plasticity, and neurodegeneration (Kucherenko *et al.* 2012; Liu *et al.* 2012; Weng and Cohen 2012; Wu *et al.* 2012). Conversely, head expression of mir-276 and mir-190 is enriched in males, and mir-210, mir-274, mir-980, and mir-981 in females (Table S4). This finding hints toward sexually dimorphic functions of these miRNAs in neuronal tissues.

Finally, miR-252 and miR-980 were previously detected by qPCR in adult male and female heads 2–4 days after eclosion, while no miR-984 could be detected (Marrone *et al.* 2012). The present analysis provides evidence that all three miRNAs are expressed in the head and establishes the expression of both mir-252 and miR-984 as slightly more prominent in female heads compared to males. The functional significance of such biases is yet to be determined.

MiRNAs in the adult body, testis, and ovary

Almost all known miRNAs (155 miRNAs) are detected in the body, the most complex sample in our data set that covers all body parts of the adult fly with the exception of the head. We find primarily mir-1, mir-8, bantam, mir-276a, mir-277, mir-276, mir-2a, mir-996, and let-7 in the fly body (Table 1). The adult fly presents striking biases for miRNAs in males and females (Figure 1E and Table S5). Mir-989 represents the strongest female-biased miRNA in the body. Among a larger set of highly male-biased miRNAs, few are detected in females. Of the 22 most strongly male-biased miRNAs in the body (above fivefold), 17 miRNAs appear exclusively in males and the remaining miRNAs (mir-960, mir-961, mir-963, mir-983, and mir-984) yield at best a few tens of reads in females. Valuable insights into the origin of these discrepancies come from the following comparisons.

We compared the populations of miRNAs in testes and ovaries. We have seen so far that from single lymphoid cells to more complex and dimorphic heads and bodies, the most abundant miRNAs remain overall conserved between males and females with a few exceptions such as mir-8. This is strikingly not the case in testes and ovaries in which the most abundant miRNAs differ. In 2- to 4-day-old flies, about half of the miRNAs cloned from ovaries correspond to mir-989, bantam, mir-8, mir-2a, and mir-318 (Table 1). In testes, this set only partially overlaps with that of ovaries and includes mir-12, mir-8, mir-305, mir-959, mir-2a, let-7, and mir-34. Younger males exhibit the same set of abundant miRNAs in testes (D. Fagegaltier, data not shown) indicating that their high expression persists in testes at least over the early adult stages.

Each tissue in our data set presents a set of miRNAs underrepresented in the other tissues examined; although their relative abundance varies between male and female, these tissue-enriched miRNAs are usually overrepresented in both sexes (Figure 1).

Ovaries and testes are enriched for certain miRNAs, but very few are enriched in both tissues. Instead, two distinct sets of miRNAs emerge: a large cluster of testis-enriched miRNAs and a smaller set of ovary-enriched miRNAs (Figure 1A). The miRNA populations of these highly sexually dimorphic tissues are highly skewed and sexually dimorphic (Figure 1H). 47 miRNAs show higher levels of expression in testes compared to ovaries (above fivefold), whereas 29 are preferentially expressed in the ovary (Table S6). Fourteen strongly testis-biased miRNAs are not detected in ovaries and may carry important and specialized functions.

During maturation, oocytes express several classes of miRNAs whose levels vary upon fertilization and later during the initiation of zygotic transcription. Maternal deposition of miRNAs has been reported in *Drosophila* to serve a variety of functions, including the destabilization of a large number of maternal mRNAs in early embryos via the SMAUG protein (Giraldez *et al.* 2006; Bushati *et al.* 2008; Soni *et al.* 2013).

In whole ovaries from 2- to 4-day-old females, we identify all but one of the reported maternally deposited miRNAs previously described in oocytes, including miRNA populations denoted as unstable (class I, restricted to stage 14 oocytes), and stable (class II, including maternally deposited and zygotically expressed miRNAs). Specifically, we identified mir-318, mir-276a, mir-34, mir-317, mir-284, let-7 (class I); mir-13b, mir-2a, mir-306, mir-184, mir-312, and mir-310 (class II). Zygote-specific miRNAs of class III were not detected, namely the miR-309 cluster zygotically expressed ~2- to 4-hr-post-fertilization (miR-309, miR-3, miR-286, miR-4,

miR-5, miR-6-1, mir-6-2, and mir-6-3). We note, however, that the expression of mir-3 and mir-5 for class III could start earlier than previously described: six to eight reads match mir-3 and mir-5. Supporting this view, low counts for mir-3 and mir-5 in 2- to 4-day-old female ovaries increase in *loqs* mutants in Czech *et al.* (2008). A low expression of these two miRNAs in the ovary therefore remains a possibility.

In summary, in addition to expressing highly divergent sets of miRNAs, both testes and ovaries express very different sets of miRNAs compared to other tissues (Figure 1A): their respective miRNA profiles appear as the most divergent of our data set.

To gain insight into the sexually dimorphic functions of miRNAs in somatic tissues, we compared the miRNA populations in testes and male body or ovaries and female body, respectively. We reasoned that a miRNA present in the male body sample (that includes testes) but not enriched in testes is likely to have at least a somatic function outside the testes. Thirty such miRNAs are enriched at least fivefold in the male body (Figure 1F and Table S7), suggesting that they carry distinct functions in the soma.

In a similar comparison between female body and ovaries, we identify 45 miRNAs enriched in female somatic tissues, 28 of which are almost exclusively detected in the female body (Figure 1G and Table S8).

Finally, the tallies of miRNAs enriched in ovaries and testes compared to the body samples establish that most of the differences in miRNA expression between male and female body come primarily from these highly dimorphic internal reproductive tissues.

Male- and female-biased somatic miRNAs

We next looked specifically for miRNAs presenting a consistent bias toward males or toward females in all somatic tissues studied. We considered miRNAs presenting at least a twofold enrichment in one sex in lymphoid cells, salivary glands, head, and/or body. Interestingly, not a single miRNA presented male biases in all four or even three tissues, suggesting that there is no ubiquitous male-biased somatic miRNA. However, a total of 23 miRNAs are male biased in two tissues, generally salivary glands and S2 cells, or head and body (Figure S2A). Of these 23 somatic male miRNAs, 10 are also enriched in testes (compared to the male body) and might therefore repress sex-specific targets in the male soma and gonads. The remaining 13 miRNAs are not enriched in testes and represent somatic male-biased miRNAs.

For females, 32 miRNAs are consistently female biased in the soma (more than twofold; Figure S2B). Interestingly, mir-318 is enriched in females in all four somatic tissues and several other miRNAs in three tissues. Eight of these female-biased miRNAs are also enriched in ovaries. The remaining 24 miRNAs represent somatic female-biased miRNAs.

Ovary and testis miRNAs

We next searched for miRNAs prevalent in ovaries, testes, or both to identify those with possible functions in gametogenesis or the organization of the adult gonads. Compared to same-sex somatic tissue, 32 miRNAs are enriched in the ovary and 51 in testis. Of these, 18 are enriched in both testis and ovary, likely underscoring important processes common to gonads of both sexes. Conversely, 8 miRNAs enriched in ovaries but not in testes and 30 miRNAs enriched in testes but not in ovaries could control sex-specific aspects of gonad development (Figure S2C).

The 30 testis-enriched miRNAs reflect a remarkable genomic homogeneity: 11 of these miRNAs are located on the X chromosome (Figure S2C). This fraction is much higher than expected ($P = 0.0018$, hypergeometric distribution) and significantly greater than the proportion of X-linked miRNAs found in other tissues (male soma, $P = 0.0747$; ovaries, $P = 0.2115$). This enrichment of miRNAs originating from the X chromosome is therefore a phenomenon specific to testes. The prevalence of X-linked miRNAs expression in testes has been reported in mouse and was explained by X-linked gene dosage (Ro *et al.* 2007; Mishima *et al.* 2008). It is tempting to speculate that such a mechanism may hold true in *Drosophila* testes as well. To date, the mechanisms regulating X-linked genes expression in testes such as meiotic sex-chromosome inactivation and dosage compensation remain unclear (Vibranovski *et al.* 2009; Deng *et al.* 2011; Meiklejohn *et al.* 2011; Vibranovski *et al.* 2012).

Are X-linked miRNAs transcriptionally regulated by dosage compensation?

We next asked whether the transcriptional regulation of X-linked miRNAs depends on dosage compensation in male somatic tissues. At the genomic level, miRNAs are evenly distributed across the *Drosophila* genome with no obvious pattern on the X chromosomes. The X chromosome represents ~20% of the *Drosophila* genome and bears an even share of miRNAs. The 149 genomic miRNA loci queried in this study are distributed evenly across all chromosomes with 34, 33, 22, 29, and 27 miRNAs on chromosomes 2L and 2R, 3L and 3R, and the X chromosome. Together, the fourth chromosome and heterochromatin of chromosome 3 (3h) account for 4 additional miRNAs. To date, no miRNA has been reported on the Y chromosome.

Two classes of miRNAs are present as typical genic miRNAs and mirtrons. A total of 37 mirtrons (24.8%) reside within introns in the genome. Compared to miRNAs regulated by their own promoter, mirtrons are slightly enriched on chromosome 2L (32.4% of chromosome 2L miRNAs) and underrepresented on chromosome 3L (13.6%); on the X chromosome, 22.2% are encoded as mirtrons.

To address whether dosage compensation controls miRNA expression directly on the X chromosome, we first examined whether X-linked miRNAs reside in regions bound by MSL-1 in ChIP–Chip experiments reported by Straub *et al.* (2008) in S2 cells and embryos. We note that X-linked miRNAs reside outside the primary "high affinity sites" defined in these studies and are therefore not primary strong binding sites for

compensasomes. MSL-1 levels were further divided into high, medium, low, or MSL-1 absent subtypes (Figure 2A). With the exception of two miRNA loci residing in regions not addressed in this study, 67% of X-linked miRNA loci reside in regions bound by compensasomes, indicating that some miRNAs could be dosage compensated.

For those X-linked miRNAs residing in regions bound by MSL1, dosage compensation could provide a direct means to equalize their expression in both sexes. To test this possibility, we assayed by quantitative PCR the levels of X-linked miRNAs expressed in salivary glands, a tissue in which dosage compensation has been extensively studied, and compared miRNA levels in wild-type animals and mutants for compensasomes function (*msl-3* and *mle*; Figure 2, B and C). In mutant males, X-linked mir-304, mir-13b, and mir-12 levels are reduced approximately twofold, as expected for genes whose expression depends on compensasomes; autosomal controls mir-100 (2L), mir-981, and mir-1013 (3R) were unaffected. However, levels of two miRNAs mir-979 and mir-210 did not change significantly in mutants, implying that some X-linked miRNAs escape dosage compensation—these join the short list of X-linked protein coding genes (*Lsp1-α*, *dpr8*, *CG9650*) that similarly avoid compensation. Interestingly, mir-12 and mir-304 belong to the same cluster as mir-283 but behave differently in mutants. The milder reduction of mir-283 levels in mutant animals supports previous observations that mir-12 and mir-304 expression patterns show little correlation with that of mir-283. Although they share a common Pol II promoter, post-transcriptional processing could account for these differences (Ryazansky *et al.* 2011).

In summary, only a few X-linked miRNAs are influenced to some extent by dosage compensation. Two X-chromosome miRNAs clearly escape dosage compensation (mir-979, mir-210). One major difference between miRNA and protein-coding genes escaping dosage compensation is that the latter tend to reside outside MSL-bound domains. Overall, it is tempting to speculate that dosage compensation presents only limited advantages for short, rapidly regulated miRNA genes.

A role for the let-7-C locus in sexual dimorphism

We investigated the functional relevance of sex-biased expression of miRNAs using the example of let-7. Two miRNAs in the let-7-C cluster, mir-125 and let-7, are highly expressed in the fly head, body, and testis and poorly in the ovary (Figure 4A). Mir-100 levels are consistently lower in all tissues expressing let-7 and mir-125. From worms to flies and humans, the let-7-C locus has an important role throughout development (Pasquinelli *et al.* 2000). In flies, let-7-C is under the control of ecdysone and mimics the hormone peaks required for each of the developmental transitions that turn an embryo into an adult (reviewed in Ambros 2011). We set out to investigate the functional implications of the male-biased expression of the let-7-C miRNAs in the gonads and more generally its function in adult males and females.

Sex-biased let-7 miRNA expression in gonadal somatic cells sustains germline differentiation

We analyzed let-7-C expression pattern in the adult *Drosophila* gonads using *Gal4* under the control of the intrinsic let-7-C promoter. In the germarium, let-7-C is expressed in some of the somatic escort (ECs) and cap cells (CpCs; Figure 3, A, B, and D). The number of let-7-C-expressing cells and the activity of the let-7-C promoter *per se* fluctuate in CpCs and ECs in different germaria and within the same germarium (compare Figure 3, D and D′), demonstrating that the expression pattern of let-7-C is highly dynamic.

In testes, somatic cells, namely cyst stem cells (CySC's), and their lineage express let-7-C (Figure 3, E–E′). We find consistently higher levels of let-7-C per cell and higher numbers of let-7-C-positive cells per testicular apex compared to positive cells in the germarium (compare Figure 3, D–D′ and E, green).

We confirmed by RT–qPCR the male-biased expression of let-7 in the gonads. Let-7 levels are about eight times higher in testes compared to those in ovaries (Figure 3C). In addition, let-7 is enriched in the gonads of both sexes compared to carcasses. Together, these findings support the biased expression of let-7-C and let-7 reported here by miRNA profiling. Further, they establish a stronger transcriptional activity of the let-7-C promoter in the testicular soma compared to the activity in the ovarian soma.

In addition, let-7 has been detected in the hub cells of old male testes, demonstrating its responsiveness to aging in males (Toledano *et al.* 2012). The dynamic expression of let-7 and its responsiveness to external and internal conditions (temperature—see below, aging) in both sexes prompted us to ask whether let-7 regulates gonadal somatic cell behavior.

We analyzed the tissue architecture of the germaria and testes upon let-7 depletion. In the ovary, Δ*let-7* clones induced specifically in somatic ECs result in a peculiar germarium architecture where both the germline and soma are abnormal (Figure 3G). Mutant germaria contain supernumerary single spectrosome germline cells (arrows) and oddly shaped somatic ECs expressing higher amounts of cell adhesion molecules (Figure 3G). Let-7 deficiency results in excessive single spectrosome germline cells (GSCs, CBs) and reduced numbers of differentiating cysts (compare Figure 3, F and G), reflective of a delayed early germline differentiation. Altered ECs lacking let-7 likely fail to protect the differentiating germline cysts from the niche signaling. The phenotypes observed imply that let-7 controls somatic ECs behavior, which in turn non-cell-autonomously modulates the efficiency of early ovarian germline differentiation.

In the testes too, let-7 deficiency affects somatic cell behavior. Normally, two squamous cells encapsulate one gonioblast, such that only small clusters of somatic cells (fewer than five cells) marked by a nuclear marker can be detected (Figure 3, H and I). Instead, CySC lineage cells lacking let-7 form large aggregates of >10 cells (Figure 3, I, J, and J′). Interestingly, these clustered cells accumulate the cell adhesion molecule FasIII, indicative of a columnar epithelium that resembles the

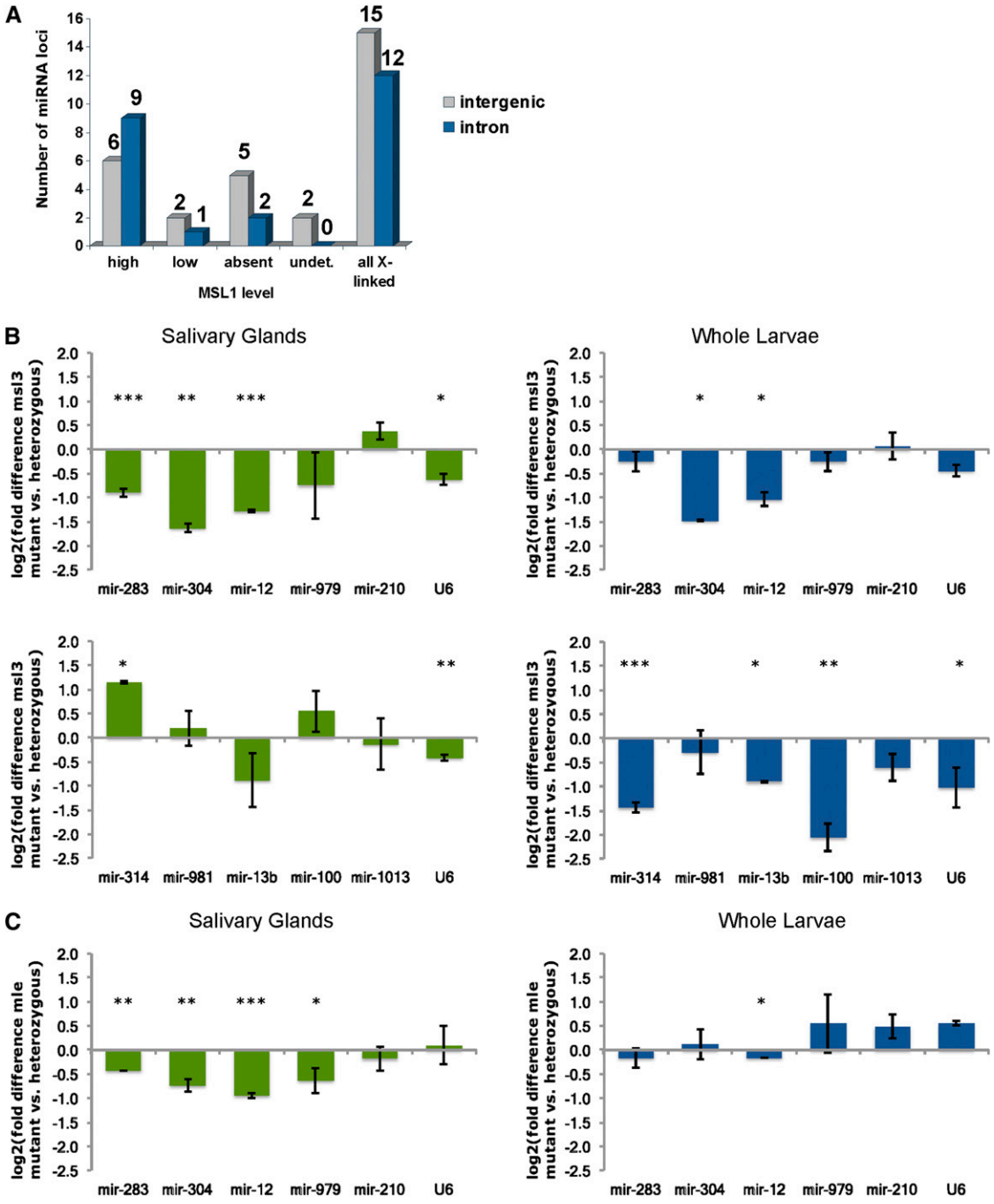

Figure 2 Effects of dosage compensation on X-linked miRNAs expression. (A) Compensasome association at the 27 X-linked miRNA loci vary, with 15 miRNAs located in regions highly populated by compensasomes (high), three miRNAs with low MSL coverage and seven miRNAs residing in regions deprived of compensasomes. Two miRNAs loci in regions not covered by the arrays (undet.) could not be assessed. We observe no difference in MSL occupancy for miRNAs residing in intronic or intergenic regions. The level of expression of miRNAs in the absence of a functional dosage-compensation complex was examined in male salivary glands (green charts) and whole larvae (blue charts) mutant for *msl3* (B) or *mle* (C). Of the six X-linked miRNAs expressed in these tissues, mir-304, mir-12, and mir-13b show the expected twofold decrease in all mutant samples compared to controls. MiRNA levels remain unchanged, however, for X-linked mir-979, mir-210, or mir-283. Autosomal mir-981, mir-100, or mir-1013 levels did not change. Mir-314 levels increase in *msl3* mutant salivary glands and decrease in whole larvae. All miRNAs were tested in triplicates on two independent biological replicates. Values were normalized to the autosomal gene standard, *Dspt4*, whose levels remain unchanged between males, females, or compensasome mutants (Chiang and Kurnit 2003). We observe similar trends between male and female salivary glands miRNAs in wild-type Oregon-R and *msl3* heterozygous mutant controls for all 10 miRNAs tested (mir-100, mir-979, mir-12, mir-314, mir-981, mir-210, mir-1013, mir-283, mir-13b, mir-304). Error bars represent standard deviations. *P*-values: (*) $P < 0.05$; (**) $P < 0.005$; (***) $P < 0.0005$. Calculations are provided in Table S11, Table S12, Table S13, Table S14, Table S15, and Table S16.

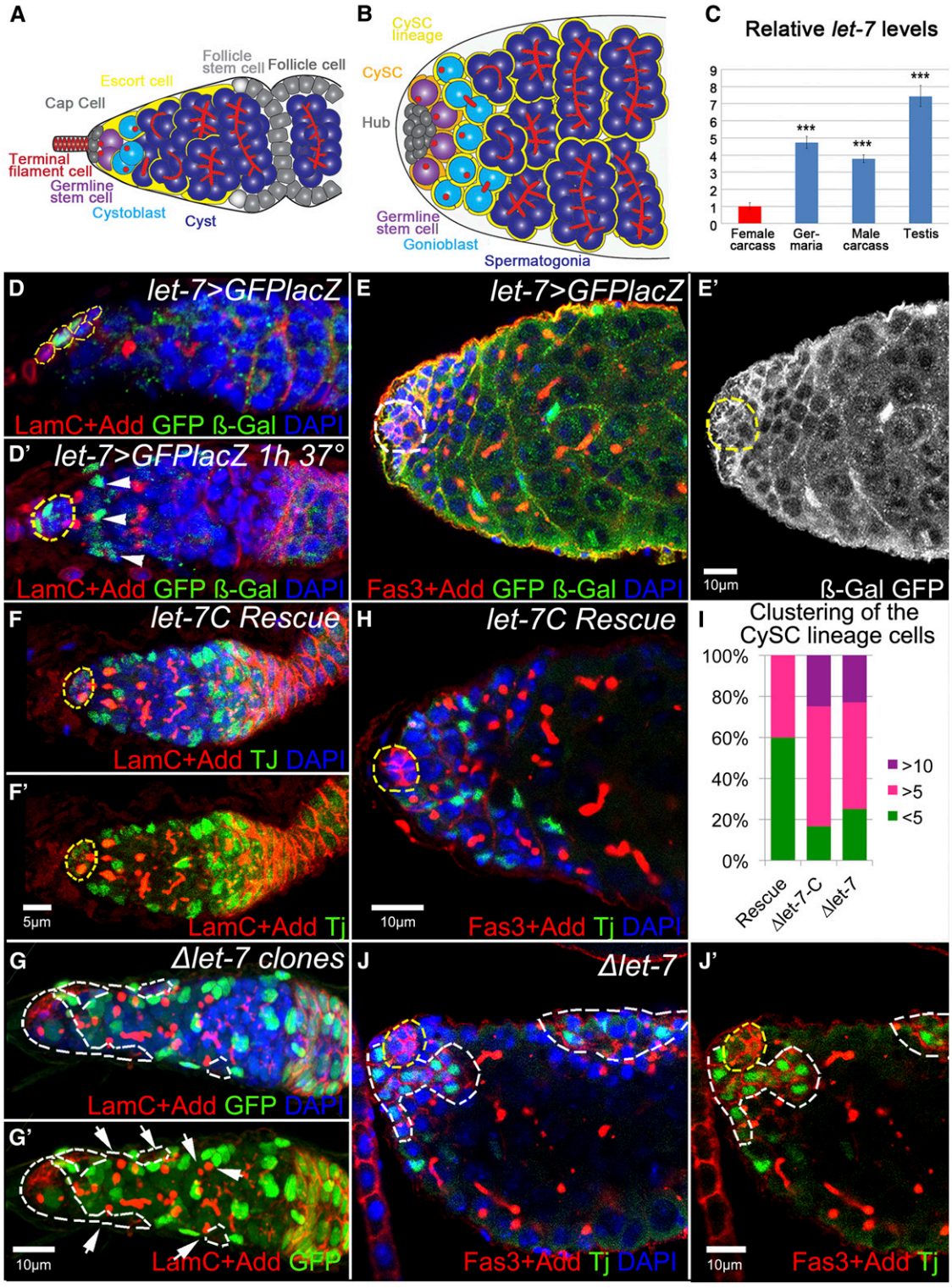

Figure 3 let-7 deficiency affects somatic cells behavior in ovaries and testes, which cell-non-autonomously influences early germline differentiation. *Drosophila* ovaries and testes present commonalities in their general organization and the type of cells they comprise (Fuller and Spradling 2007). The ovary is a paired organ consisting of 16–20 ovarioles, each representing a string of progressively developing egg chambers. (A) At the apex of an ovariole, the germarium comprises somatic cells (terminal filament, TF; cap cells, CpC's; escort cells, ECs; follicle stem cells, FSCs; follicle cells, FCs) and germline cells (germline stem cells, GSCs; cystoblast, CB; differentiating cyst, Cyst). GSCs are physically attached to the somatic cluster of cap cells that, with the terminal filament cells, represent the GSC niche. GSCs divide into a differentiating cystoblast, which then divides four times with incomplete cytokinesis, producing a 16-cell cyst in which 1 cell becomes the oocyte while the others develop as nurse cells. These different germline cell populations can be easily identified by their location and specific markers in the germarium. For example, *Drosophila* adducin homolog antibody marks an actin-rich cellular organelle represented as a dot-like structure in single

ovarian follicular epithelium. Such aggregates do not develop in let-7-C rescue flies (Figure 3, H and I).

Let-7 levels are important to specify male and female sexual identify

Let-7 levels fluctuate at each developmental transition of the fly, including a major pulse in late pupae. During development, let-7 miRNA first appears in L3 larvae and has been detected in genital discs of L3 male and female larvae (Sokol *et al.* 2008). Dsx levels vary as well during development and are especially important from the L3 larval to the late pupal stages to transform genital discs into adult genital and anal structures. To ask whether let-7 influences the transformation of these structures, we expressed *UAS–let-7-C* in patterns that mimic pulses of the major controller of the sex-determination hierarchy DSX using the *dsx–Gal4* driver. Animals overexpressing let-7-C in *dsx*-expressing cells develop severe phenotypes: males and females fail to develop segments A8–A10 and lack a terminalia (analia and genitalia) (Figure 4B). Overexpressing individual miRNAs from the cluster alters the same segments (Figure 4, B and C): females overexpressing mir-125 form additional vaginal teeth, up to a full second row of teeth, and a vulva overgrowth. Additional vaginal teeth appear toward the posterior part of the vulva in females overexpressing let-7. Males overexpressing let-7 show an overgrowth of the genital ring/arch. In males overexpressing mir-125, this structure proliferates yet collapses into a more compact bulged ring (Figure 4, B and C). In addition, overexpressing let-7 or mir-125 in *dsx*-expressing cells results in the overall reduction of the male external genital structures. Importantly, the external terminalia of males and females lacking let-7 present similar defects (Figure 4C). Finally, in animals overexpressing mir-125, the typical female abdominal pigmentation darkens in the posterior stripes of segments A3–A5 and in the terminal A6 and A7 segments where it widens (Figure 4B). Females overexpressing the whole let-7-C cluster show a similar increase in pigment, but not those overexpressing let-7 alone, pointing at mir-125 as the miRNA responsible for the pigment defects. Controls expressing *UAS–NLS–GFP* or *UAS–mir-100* constructs do not present such phenotypes. Together, these results suggest that the ectopic expression of let-7-C, let-7, or mir-125 in *dsx*-expressing cells represses gene(s) necessary for pigmentation in most abdominal segments and importantly, gene(s) critical for the formation of the highly dimorphic segments A8–A10 in both sexes. The transformation of the genital disc into a male or female adult terminalia and the sexually dimorphic pigmentation pathway are both orchestrated by DSX during the pupal stages. It is likely that the respective timing and levels of expression of let-7-C miRNAs and *dsx* at this stage are important. None of the miRNAs in the let-7-C cluster, however, are predicted to target the *dsx* transcripts, suggesting that the phenotypes reflecting alterations of the levels of DSX or of the genes it acts with are generated upstream or in parallel to DSX action rather than from a direct interaction.

To test whether sex determination is affected by let-7, we quantified in animals lacking let-7 the male- (dsx^M) and female-specific transcripts (*Sxl*, *tra*) of the sex-determination hierarchy and DSX downstream target Yp1 (Figure 5, A and B). In *let-7* mutant females, the levels of *Sxl* and *tra* remain unchanged but *Yp1* mRNA levels are significantly lower. The background levels of dsx^M remain stable in females lacking let-7, implying that the levels of the direct activator of Yp1,

cells (GSCs and CBs) and as a branched fusome in the developing cysts. There is another class of somatic cells at the anterior of the germarium, called the escort cells. These squamous cells are mitotically quiescent and envelop differentiating cysts to protect them from niche signaling, an important role for germline differentiation (Chen *et al.* 2011). ECs guide differentiating cysts to the posterior end of the germarium, where the germline becomes encapsulated by the follicular epithelium and pinched off from the germarium. (B) The *Drosophila* testes are a paired tubular organ that consists of somatic and germline cells. Scheme depicting the testis apex somatic cells (hub cells, Hub; cyst stem cells, CySC's; cyst stem cells lineage, CySC lineage) and germline cells (germline stem cells, GSCs; gonioblast, GB; differentiating spermatocysts and spermatogonia). Attached to the stem cell niche, termed the hub, reside two types of stem cells: GSCs and CySC's. While the hub is made by a cluster of postmitotic somatic cells, both stem cell types divide in synchrony to produce differentiating germline cysts, each of which is encapsulated by two somatic CySC's lineage cells. This encapsulation is critical for proper germline differentiation (Leatherman and Dinardo 2010). Similar to the ovarian GSC progeny, the germline gonioblast undergoes four rounds of incomplete cytokinesis to produce 16 primary spermatocytes in a cyst, eventually generating 64 sperm cells. (C) The relative expression levels of miRNA let-7 in female and male carcasses, ovaries, and testes show that let-7 miRNA is sex biased and expressed at the higher levels in testes (see also Table S17). (D, D′, E, E′) Localization of let-7-C miRNAs in the ovaries and testes, detected via membrane *GFP* and nuclear *lacZ* expressed under the control of the *let-7-C* promoter (*let-7-C^{GK1}–Gal4/UAS–CD8-GFP::nuc–lacZ*). In the ovary, *let-7-C* is expressed in the somatic cells of the germarium, CpCs and ECs (D). (D′) More ECs express let-7-C, shown by the presence of lacZ (β-Gal, green) when adult flies were subject to a heat shock for 1 hr prior to dissection. (E and E′) In the testis, *let-7-C* is broadly expressed in all somatic cells, CySC's and their lineage and the hub cells (*let-7-C^{GK1}-Gal4/UAS-CD8-GFP::nuc-lacZ*). (F and F′) Control *let-7-C* rescue germaria (*P{W8, let-7-C}/+; let-7-C$^{GK1/KO1}$*) show typical numbers of germline SSCs and developing cysts (marked by the spectrosome and fusome marker Adducin, Add, red) as well as somatic ECs (marked by Traffic jam, Tj, green). The GSC niche (marked by Lamin C, LamC, red) is outlined by yellow dashed lines. (G and G′) Somatic cell Δ*let-7* clones (*Ubi–GFP, FRT40A/ FRT40A, let-7 miR-125; bab1–Gal4, UAS–Flp/P{W8, let-7-C$^{\Delta let-7}$}*) are marked by the absence of GFP and outlined by white dashed lines. Upon let-7 depletion in the soma of the germarium, the number of somatic ECs and germline SSCs increases, while the number of fusome-containing cysts decreases. The magnification is the same in F and G. (H) The testicular apex of a control let-7-C rescue (*P{W8, let-7-C}; let-7-C$^{GK1/KO1}$*) displays typical numbers of germline CBs and cysts (marked by spectrosome and fusome marker Add, red) and the CySC lineage cells (marked by Tj, green); yellow dashed lines outline the hub (marked by Fasciclin III, Fas3, red). (J) In Δ*let-7* mutant testis (*let-7-C$^{GK1/KO1}$; P{W8, let-7-C$^{\Delta let-7}$}/+*) the CySC lineage cells cluster in larger groups and express the ovarian follicular epithelium marker, Fas3. These clusters (outlined by white dashed lines) can be found at the apex or the side of the testicular tube. (I) Percentages of mutant testes containing large ≥5 or >10 somatic cell clusters in comparison to control let-7-C Rescue. Ten to 20 testes were analyzed for each genotype. Red: LamC + Add in D, D′, F, F′, G, G′ ; Fas3 + Add in E, H, J, J′. Green: GFP + β-Gal in D and E; GFP in G, G′; Tj in F, F′, H, J, J′. White: GFP + β-Gal in E′. Blue: DAPI in D–H, G–J′. D, E + E′, H, J + J′ are single confocal sections while D′, F + F′, and G + G′ are projections of several z-stacks.

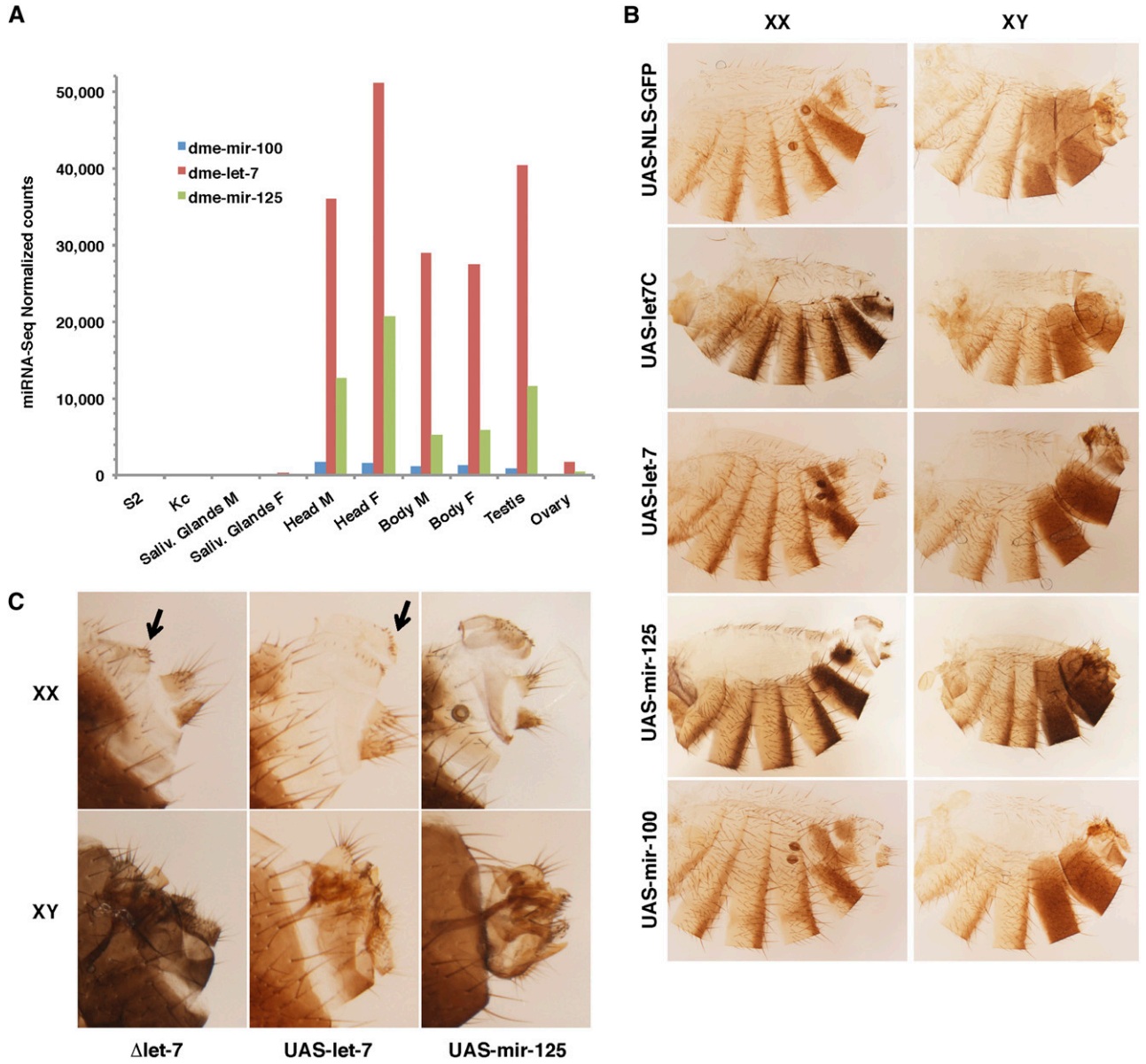

Figure 4 Let-7-C miRNAs abundance across tissues and overexpression. (A) The three miRNAs of the let-7-C locus are almost undetectable in salivary glands and lymphoid cells and highly expressed in male and female heads and body. All let-7-C miRNAs are highly expressed in testes compared to ovaries. Let-7 is consistently more abundant than mir-125 in all tissues expressing let-7-C, while mir-100 remain comparably low. (B) Cuticle preparations of *dsx–Gal4 > UAS–let-7-C* males (XY) and females (XX): both fail to transform A8–A10 segments into a proper genitalia and analia. Increased abdominal pigmentation in let-7-C and mir-125 overexpressing flies (compare *UAS–let-7-C* or *UAS–mir-125* to *UAS–NLS–GFP*). (B and C) Terminalia phenotypes of flies overexpressing single miRNAs of the locus: additional vaginal teeth toward the posterior section of the vulva in *dsx–Gal4 > UAS–let-7* females, similar to *Δlet7* flies (arrows in closeups in C); additional row of vaginal teeth and overgrowth of the anterior vulva in *dsx–Gal4 > UAS–mir-125* females; overgrowth of the genital ring/arch *dsx–Gal4 > UAS–let-7* male genitalia; *dsx–Gal4 > UAS–mir-125* male genital ring collapses into a more compact bulged ring (lateral view in C). Note the reduced size of male external genital and anal structures in *UAS–let-7*, *UAS–mir-125*, and *Δlet7* males. *Dsx–Gal4> UAS–NLS–GFP*, and *dsx–Gal4 > UAS–mir-100* males and females appear normal.

DSX^F, but not its repressor DSX^M, are compromised. A general depletion of let-7 during development generates more dramatic effects in males. Specifically, males deficient for let-7 present a spurious expression of two genes normally restricted to females, *Sxl* and *Yp1*. Altogether these results point at a role of let-7 in modulating the sex-determination cascade during development, at least during the late-larval to late-pupal stages.

Ecdysone signaling via let-7 maintains sexual identity during adulthood

We attempted to determine what signaling pathway acts upstream of let-7 in the process of sexual identity establishment but also its maintenance. Hormonal signaling is a strong candidate for this type of regulation, since it may coordinate the sex-specific differentiation of different tissues in the whole organism. The ecdysteroid signaling cascade governs various

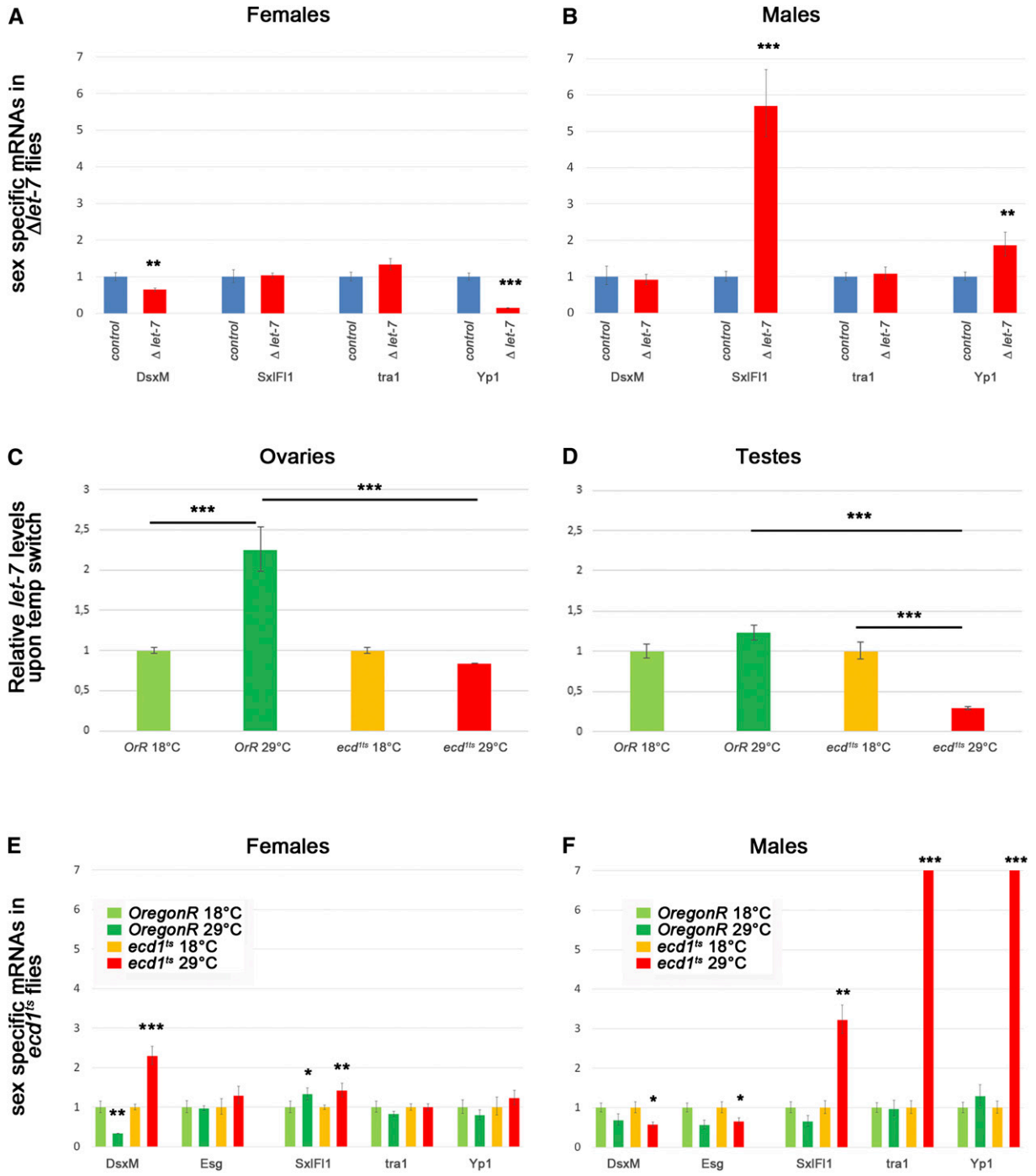

Figure 5 Levels of sex-specific mRNAs are altered due to loss of function of steroid-dependent miRNA let-7 and ecdysone deficiency. (A and B) Relative levels of sex-specific mRNAs in *Δlet-7* mutant *(let-7-C$^{GK1/KO1}$*; *P{W8, let-7-C$^{Δlet-7}$}/+*) and control rescue *(P{W8, let-7-C}/+*; *let-7-C$^{GK1/KO1}$)* females (A) and males (B). (C and D) Relative levels of let-7 miRNA expression in wild-type (Oregon-R) and *ecd^{1ts}* mutants kept at permissive (18°) and restrictive (29°) temperatures measured in the anterior parts of ovaries (C) and testes (D). (E and F) Relative levels of sex-specific mRNAs in wild-type (Oregon-R) and *ecd^{1ts}* females (E) and males (F) kept at permissive (18°) and restrictive (29°) temperatures. Samples at restrictive temperature were compared to the respective genotype and sex at permissive temperature. Error bars represent the range of mRNA levels; *P*-values are calculated by Student *t*-test: (*) $P < 0.05$, (**) $P < 0.005$, (***) $P < 0.0005$. See also Table S18, Table S19, and Table S20.

biological responses during *Drosophila* lifetime. Its specificity depends on the differential spatiotemporal expression of downstream components specific to various cell types and developmental stages. Steroid-coupled regulation of let-7 expression takes place during the developmental transition from larval-to-reproductive animals (Sempere *et al.* 2002, 2003; Garbuzov and Tatar 2010; Chawla and Sokol 2012; Kucherenko *et al.* 2012). During this period, DSX most actively controls the

transformation of the A8–A10 genital primordia into dimorphic male and female terminal structures. In addition, we and others have reported that a deficit in ecdysone signaling generates non-cell-autonomous defects in early female germline differentiation (König *et al.* 2011; Morris and Spradling 2012). These defects resemble the *let-7* loss-of-function defects described here in ovaries. Moreover, we report similar germline differentiation defects in *let-7* mutant testes. Together, the steroid-dependent onset of let-7 expression during development and the similarity of the germline phenotypes observed in adult males and females lacking let-7 converge toward a model in which ecdysone signaling acts upstream of the let-7 miRNA to modulate (i) sex determination in tissues and (ii) germ-cell differentiation via the gonadal soma.

Whether let-7 also depends on ecdysone signaling in adults has not been addressed previously. To address this, we took advantage of a temperature-sensitive *ecdysoneless* mutation, ecd^{1ts}, that blocks the production of ecdysone at restrictive temperature (29°) (Garen *et al.* 1977). After impairing ecdysone signaling specifically in adults, we analyzed let-7 levels in germaria and testes of Oregon-R and ecd^{1ts} flies. Shifting Oregon-R male and female adults to 29° results in increased let-7 levels, showing that let-7 expression is dependent on temperature (Figure 5, C and D). Enhanced activity of the let-7-C promoter is also visible at the cellular level in the ovarian CpC's and ECs upon heat shock (Figure 3D′). Contrary to wild-type flies, let-7 levels drop at the restrictive temperature in ecd^{1ts} mutant female and more significantly in male gonads, demonstrating that let-7 expression depends on ecdysone signaling in the adult germaria and testes (Figure 5, C and D).

While the signaling cascade that establishes sexual identity has been studied extensively, the question of whether certain cues are needed to actively maintain sexual identity throughout the adult life has not been addressed. We quantified the expression of female- and male-specific components of the sex-determination hierarchy 3 days after inducing an ecdysone deficit in mature adults. Females lacking ecdysone begin to express the male-specific isoform of *dsx*, dsx^{M} (Figure 5E). In males lacking ecdysone, conversely, male-specific mRNA levels of dsx^{M} and *escargot* (*esg*) fall significantly while the female *Sxl*, *tra*, and *Yp1* transcripts undergo a dramatic burst in expression (Figure 5F). Because *Sxl* and *tra* become aberrantly produced in males, and both are required to produce the female-specific isoform of *dsx*, it is likely that *Yp1* hyperactivation in males is a consequence of the production of DSX^{F} when ecdysone signaling is disrupted.

Together, our data support the hypothesis that ecdysone is required to maintain the sexual fate of adult cells. Interestingly, ecdysone effect on sex-specific mRNAs expression is significantly stronger than that of let-7 alone (compare Figure 5, A, B, E, and F), indicating that this systemic hormonal signaling regulates in addition to let-7 other key players in the maintenance of sexual identity during adulthood. Critically, these data suggest that ecdysone signaling plays an essential role in the maintenance of sexual identity in the adult *Drosophila*, primarily in males, and that this function is mediated at least in part by let-7 miRNA.

Ecdysone signaling via let-7 maintains male cell fate of the testicular soma during adulthood

Ecdysone-deficient (ecd^{1ts}) males have reduced fertility and most become completely sterile after 3 days at restrictive temperature (Garen *et al.* 1977). At the tissue level, ecdysone signaling appears important to maintaining the proper behavior and function of the somatic CySC's lineage in the adult testis (Figure 6, A–C). In adult males subject to ecdysone deficiency, the CySC's lineage overproliferates, expresses epithelial markers, and non-cell-autonomously affects germline differentiation. Massive clusters of somatic cells appear at the testis apex, forming occasionally epithelial-like sheaths surrounding the testicular tube (Figure 6, B and C). The appearance of aggregates coincides with defects in germline differentiation at two levels. First, somatic cells clustering at the apex displace germline stem cells from the hub, forcing their premature differentiation (Figure 6B′). Second, somatic cells accumulating in lateral sheaths further disrupt their progression through germline differentiation programs (Figure 6C′). Flies deprived of ecdysone for a longer period show more severe phenotypes (Figure 6, D and E). Still, these alterations remain partial sex transformations. We never observed a full transformation resulting in the production of sperm or egg in mutants of the opposite sex. These findings suggest that sustained steroid activity is required to maintain let-7 levels within testicular somatic cells.

Taken together, our analyses show that steroid signaling is involved in the maintenance of sexual identity in adult flies and in the maintenance of germline differentiation programs in the gonads. This hormonal signal engages miRNAs to execute this regulation in a gender-specific manner. Therefore the maintenance of sexual identity in the adult life requires a systemic signaling that strongly depends on the general state of the organism and external conditions. This type of regulation is common in higher vertebrates including humans, implying that the analysis of sex-biased miRNAs and their targets will be of great importance to better understanding of sexual identity safeguarding throughout life at the cellular level in different organisms.

Evidence supporting the existence of a long-range gonadal axis in flies has emerged recently. Ecdysone is metabolized in the fat body in both sexes and is also present exclusively in the female germline late follicles. As a result, ecdysone titers are higher in females (Bownes *et al.* 1983; Parisi *et al.* 2010). Germline ablation largely decreases ecdysone titers and affects sex-biased somatic genes, including ecdysone biosynthesis genes exclusively in females (Parisi *et al.* 2004, 2010). In fact, half of the sex-biased genes in the female soma are estimated to be germline-dependent genes that respond to ecdysone, the other half comprising germline-independent sex-biased genes regulated by the sex-determination hierarchy. The absence of germline, however, does not affect somatic expression of the canonical

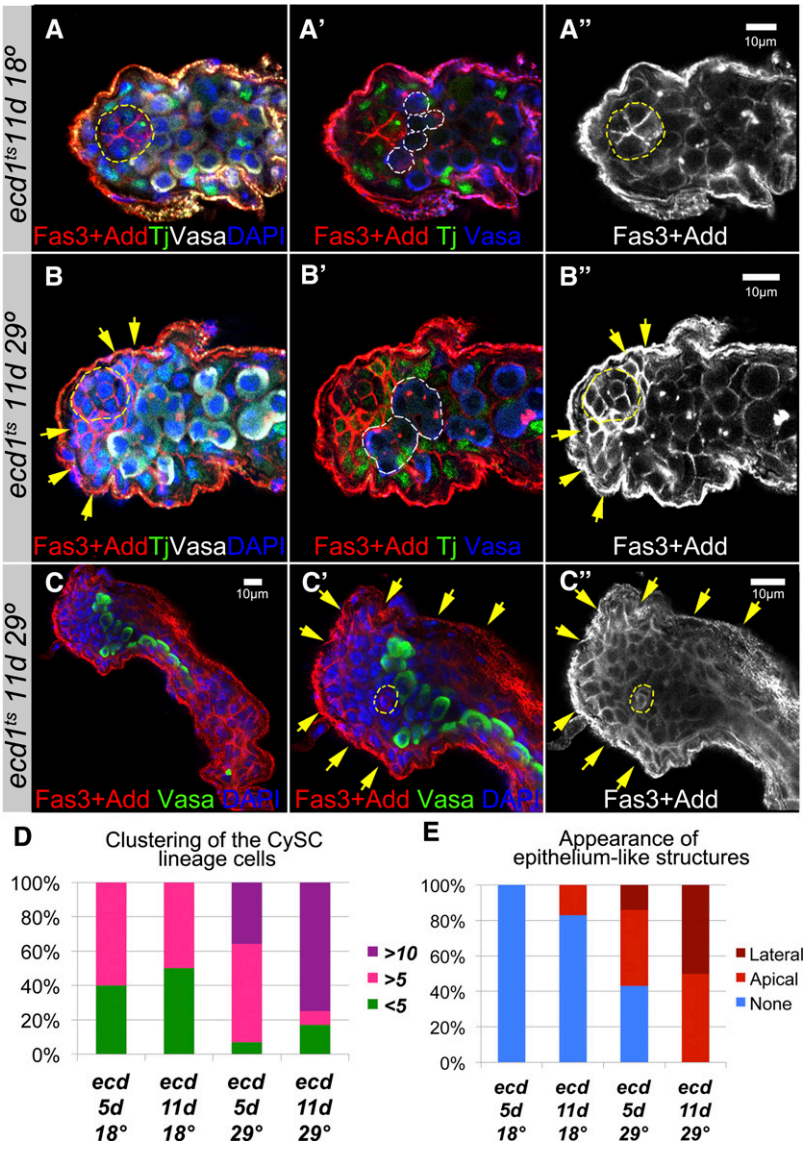

Figure 6 Ecdysone signaling controls testicular soma behavior and function. (A) In control (*ecd*^{1ts}, 11 days at 18°), the hub (outlined in yellow, A, A′′) is surrounded by proportional numbers of CySC's and GSCs (outlined in white, A′). (B and C) In mutants (*ecd*^{1ts}, 11 days at 29°), somatic cells aggregate in large epithelium-like clusters next to the hub (yellow arrows, B, B′′). In contrast, GSCs that would be seen as germline cells with a single spectrosome are no longer attached to the hub, indicating that they were pushed away from the niche and their differentiation was induced. Differentiating cysts are outlined in white, B′. Sometimes these abnormal epithelial-like sheets are found around the whole testicular tube (yellow arrows, C′, C′′), affecting germline differentiation: differentiating cysts that would be marked by branched fusomes are not seen. Note that the aberrant somatic cells express the Fas3 marker of hub cells and ovarian follicular epithelium. (D and E) The frequency of testes displaying clustering of the CySC lineage cells (D) and the appearance of epithelium sheets (E) increase with the time flies were deprived of ecdysone (5 or 11 days). See also Table S21. Red: Fas3 + Add in A, A′, B, B′, C, C′. White: Vasa in A, B; Fas3 + Add in A′′, B′′, C′′. Green: Tj in A, A′, B, B′; Vasa in C, C′. Blue: DAPI in A, B, C; Vasa in A′, B′, C′. All pictures are single confocal sections.

sex-determination genes in either sex. Our study shows that sex-determination gene expression depends largely on ecdysone-mediated let-7 signaling in the soma, primarily in males. The pronounced effects on *dsx* and *Sxl* in males suggest that ecdysone and let-7 constitute the system that supports the expression of somatic sex-biased genes in males.

The effects of let-7 depletion on Yp1 and, importantly, the influence of ecdysone signaling on the sex-determination hierarchy in males raise the possibility that, although more weakly, all sex-biased genes eventually depend on hormones in females as well. If true, their sex-biased expression would result from two pathways regulated by ecdysone: a germline-dependent influence of ecdysone known as the gonadal sex hormone axis and a second pathway regulated by the sex-determination hierarchy that is germline independent but, as shown here, influenced mildly by hormones and let-7. Supporting this view, females require ecdysone receptor (EcR) expression in FRU expressing neurons to modulate precopulatory behavior just like males (see below), and ecdysone deficient females present male behaviors (Dalton *et al.* 2009; Ganter *et al.* 2012).

Intrinsic sex-specific specific factors and the proper sexual identity of the fat body are important for courtship behavior orchestrated by DSX and FRU in the brain, suggesting a fine interplay between signaling from the fat body and the sex-specific regulation of the nervous system (Lazareva *et al.* 2007; Camara *et al.* 2008). In particular, the EcR-A isoform that may interact with let-7 signaling is required in the FRU^{M} neural circuit for male courtship behavior (Sanders and Arbeitman 2008; Dalton *et al.* 2009).

FRU^{M} and DSX establish neural circuits differentially in each sex at mid-metamorphosis, a time at which they show strongest expression. Let-7 pulses could affect the FRU and DSX branches of the sex-determination hierarchy in the neural circuitry during this period. Let-7 may well contribute to a feedback loop in the nervous system since FRU targets include a preponderance of genes regulated by the steroid

hormone ecdysone (Dalton *et al.* 2009, 2013; Neville *et al.* 2014). However, the reported FRU^M and DSX binding sites in Luo *et al.* (2011) do not include the let-7-C locus, suggesting an indirect interaction.

In addition to ecdysone titers, let-7 levels and its mode of action are particularly important to understanding the impact of hormones in each sex and how they may regulate sex determination. Let-7 expression is dependent on ecdysteroids in both male and female adult gonads; however, ecdysone signaling facilitates cell gender maintenance in the organism via let-7 primarily in males, suggesting that let-7 response to ecdysone signaling and/or its effectors differ between the sexes. During metamorphosis, let-7 is induced by ecdysone signaling to control the timing of neuronal differentiation by way of BTB transcription factors. Two of them, Abrupt and Chinmo, act as negative regulators of ecdysone signaling, therefore creating a feedback loop (Zhu *et al.* 2006; Wu *et al.* 2012). By targetting repressors, let-7 finely modulates and reinforces steroid hormone signaling pulses in the brain. Interestingly, Abrupt modulates ecdysone signaling in the ovary as well (Jang *et al.* 2009). Increasing ecdysone titers established during oocyte development coincide with the gradual decrease of Abrupt concentration in the ovary. When ecdysone signaling is very high, Abrupt fails to bind the EcR coactivator Taiman, resulting in ecdysone signaling block. Whether let-7 controls Abrupt in the gonads and contributes to reinforcing ecdysone signaling via a feedback loop has not been studied. Nonetheless, naturally low levels of let-7 in the ovary where ecdsyone levels are plenty, contrary to testes, allows *let-7* to generate in the germarium soma a sharper threshold response to the systemic signaling only when ecdysone titers are high (A. Konig and H. Shcherbata, unpublished results). In turn, because ecdysone and let-7-deficient phenotypes are just as strong in male and female gonads, higher levels of let-7 seem required to respond to lower ecdysone titers in males.

The two *bona fide* targets of let-7 in the brain present intriguing parallels in the gonads. Under the control of ecdysone, Chinmo and Abrupt control the differentiation of the gonadal soma specifically in one sex: Abrupt acts in the germarium and Chinmo in testis (Jang *et al.* 2009; Flaherty *et al.* 2010). Both are effectors of the JAK/STAT pathway, known to act differently in male and female gonads (Decotto and Spradling 2005). As examplified by the JAK/STAT pathway in the gonads, sex-specific transcription factors controlled by differential levels of let-7 may respond differently to ecdysone signaling and lead to sex-specific functions. This may hold true in the brain where Chinmo is a direct target of Fru^M in males (Neville *et al.* 2014).

Another important aspect of our findings is the temporal character of ecdysone-let-7 involvement in the gonadal soma. It has been shown previously that there are differential requirements for the miRNA pathway in preadult and adult stages for the maintenance of germline stem cells (Shcherbata *et al.* 2007). In addition, augmentation of JAK/STAT signaling via let-7 miRNA in the testicular stem cell niche is essential for male germline stem cell preservation in aging flies (Toledano *et al.* 2012).

The temporal ecdysteroid–let-7 signaling cascade also cooperates with the JAK/STAT cytokine pathway in neuronal cell fate determination (Kucherenko and Shcherbata 2013). One possibility is that the ecdysteroid–let-7 effect on somatic gender identity also has a temporal character and incorporates JAK/STAT cytokine signaling to control sex determination in the somatic cells.

Interestingly, one of the JAK/STAT pathway ligands, Unpaired (*Upd*), is an X-linked signal element gene that affects *Sxl* expression (Sefton *et al.* 2000). Upd is a genuine target of miR-279 that regulates circadian rhythms (Luo and Sehgal 2012). Knockdown of *Upd* rescues the behavioral phenotype of *miR-279* mutants. Further studies of the ecdysone–miRNA-JAK/STAT signaling cascade will determine upstream and downstream components sustaining cellular sexual identity during the postembryonic stages, adulthood, and aging.

Finally, the significant upregulation of *Sxl* in both wild-type and ecd^{1ts} females upon temperature shift (Figure 5E) indicates that *Sxl* expression is temperature dependent in flies and also modulated by ecdysteroid hormones. This provides a direct role for hormones in regulating sex determination in females. Clearly our understanding of this unprecedented complexity of sex determination requires both temporal and cell-specific examinations of the interplay between miRNAs, steroid hormones, and sex determination.

These results comprehensively demonstrate an important role for miRNAs as regulators of sexual dimorphism and identify several sets of candidate miRNAs to achieve differential functions in each sex. The function of let-7 provides a proof of concept of the importance of sex-biased miRNA expression in the developing and aging adult gonad and reproductive apparatus. In mammals, sex hormones produced in the gonads coordinate gene expression in distant tissues and organs. The existence of a similar hormonal axis in *Drosophila* has remained elusive. We show here for the first time that ecdysone signaling controls sex-determination genes in flies, via the miRNA let-7. Misregulation of let-7 in mammals has been shown to impair differentiation and leads to the development of diseases including cancer. Let-7 appears as a master regulator of the cell-proliferation pathways altered in lung, breast, colon, and prostate cancer (Takamizawa 2004; Johnson *et al.* 2007; Trang *et al.* 2009; reviewed in Lo *et al.* 2013). Notably, such cancer cells present unusually low levels of let-7. In addition, connections between let-7 and hormone signaling have been established in mammals. Let-7c plays an important role in the regulation of androgen signaling in castration-resistant prostate cancers, acting by downregulation of the androgen receptor. In turn, androgen signaling further increases cellular levels of miR-125b (Shi *et al.* 2007), suggesting that both mir-125 and let-7 respond to hormonal imbalances. Whether sex determination is affected in these contexts will require future studies.

We provide an extensive repertoire of sex-biased and gender neutral miRNAs that will help address the varied

functions of miRNA activity across development and aging, as well as in the context of human diseases.

Acknowledgments

We thank Laura Johnston, Nicholas Sokol, Frank Hirth, Ralf Pflanz, Bruce Baker, Carmen Robinett, Acaimo Gonzalez-Reyes, the Bloomington Stock Center for providing flies and reagents, and Mark Siegal for advice on cuticle preparations. We thank all members of the Hannon lab, Ilaria Falciatori, the Department of Herbert Jäckle and the Shcherbata Lab for helpful discussions, the two reviewers and Alexander Vaughan for providing constructive comments that helped improve this manuscript. This work was supported by grants from the National Institutes of Health, a kind gift from Kathryn W. Davis to G.J.H., and by the Max Planck Society to A.K. and H.R.S.

Literature Cited

Alekseyenko, A. A., E. Larschan, W. R. Lai, P. J. Park, and M. I. Kuroda, 2006 High-resolution ChIP-chip analysis reveals that the Drosophila MSL complex selectively identifies active genes on the male X chromosome. Genes Dev. 20: 848–857.

Alekseyenko, A. A., J. W. K. Ho, S. Peng, M. Gelbart, M. Y. Tolstorukov *et al.*, 2012 Sequence-specific targeting of dosage compensation in Drosophila favors an active chromatin context. PLoS Genet. 8: e1002646.

Ambros, V., 2011 MicroRNAs and developmental timing. Curr. Opin. Genet. Dev. 21: 511–517.

Ambros, V., and X. Chen, 2007 The regulation of genes and genomes by small RNAs. Development 134: 1635–1641.

Aravin, A. A., M. Lagos-Quintana, A. Yalcin, M. Zavolan, D. Marks *et al.*, 2003 The small RNA profile during *Drosophila melanogaster* development. Dev. Cell 5: 337–350.

Arbeitman, M. N., E. E. M. Furlong, F. Imam, E. Johnson, B. H. Null *et al.*, 2002 Gene expression during the life cycle of *Drosophila melanogaster*. Science 297: 2270–2275.

Baker, B. S., and K. A. Ridge, 1980 Sex and the single cell. I. On the action of major loci affecting sex determination in *Drosophila melanogaster*. Genetics 94: 383–423.

Baker, B. S., K. Burtis, T. Goralski, W. Mattox, and R. Nagoshi, 1989 Molecular genetic aspects of sex determination in *Drosophila melanogaster*. Genome 31: 638–645.

Baley, J., and J. Li, 2012 MicroRNAs and ovarian function. J. Ovarian Res.

Bartel, D. P., 2009 MicroRNAs: target recognition and regulatory functions. Cell 136: 215–233.

Bashaw, G. J., and B. S. Baker, 1997 The regulation of the Drosophila msl-2 gene reveals a function for Sex-lethal in translational control. Cell 89: 789–798.

Bejarano, F., D. Bortolamiol-Becet, Q. Dai, K. Sun, A. Saj *et al.*, 2012 A genome-wide transgenic resource for conditional expression of Drosophila microRNAs. Development 139: 2821–2831.

Belote, J. M., M. B. McKeown, D. J. Andrew, T. N. Scott, M. F. Wolfner *et al.*, 1985 Control of sexual differentiation in *Drosophila melanogaster*. Cold Spring Harb. Symp. Quant. Biol. 50: 605–614.

Belote, J. M., M. McKeown, R. T. Boggs, R. Ohkawa, and B. A. Sosnowski, 1989 Molecular genetics of transformer, a genetic switch controlling sexual differentiation in Drosophila. Dev. Genet. 10: 143–154.

Bownes, M., M. Blair, R. Kozma, and M. Dempster, 1983 20-Hydroxyecdysone stimulates tissue-specific yolk-protein gene transcription in both male and female Drosophila. J. Embryol. Exp. Morphol. 78: 249–268.

Bridges, C. B., 1921 Triploid intersexes in *Drosophila melanogaster*. Science 54: 252–254.

Burtis, K. C., K. T. Coschigano, B. S. Baker, and P. C. Wensink, 1991 The doublesex proteins of *Drosophila melanogaster* bind directly to a sex-specific yolk protein gene enhancer. EMBO J. 10: 2577–2582.

Bushati, N., A. Stark, J. Brennecke, and S. M. Cohen, 2008 Temporal reciprocity of miRNAs and their targets during the maternal-to-zygotic transition in Drosophila. Curr. Biol. 18: 501–506.

Camara, N., C. Whitworth, and M. Van Doren, 2008 The creation of sexual dimorphism in the Drosophila soma. Curr. Top. Dev. Biol. 83: 65–107.

Caygill, E. E., and L. A. Johnston, 2008 Temporal regulation of metamorphic processes in Drosophila by the let-7 and miR-125 heterochronic microRNAs. Curr. Biol. 18: 943–950.

Chatterjee, S. S., L. D. Uppendahl, M. A. Chowdhury, P.-L. Ip, and M. L. Siegal, 2011 The female-specific doublesex isoform regulates pleiotropic transcription factors to pattern genital development in Drosophila. Development 138: 1099–1109.

Chawla, G., and N. S. Sokol, 2012 Hormonal activation of let-7-C microRNAs via EcR is required for adult *Drosophila melanogaster* morphology and function. Development 139: 1788–1797.

Chen, S., S. Wang, and T. Xie, 2011 Restricting self-renewal signals within the stem cell niche: multiple levels of control. Curr. Opin. Genet. Dev. 21: 684–689.

Chiang, P.-W., and D. M. Kurnit, 2003 Study of dosage compensation in Drosophila. Genetics 165: 1167–1181.

Christiansen, A. E., E. L. Keisman, S. M. Ahmad, and B. S. Baker, 2002 Sex comes in from the cold: the integration of sex and pattern. Trends Genet. 18: 510–516.

Chung, W.-J., K. Okamura, R. Martin, and E. C. Lai, 2008 Endogenous RNA interference provides a somatic defense against Drosophila transposons. Curr. Biol. 18: 795–802.

Cline, T. W., 1978 Two closely linked mutations in *Drosophila melanogaster* that are lethal to opposite sexes and interact with daughterless. Genetics 90: 683–698.

Clough, E., and B. Oliver, 2012 Genomics of sex determination in Drosophila. Brief Funct Genomics 11: 387–394.

Czech, B., C. D. Malone, R. Zhou, A. Stark, C. Schlingeheyde *et al.*, 2008 An endogenous small interfering RNA pathway in Drosophila. Nature 453: 798–802.

Dai, Q., P. Smibert, and E. C. Lai, 2012 Exploiting Drosophila genetics to understand microRNA function and regulation. Curr. Top. Dev. Biol. 99: 201–235.

Dalton, J. E., M. S. Lebo, L. E. Sanders, F. Sun, and M. N. Arbeitman, 2009 Ecdysone receptor acts in fruitless: expressing neurons to mediate Drosophila courtship behaviors. Curr. Biol. 19: 1447–1452.

Dalton, J. E., J. M. Fear, S. Knott, B. S. Baker, L. M. McIntyre *et al.*, 2013 Male-specific Fruitless isoforms have different regulatory roles conferred by distinct zinc finger DNA binding domains. BMC Genomics 14: 659.

Decotto, E., and A. C. Spradling, 2005 The Drosophila ovarian and testis stem cell niches: similar somatic stem cells and signals. Dev. Cell 9: 501–510.

Deng, X., J. B. Hiatt, D. K. Nguyen, S. Ercan, D. Sturgill *et al.*, 2011 Evidence for compensatory upregulation of expressed X-linked genes in mammals, *Caenorhabditis elegans* and *Drosophila melanogaster*. Nat. Genet. 43: 1179–1185.

Dillies, M.-A., A. Rau, J. Aubert, C. Hennequet-Antier, M. Jeanmougin *et al.*, 2013 A comprehensive evaluation of normalization methods for Illumina high-throughput RNA sequencing data analysis. Brief. Bioinform. 14: 671–683.

Duncan, K., M. Grskovic, C. Strein, K. Beckmann, R. Niggeweg *et al.*, 2006 Sex-lethal imparts a sex-specific function to UNR by recruiting it to the msl-2 mRNA 3′ UTR: translational repression for dosage compensation. Genes Dev. 20: 368–379.

Fagegaltier, D., and B. S. Baker, 2004 X chromosome sites autonomously recruit the dosage compensation complex in Drosophila males. PLoS Biol. 2: e341.

Flaherty, M. S., P. Salis, C. J. Evans, L. A. Ekas, A. Marouf *et al.*, 2010 chinmo is a functional effector of the JAK/STAT pathway that regulates eye development, tumor formation, and stem cell self-renewal in Drosophila. Dev. Cell 18: 556–568.

Fuller, M. T., and A. C. Spradling, 2007 Male and female Drosophila germline stem cells: two versions of immortality. Science 316: 402–404.

Ganter, G. K., J. B. Desilets, J. A. Davis-Knowlton, A. E. Panaitiu, M. Sweezy *et al.*, 2012 Drosophila female precopulatory behavior is modulated by ecdysteroids. J. Insect Physiol. 58: 413–419.

Garbuzov, A., and M. Tatar, 2010 Hormonal regulation of Drosophila microRNA let-7 and miR-125 that target innate immunity. Fly 4: 306–311.

Garen, A., L. Kauvar, and J. A. Lepesant, 1977 Roles of ecdysone in Drosophila development. Proc. Natl. Acad. Sci. USA 74: 5099–5103.

Giraldez, A. J., Y. Mishima, J. Rihel, R. J. Grocock, S. Van Dongen *et al.*, 2006 Zebrafish MiR-430 promotes deadenylation and clearance of maternal mRNAs. Science 312: 75–79.

Hempel, L. U., and B. Oliver, 2007 Sex-specific DoublesexM expression in subsets of Drosophila somatic gonad cells. BMC Dev. Biol. 7: 113.

Hildreth, P. E., 1965 Doublesex, recessive gene that transforms both males and females of Drosophila into intersexes. Genetics 51: 659–678.

Jang, A. C.-C., Y.-C. Chang, J. Bai, and D. Montell, 2009 Border-cell migration requires integration of spatial and temporal signals by the BTB protein Abrupt. Nat. Cell Biol. 11: 569–579.

Johnson, C. D., A. Esquela-Kerscher, G. Stefani, M. Byrom, K. Kelnar *et al.*, 2007 The let-7 microRNA represses cell proliferation pathways in human cells. Cancer Res. 67: 7713–7722.

Kato, M., A. de Lencastre, Z. Pincus, and F. J. Slack, 2009 Dynamic expression of small non-coding RNAs, including novel microRNAs and piRNAs/21U-RNAs, during *Caenorhabditis elegans* development. Genome Biol. 10: R54.

Kerman, B. E., A. M. Cheshire, and D. J. Andrew, 2006 From fate to function: the Drosophila trachea and salivary gland as models for tubulogenesis. Differentiation 74: 326–348.

König, A., and H. R. Shcherbata, 2013 Visualization of adult stem cells within their niches using the Drosophila germline as a model system. Methods Mol. Biol. 1035: 25–33.

König, A., A. S. Yatsenko, M. Weiss, and H. R. Shcherbata, 2011 Ecdysteroids affect Drosophila ovarian stem cell niche formation and early germline differentiation. EMBO J. 30: 1549–1562.

Kucherenko, M. M., and H. R. Shcherbata, 2013 Steroids as external temporal codes act via microRNAs and cooperate with cytokines in differential neurogenesis. Fly 7: 173–183.

Kucherenko, M. M., J. Barth, A. Fiala, and H. R. Shcherbata, 2012 Steroid-induced microRNA let-7 acts as a spatio-temporal code for neuronal cell fate in the developing Drosophila brain. EMBO J. 31: 4511–4523.

Lazareva, A. A., G. Roman, W. Mattox, P. E. Hardin, and B. Dauwalder, 2007 A role for the adult fat body in Drosophila male courtship behavior. PLoS Genet. 3: e16.

Leatherman, J. L., and S. Dinardo, 2010 Germline self-renewal requires cyst stem cells and stat regulates niche adhesion in Drosophila testes. Nat. Cell Biol. 12: 806–811.

Lebo, M. S., L. E. Sanders, F. Sun, and M. N. Arbeitman, 2009 Somatic, germline and sex hierarchy regulated gene expression during Drosophila metamorphosis. BMC Genomics 10: 80.

Lee, G., J. C. Hall, and J. H. Park, 2002 Doublesex gene expression in the central nervous system of *Drosophila melanogaster*. J. Neurogenet. 16: 229–248.

Legube, G., S. K. McWeeney, M. J. Lercher, and A. Akhtar, 2006 X-chromosome-wide profiling of MSL-1 distribution and dosage compensation in Drosophila. Genes Dev. 20: 871–883.

Li, W., M. Cressy, H. Qin, T. Fulga, D. Van Vactor *et al.*, 2013 MicroRNA-276a functions in ellipsoid body and mushroom body neurons for naive and conditioned olfactory avoidance in Drosophila. J. Neurosci. 33: 5821–5833.

Liu, N., M. Landreh, K. Cao, M. Abe, G.-J. Hendriks *et al.*, 2012 The microRNA miR-34 modulates ageing and neurodegeneration in Drosophila. Nature 482: 519–523.

Lo, U., D. Yang, and J. T. Hsieh, 2013 The role of microRNAs in prostate cancer progression. Transl. Androl. Urol. 2(3): 228–241.

Luo, S. D., G. W. Shi, and B. S. Baker, 2011 Direct targets of the *D. melanogaster* DSXF protein and the evolution of sexual development. Development 138: 2761–2771.

Luo, W., and A. Sehgal, 2012 Regulation of circadian behavioral output via a MicroRNA-JAK/STAT circuit. Cell 148: 765–779.

Malone, C., J. Brennecke, B. Czech, A. Aravin, and G. J. Hannon, 2012 Preparation of small RNA libraries for high-throughput sequencing. Cold Spring Harb Protoc 2012: 1067–1077.

Marrone, A. K., E. V. Edeleva, M. M. Kucherenko, N.-H. Hsiao, and H. R. Shcherbata, 2012 Dg-Dys-Syn1 signaling in Drosophila regulates the microRNA profile. BMC Cell Biol. 13: 26.

Meiklejohn, C. D., E. L. Landeen, J. M. Cook, S. B. Kingan, and D. C. Presgraves, 2011 Sex chromosome-specific regulation in the Drosophila male germline but little evidence for chromosomal dosage compensation or meiotic inactivation. PLoS Biol. 9: e1001126.

Mishima, T., T. Takizawa, S.-S. Luo, O. Ishibashi, Y. Kawahigashi *et al.*, 2008 MicroRNA (miRNA) cloning analysis reveals sex differences in miRNA expression profiles between adult mouse testis and ovary. Reproduction 136: 811–822.

Morris, L. X., and A. C. Spradling, 2012 Steroid signaling within Drosophila ovarian epithelial cells sex-specifically modulates early germ cell development and meiotic entry. PLoS ONE 7: e46109.

Neville, M. C., T. Nojima, E. Ashley, D. J. Parker, J. Walker *et al.*, 2014 Male-specific fruitless isoforms target neurodevelopmental genes to specify a sexually dimorphic nervous system. Curr. Biol. 24: 229–241.

Parisi, M., R. Nuttall, P. Edwards, J. Minor, D. Naiman *et al.*, 2004 A survey of ovary-, testis-, and soma-biased gene expression in *Drosophila melanogaster* adults. Genome Biol. 5: R40.

Parisi, M. J., V. Gupta, D. Sturgill, J. T. Warren, J.-M. Jallon *et al.*, 2010 Germline-dependent gene expression in distant non-gonadal somatic tissues of Drosophila. BMC Genomics 11: 346.

Pasquinelli, A. E., B. J. Reinhart, F. Slack, M. Q. Martindale, M. I. Kuroda *et al.*, 2000 Conservation of the sequence and temporal expression of let-7 heterochronic regulatory RNA. Nature 408: 86–89.

Rideout, E. J., A. J. Dornan, M. C. Neville, S. Eadie, and S. F. Goodwin, 2010 Control of sexual differentiation and behavior by the doublesex gene in *Drosophila melanogaster*. Nat. Neurosci. 13: 458–466.

Ro, S., C. Park, K. M. Sanders, J. R. McCarrey, and W. Yan, 2007 Cloning and expression profiling of testis-expressed microRNAs. Dev. Biol. 311: 592–602.

Robinett, C. C., A. G. Vaughan, J.-M. Knapp, and B. S. Baker, 2010 Sex and the single cell. II. There is a time and place for sex. PLoS Biol. 8: e1000365.

Ruby, J. G., A. Stark, W. K. Johnston, M. Kellis, D. P. Bartel *et al.*, 2007 Evolution, biogenesis, expression, and target predictions of a substantially expanded set of Drosophila microRNAs. Genome Res. 17: 1850–1864.

Ryazansky, S. S., V. A. Gvozdev, and E. Berezikov, 2011 Evidence for post-transcriptional regulation of clustered microRNAs in Drosophila. BMC Genomics 12: 371.

Ryner, L. C., and B. S. Baker, 1991 Regulation of doublesex pre-mRNA processing occurs by 3′-splice site activation. Genes Dev. 5: 2071–2085.

Salz, H. K., 2011 Sex determination in insects: a binary decision based on alternative splicing. Curr. Opin. Genet. Dev. 21: 395–400.

Sanders, L. E., and M. N. Arbeitman, 2008 Doublesex establishes sexual dimorphism in the Drosophila central nervous system in an isoform-dependent manner by directing cell number. Dev. Biol. 320: 378–390.

Sefton, L., J. R. Timmer, Y. Zhang, F. Béranger, and T. W. Cline, 2000 An extracellular activator of the Drosophila JAK/STAT pathway is a sex-determination signal element. Nature 405: 970–973.

Sempere, L. F., E. B. Dubrovsky, V. A. Dubrovskaya, E. M. Berger, and V. Ambros, 2002 The expression of the let-7 small regulatory RNA is controlled by ecdysone during metamorphosis in *Drosophila melanogaster*. Dev. Biol. 244: 170–179.

Sempere, L. F., N. S. Sokol, E. B. Dubrovsky, E. M. Berger, and V. Ambros, 2003 Temporal regulation of microRNA expression in *Drosophila melanogaster* mediated by hormonal signals and broad-Complex gene activity. Dev. Biol. 259: 9–18.

Shcherbata, H. R., E. J. Ward, K. A. Fischer, J.-Y. Yu, S. H. Reynolds *et al.*, 2007 Stage-specific differences in the requirements for germline stem cell maintenance in the Drosophila ovary. Cell Stem Cell 1: 698–709.

Shi, X.-B., L. Xue, J. Yang, A.-H. Ma, J. Zhao *et al.*, 2007 An androgen-regulated miRNA suppresses Bak1 expression and induces androgen-independent growth of prostate cancer cells. Proc. Natl. Acad. Sci. USA 104: 19983–19988.

Smibert, P., and E. C. Lai, 2010 A view from Drosophila: multiple biological functions for individual microRNAs. Semin. Cell Dev. Biol. 21: 745–753.

Sokol, N. S., P. Xu, Y.-N. Jan, and V. Ambros, 2008 Drosophila let-7 microRNA is required for remodeling of the neuromusculature during metamorphosis. Genes Dev. 22: 1591–1596.

Soni, K., A. Choudhary, A. Patowary, A. R. Singh, S. Bhatia *et al.*, 2013 miR-34 is maternally inherited in *Drosophila melanogaster* and *Danio rerio*. Nucleic Acids Res. 41: 4470–4480.

Sosnowski, B. A., J. M. Belote, and M. McKeown, 1989 Sex-specific alternative splicing of RNA from the transformer gene results from sequence-dependent splice site blockage. Cell 58: 449–459.

Straub, T., C. Grimaud, G. D. Gilfillan, A. Mitterweger, and P. B. Becker, 2008 The chromosomal high-affinity binding sites for the Drosophila dosage compensation complex. PLoS Genet. 4: e1000302.

Takamizawa, J., 2004 Reduced expression of the let-7 microRNAs in human lung cancers in association with shortened postoperative survival. Cancer Res. 64: 3753–3756.

Tanaka, K., O. Barmina, L. E. Sanders, M. N. Arbeitman, and A. Kopp, 2011 Evolution of sex-specific traits through changes in HOX-dependent doublesex expression. PLoS Biol. 9: e1001131.

Toledano, H., C. D'Alterio, B. Czech, E. Levine, and D. L. Jones, 2012 The let-7-Imp axis regulates ageing of the Drosophila testis stem-cell niche. Nature 485: 605–610.

Trang, P., P. P. Medina, J. F. Wiggins, L. Ruffino, K. Kelnar *et al.*, 2009 Regression of murine lung tumors by the let-7 microRNA. Oncogene 29: 1580–1587.

Vibranovski, M. D., H. F. Lopes, T. L. Karr, and M. Long, 2009 Stage-specific expression profiling of Drosophila spermatogenesis suggests that meiotic sex chromosome inactivation drives genomic relocation of testis-expressed genes. PLoS Genet. 5: e1000731.

Vibranovski M. D., Zhang Y. E., Kemkemer C., Lopes H. F., Karr T. L., Long M., 2012 Re-analysis of the larval testis data on meiotic sex chromosome inactivation revealed evidence for tissue-specific gene expression related to the Drosophila X chromosome. BMC Biol. 10: 49–50.

Weng, R., and S. M. Cohen, 2012 Drosophila miR-124 regulates neuroblast proliferation through its target anachronism. Development 139: 1427–1434.

Whitworth, C., E. Jimenez, and M. Van Doren, 2012 Development of sexual dimorphism in the Drosophila testis. Spermatogenesis 2: 129–136.

Williams, T. M., J. E. Selegue, T. Werner, N. Gompel, A. Kopp *et al.*, 2008 The regulation and evolution of a genetic switch controlling sexually dimorphic traits in Drosophila. Cell 134: 610–623.

Wu, Y.-C., C.-H. Chen, A. Mercer, and N. S. Sokol, 2012 Let-7-complex microRNAs regulate the temporal identity of Drosophila mushroom body neurons via chinmo. Dev. Cell 23: 202–209.

Xu, P., S. Y. Vernooy, M. Guo, and B. A. Hay, 2003 The Drosophila microRNA Mir-14 suppresses cell death and is required for normal fat metabolism. Curr. Biol. 13: 790–795.

Zhu, S., S. Lin, C.-F. Kao, T. Awasaki, A.-S. Chiang *et al.*, 2006 Gradients of the Drosophila Chinmo BTB-zinc finger protein govern neuronal temporal identity. Cell 127: 409–422.

Communicating editor: B. Andrews

GENETICS

Supporting Information
http://www.genetics.org/lookup/suppl/doi:10.1534/genetics.114.169268/-/DC1

A Genome-Wide Survey of Sexually Dimorphic Expression of *Drosophila* miRNAs Identifies the Steroid Hormone-Induced miRNA let-7 as a Regulator of Sexual Identity

Delphine Fagegaltier, Annekatrin König, Assaf Gordon, Eric C. Lai, Thomas R. Gingeras, Gregory J. Hannon and Halyna R. Shcherbata

DOI: 10.1534/genetics.114.169268

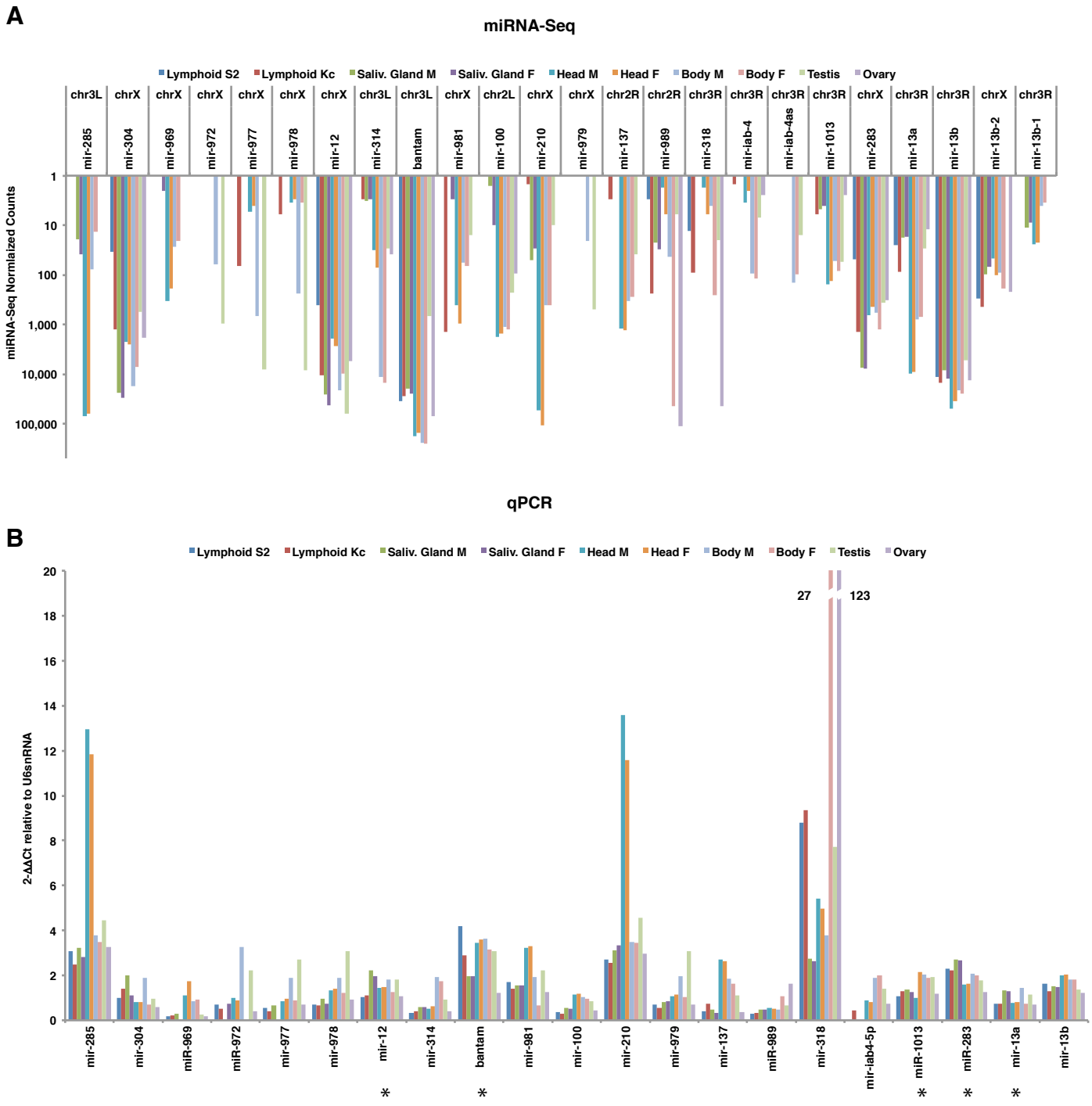

FIGURE S1: **qPCR validation of the expression levels of 22 miRNAs across all samples**. The trends of miRNA expression levels and relative abundance across all samples by miRNA-Seq (A) and qPCR (B) are similar for 16 miRNAs. Five additional miRNAs showing differences between miRNA-Seq and qPCR trends in one or more tissues (miR-12, bantam, miR-1013, miR-283, and miR-13a) are denoted with an asterisk. The genome presents several copies of mature miR-13b undistinguishable by qPCR: mir-13b and mir-13b-1 on chr3R, and mir-13b-2 on chrX. MiRNA normalized reads are reported in (A). qPCR assays were performed with at least two independent biological replicates and gave similar trends in (B). M: male ; F: female.

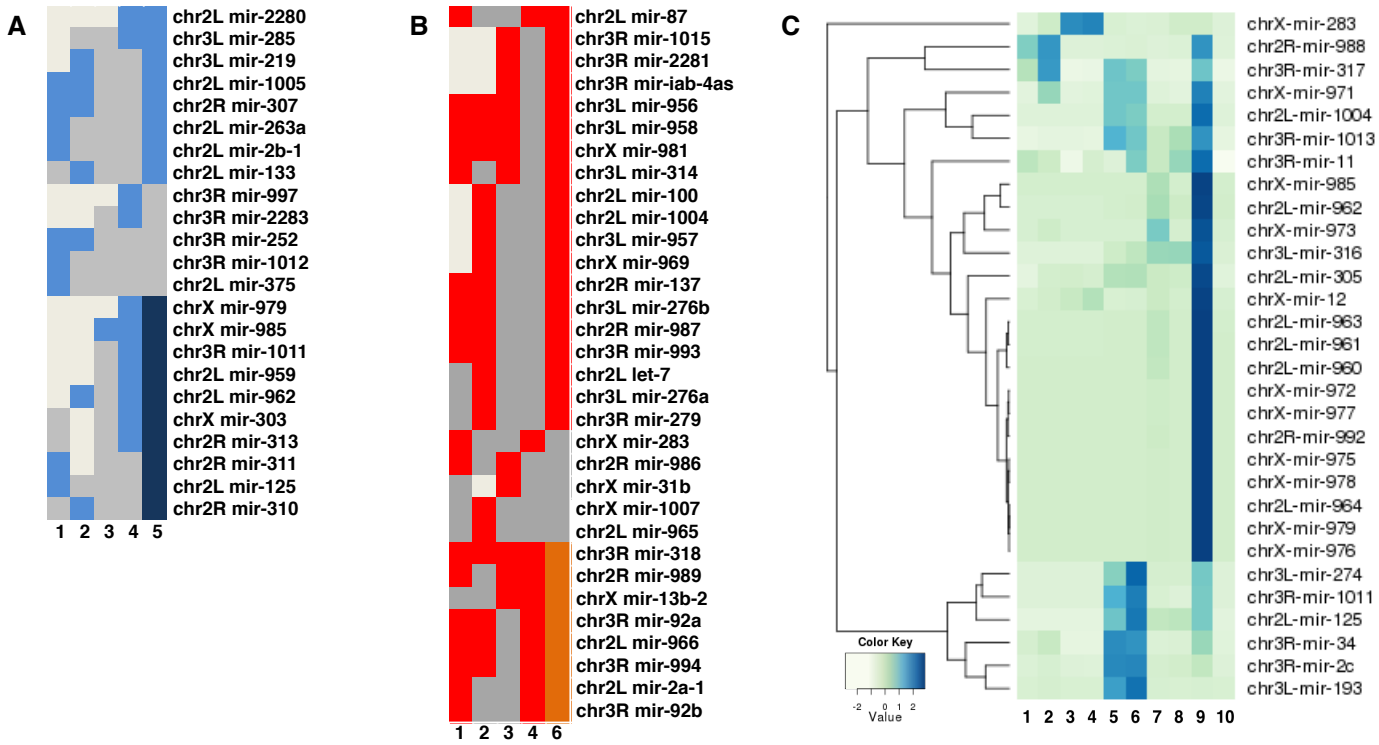

Figure S2: Male-enriched, female-enriched and X-linked testis-enriched miRNAs. (A) 23 miRNAs enriched in male somatic tissues in pairwise comparisons of S2 vs. Kc cells (1), male vs. female salivary glands (2), heads (3), and decapitated body (4). Colors indicate male-enriched miRNAs (light blue), miRNAs present at similar levels in both sexes (grey), poorly expressed miRNAs (white) and whether these miRNAs are more abundant in the male body (light blue) or testis (dark blue) in (5). (B) 32 female-enriched miRNAs in somatic tissues. Colors indicate female-enriched miRNAs (red), miRNAs present at similar levels in both sexes (grey), poorly expressed miRNAs (white) in somatic tissues [tissues (1) to (4) as in (A)], and whether these miRNAs are more abundant in the female body (red) or ovary (orange) in (6). (C) Relative abundance across all sexed tissues of the 30 miRNAs enriched exclusively in testis compared to the male body and not enriched in ovaries in females. 11 of the 30 testis-enriched miRNAs reside on the X chromosome. These miRNAs are highly and almost exclusively expressed in testis. S2 cells (1), Kc cells (2), male (3) and female (4) salivary glands, heads [male (5), female (6)], body [male (7), female (8)], testis (9), ovary (10).

TABLE S1: PCR primers used in this study

2S rRNA depletion:

5'-AGTCTTACAACCCTCAACCATATGTAGTCCAAGCAGCACT-3'

qPCR (miScript assay):

bantam-fwd	5'-GAGATCATTTTGAAAGCTGATT-3'	
miR-12-fwd	5'-GAGTATTACATCAGGTACTGGT-3'	
mir-13b-1-2-fwd	5'-TATCACAGCCATTTTGACGAGT-3'	
mir-13a-fwd	5'-TATCACAGCCATTTTGATGAGT-3'	
mir-283-fwd	5'-TAAATATCAGCTGGTAATTCT-3'	
mir-304-fwd	5'-AATCTCAATTTGTAAATGTGAG-3'	
mir-210-fwd	5'-TTGTGCGTGTGACAGCGGCTA-3'	
mir-iab-4-5p-fwd	5'-ACGTATACTGAATGTATCCTGA-3'	
mir-iab-4-3p-fwd	5'-GTATACCTTCAGTATACGTAAC-3'	
mir-318-fwd	5'-TCACTGGGCTTTGTTTATCTCA-3'	
mir-985-fwd	5'-CAAATGTTCCAATGGTCGGGCA-3'	
mir-979-fwd	5'-TTCTTCCCGAACTCAGGCTAA-3'	
mir-981-fwd	5'-TTCGTTGTCGACGAAACCTGCA-3'	
mir-977-fwd	5'-TGAGATATTCACGTTGTCTAA-3'	
mir-285-fwd	5'-TAGCACCATTCGAAATCAGTGC-3'	
mir-969-fwd	5'-GAGTTCCACTAAGCAAGTTTT-3'	
mir-972-fwd	5'-TGTACAATACGAATATTTAGGC-3'	
mir-978-fwd	5'-TGTCCAGTGCCGTAAATTGCAG-3'	
mir-314-fwd	5'-TATTCGAGCCAATAAGTTCGG-3'	
mir-100-fwd	5'-AACCCGTAAATCCGAACTTGTG-3'	
mir-137-Fwd	5'-TATTGCTTGAGAATACACGTAG-3'	
mir-989-fwd	5'-ATGTGATGTGACGTAGTGGAAC-3'	
mir-1013-fwd	5'-AATAAAAGTATGCCGAACTCG-3'	
mir-Spike-fwd	5'-CTCAGGATGGCGGAGCGGTGT-3'	external reference
U6snRNA-fwd	5'-ATTGGAACGATACAGAGAAGATTAG-3'	reference
Dspt-4-fwd	5'-TTGACGCGATACCCAAGGAT-3'	reference
Dspt4-rev	5'-CTAGTGTGATCATAGACATTGTCCTTGTT-3'	

qPCR on sex-specific transcripts:

RpL32-fwd	5'-AAGATGACCATCCGCCCAGC-3'	endogenous control
RpL32-rev	5'-GTCGATACCCTTGGGCTTGC-3'	
Esg-fwd	5'-CGCCCATGAGATCTGAAATC-3'	
Esg rev	5'-GGTCTTGTCACAATCCTTGC-3'	(Chau *et al.* 2009)
DsxM fwd	5'-TCCTTGGGAGCTGATGCCAC-3'	
DsxM rev	5'-GGCTACAGTGCGATTTATT-3'	
Yp1-fwd	5'-TGAGCGTCTGGAGAACATGAA-3'	
Yp1-rev	5'-GCGACAGGTGGTAGACTTGCT-3'	
tra1-fwd	5'-GGAACCCAGCATCGAGATTC-3'	
tra1-rev	5'-ATCGCCCATGGTATTCTCTTTC-3'	
Sxl-fwd	5'-ACAACGACAGCAGCAGGCCA-3'	
Sxl-rev	5'-TTGTAACCACGACGCGACGAT-3'	(Hashiyama *et al.* 2011)

TABLE S2: Late embryo-derived Lymphoid S2 (male) and Kc (female) cells biased miRNAs

S2 biased

chrom	miRNA	S2 reads	Kc reads	M/M+F	F/M+F	Sum reads	% miRNA
chr3R	dme-mir-252	13294	205	0.98479	0.01521	**13499**	1.1771
chr2R	dme-mir-307	932	33	0.96584	0.03416	**965**	0.0841
chr2L	dme-mir-263a	66	4	0.93623	0.06377	**70**	0.0061
chrX	dme-mir-980	1534	453	0.77219	0.22781	**1987**	0.1732
chr3L	dme-mir-282	13543	4622	0.74557	0.25443	**18165**	1.5839
chr2R	dme-mir-311	8	3	0.72746	0.27254	**11**	0.001
chr3R	dme-mir-1012	164	63	0.72266	0.27734	**227**	0.0198
chr2L	dme-mir-2b-1	498	207	0.70658	0.29342	**705**	0.0615
chr2L	dme-mir-125	10	4	0.68986	0.31014	**14**	0.0013
chr2R	dme-mir-286	43	21	0.67209	0.32791	**64**	0.0056

Kc biased

chrom	miRNA	S2	Kc reads	M/M+F	F/M+F	Sum reads	% miRNA
chrX	dme-mir-971	0	52	0	1	**52**	0.0046
chrX	dme-mir-973	0	12	0	1	**12**	0.001
chrX	dme-mir-982	0	16	0	1	**16**	0.0014
chrX	dme-mir-981	1	1427	0.00070	0.99930	**1428**	0.1245
chr3R	dme-mir-1000	1	1299	0.00077	0.99923	**1300**	0.1134
chr3R	dme-mir-92a	13	2215	0.00584	0.99416	**2228**	0.1943
chr3R	dme-mir-1010	1	106	0.00931	0.99069	**107**	0.0094
chr2R	dme-mir-989	3	237	0.01251	0.98749	**240**	0.0209
chrX	dme-mir-977	1	66	0.01494	0.98506	**67**	0.0058
chr3L	dme-mir-276b	5	187	0.02600	0.97400	**192**	0.0168
chrX	dme-mir-304	34	1260	0.02627	0.97373	**1294**	0.1129
chr2L	dme-mir-932	5	177	0.02750	0.97250	**182**	0.0159
chr2R	dme-mir-278	47	1647	0.02775	0.97225	**1694**	0.1477
chr3R	dme-mir-92b	20	670	0.02899	0.97101	**690**	0.0602
chr3L	dme-mir-193	3	96	0.03033	0.96967	**99**	0.0086
chrX	dme-mir-283	48	1394	0.03330	0.96670	**1442**	0.1257
chr3L	dme-mir-958	1	28	0.03393	0.96607	**29**	0.0026
chr3R	dme-mir-10	1	27	0.03575	0.96425	**28**	0.0024
chrX	dme-mir-12	415	10569	0.03778	0.96222	**10984**	0.9578
chr2R	dme-mir-986	3	43	0.06457	0.93543	**46**	0.0041
chr2L	dme-mir-124	8	94	0.07812	0.92188	**102**	0.0089
chr4	dme-mir-954	11	91	0.10741	0.89259	**102**	0.0089
chr3R	dme-mir-994	5	40	0.10998	0.89002	**45**	0.004
chr2R	dme-mir-8	4003	27812	0.12582	0.87418	**31815**	2.7742
chr3R	dme-mir-318	13	90	0.12632	0.87368	**103**	0.009
chr2L	dme-mir-9b	2463	11885	0.17166	0.82834	**14348**	1.2511
chr2L	dme-mir-2a-2	2015	9699	0.17202	0.82798	**11714**	1.0214
chrX	dme-mir-984	25	102	0.19700	0.80300	**127**	0.0111
chr2L	dme-mir-966	15	58	0.20424	0.79576	**73**	0.0064
chr2L	dme-mir-2b-2	431	1648	0.20727	0.79273	**2079**	0.1813
chr2L	dme-mir-2a	7839	29779	0.20838	0.79162	**37618**	3.2803
chr2R	dme-mir-31a	5	18	0.21756	0.78244	**23**	0.002

chr2L	dme-mir-1	23	82	0.21817	0.78183	**105**	0.0092
chr3R	dme-mir-13a	25	85	0.22641	0.77359	**110**	0.0096
chr3L	dme-mir-276	4524	15417	0.22687	0.77313	**19941**	1.7389
chr2L	dme-mir-305	3321	10310	0.24364	0.75636	**13631**	1.1886
chr2R	dme-mir-312	3	9	0.25018	0.74982	**12**	0.001
chr2L	dme-mir-9c	1896	5648	0.25132	0.74868	**7544**	0.6578
chr2R	dme-mir-1008	94	262	0.26386	0.73614	**356**	0.0311
chr2L	dme-mir-275	461	1247	0.26994	0.73006	**1708**	0.1489
chr3L	dme-mir-190	171	462	0.27033	0.72967	**633**	0.0552
chr2L	dme-mir-79	2043	5420	0.27374	0.72626	**7463**	0.6508
chr3L	dme-mir-9a	49	124	0.28262	0.71738	**173**	0.0151
chr2L	dme-mir-1006	58	145	0.28521	0.71479	**203**	0.0177
chr2L	dme-mir-306	2500	6128	0.28977	0.71023	**8628**	0.7523
chr3R	dme-mir-317	9157	21083	0.30281	0.69719	**30240**	2.6369
chr3R	dme-mir-999	247	560	0.30590	0.69410	**807**	0.0704
chr2R	dme-mir-1009	4	9	0.30790	0.69210	**13**	0.0011
chrX	dme-mir-983	6	13	0.30790	0.69210	**19**	0.0017
chr2L	dme-mir-2a-1	173	388	0.30831	0.69169	**561**	0.0489
chr3R	dme-mir-2c	9	19	0.31600	0.68400	**28**	0.0025
chr3L	dme-mir-33	1927	4040	0.32294	0.67706	**5967**	0.5203
chr2L	dme-mir-2b	9981	20837	0.32387	0.67613	**30818**	2.6874
chr2R	dme-mir-184	54062	109778	0.32997	0.67003	**163840**	14.2868

At least 10 normalized reads in the summed normalized reads were required. S2: Male (M); Kc: Female (F).
A ratio (F/M+F) >=0.66 is female biased. A ratio (M/M+F) >=0.66 is male biased.

TABLE S3: Male and female biased miRNAs in L3 larval salivary glands

Male biased

chrom	miRNA	Male S. Gland reads	Female S. Gland reads	M/M+F	F/M+F	Sum Reads	% miRNA
chr2L	dme-mir-275	21773	2588	0.89376	0.10624	**24361**	2.63097
chr2R	dme-mir-1009	8	2	0.80000	0.20000	**10**	0.00108
chr2R	dme-mir-278	1275	526	0.70797	0.29203	**1801**	0.19453
chr2L	dme-mir-133	10	4	0.70588	0.29412	**14**	0.00147
chr2L	dme-mir-1005	26	11	0.69945	0.30055	**37**	0.00395
chr3R	dme-mir-252	1330	644	0.67369	0.32631	**1974**	0.21315

Female biased

chrom	miRNA	Male S. Gland reads	Female S. Gland reads	M/M+F	F/M+F	Sum Reads	% miRNA
chr2L	dme-mir-100	2	10	0.13793	0.86207	**12**	0.00125
chr3L	dme-mir-282	6635	31936	0.17202	0.82798	**38571**	4.1657
chr2L	dme-let-7	48	219	0.17978	0.82022	**267**	0.02884
chr3R	dme-mir-279	514	1492	0.25608	0.74392	**2006**	0.21661
chr2L	dme-mir-965	210	567	0.26989	0.73011	**777**	0.08387
chr2R	dme-mir-987	14	36	0.28571	0.71429	**50**	0.00544
chr2L	dme-mir-305-as	3	7	0.31373	0.68627	**10**	0.0011
chr3R	dme-mir-92a	3	7	0.31373	0.68627	**10**	0.0011
chr3L	dme-mir-957	3	7	0.31373	0.68627	**10**	0.0011
chr2R	dme-mir-307-as	8	17	0.32000	0.68000	**25**	0.0027
chr3L	dme-mir-276a	1853	3728	0.33200	0.66800	**5581**	0.60273
chr3L	dme-mir-285	19	38	0.33566	0.66434	**57**	0.00618

At least 10 normalized reads in the summed normalized reads were required. M: male ; F: female.
A ratio (F/M+F) >=0.66 is female biased in salivary glands (S. glands). A ratio(M/M+F) >=0.66 is male biased.

TABLE S4: Male and female biased miRNAs in adult heads

Male biased

chrom	miRNA	Male Head reads	Female Head reads	M/M+F	F/M+F	Sum Reads	% miRNA
chrX	dme-mir-974	9	2	0.81405	0.18595	**11**	0.000247
chr3L	dme-mir-190	2189	634	0.77540	0.22460	**2823**	0.06472
chr2L	dme-mir-305-as	21	8	0.72426	0.27574	**29**	0.000665
chr3L	dme-mir-276	119752	58112	0.67328	0.32672	**177864**	4.077941
chr2R	dme-mir-1008	208	104	0.66707	0.33293	**312**	0.007162

Female biased

chrom	miRNA	Male Head reads	Female Head reads	M/M+F	F/M+F	Sum Reads	% miRNA
chr3L	dme-mir-958	5	29	0.15336	0.84664	**34**	0.000785
chrX	dme-mir-31b	12	44	0.21788	0.78212	**56**	0.00129
chr2L	dme-mir-964	12	41	0.23015	0.76985	**53**	0.001221
chr3L	dme-mir-956	7	20	0.25938	0.74062	**27**	0.000619
chrX	dme-mir-980	611	1464	0.29450	0.70550	**2075**	0.047577
chrX	dme-mir-981	404	968	0.29472	0.70528	**1372**	0.031468
chr3L	dme-mir-274	24301	55708	0.30373	0.69627	**80009**	1.834398
chr3L	dme-mir-314	32	72	0.30448	0.69552	**104**	0.002373
chr2L	dme-mir-961	9	20	0.30448	0.69552	**29**	0.000659
chr2L	dme-mir-963	9	20	0.30448	0.69552	**29**	0.000659
chr3R	dme-mir-284	907	2009	0.31105	0.68895	**2916**	0.066857
chr2R	dme-mir-286	7	15	0.31831	0.68169	**22**	0.000504
chr2L	dme-mir-275	1170	2503	0.31849	0.68151	**3673**	0.084205
chrX	dme-mir-13b-2	47	101	0.31885	0.68115	**148**	0.0034
chr2R	dme-mir-986	475	1006	0.32052	0.67948	**1481**	0.033945
chrX	dme-mir-210	54115	106957	0.33597	0.66403	**161072**	3.692947
chr3R	dme-mir-11	10872	21450	0.33637	0.66363	**32322**	0.741065
chr2L	dme-mir-960	53	103	0.33776	0.66224	**156**	0.003566
chr2L	dme-mir-133	8468	16473	0.33953	0.66047	**24941**	0.571834

At least 10 normalized reads in the summed normalized reads were required.

A ratio (F/M+F) >=0.66 is female biased in the head. A ratio(M/M+F) >=0.66 is male biased. F: female; M: Male.

TABLE S5: Male vs. female biased miRNAs in the adult body

Male body biased

chrom	miRNA	Male Body reads	Female Body reads	M/M+F	F/M+F	Sum Reads	% miRNA
chrX	dme-mir-972	61	0	1	0	**61**	0.001355886
chrX	dme-mir-975	33	0	1	0	**33**	0.000733512
chrX	dme-mir-977	680	0	1	0	**680**	0.015114796
chrX	dme-mir-979	21	0	1	0	**21**	0.00046678
chr3R	dme-mir-997	184	0	1	0	**184**	0.004089886
chrX	dme-mir-978	241	3	0.98597	0.01403	**244**	0.00543307
chrX	dme-mir-974	236	3	0.98568	0.01432	**239**	0.005321932
chrX	dme-mir-976	380	7	0.98227	0.01773	**387**	0.008598921
chr2L	dme-mir-959	478	10	0.97894	0.02106	**488**	0.010853439
chrX	dme-mir-303	142	3	0.97642	0.02358	**145**	0.003232534
chrX	dme-mir-985	214	7	0.96895	0.03105	**221**	0.004909133
chrX	dme-mir-983	724	24	0.96791	0.03209	**748**	0.016626275
chrX	dme-mir-984	551	24	0.95826	0.04174	**575**	0.012780893
chrX	dme-mir-973	76	3	0.95683	0.04317	**79**	0.00176551
chr2L	dme-mir-963	368	21	0.94706	0.05294	**389**	0.008637026
chr2R	dme-mir-991	120	7	0.94595	0.05405	**127**	0.002819735
chr2L	dme-mir-960	1717	117	0.93642	0.06358	**1834**	0.040755964
chr2R	dme-mir-992	45	3	0.92920	0.07080	**48**	0.001076453
chr2L	dme-mir-964	437	34	0.92725	0.07275	**471**	0.010475569
chrX	dme-mir-982	118	10	0.91982	0.08018	**128**	0.002851489
chr2L	dme-mir-961	177	17	0.91170	0.08830	**194**	0.004315337
chr3L	dme-mir-285	76	14	0.84713	0.15287	**90**	0.001994137
chr2R	dme-mir-1009	38	10	0.78698	0.21302	**48**	0.001073277
chr3L	dme-mir-193	12	3	0.77778	0.22222	**15**	0.000342941
chr2L	dme-mir-962	401	134	0.74993	0.25007	**535**	0.011885434
chrX	dme-mir-304	17186	7227	0.70396	0.29604	**24413**	0.542652738
chrX	dme-mir-12	21306	9603	0.68930	0.31070	**30909**	0.687043433
chr2R	dme-mir-313	59	27	0.68264	0.31736	**86**	0.001921103

Female body biased

chrom	miRNA	Male Body reads	Female Body reads	M/M+F	F/M+F	Sum Reads	% miRNA
chr2R	dme-mir-989	44	45010	0.00098	0.99902	**45054**	1.001449337
chr3R	dme-mir-318	4	261	0.01512	0.98488	**265**	0.005880792
chr3R	dme-mir-994	4	261	0.01512	0.98488	**265**	0.005880792
chr3R	dme-mir-92b	42	233	0.15265	0.84735	**275**	0.006115771
chr2L	dme-mir-966	5	21	0.19553	0.80447	**26**	0.000568392
chr2L	dme-mir-2a-1	21	75	0.21778	0.78222	**96**	0.002143378
chr3L	dme-mir-190	162	579	0.21850	0.78150	**741**	0.016480193
chr3L	dme-mir-276	47955	128270	0.27212	0.72788	**176225**	3.917056396
chr2L	dme-mir-275	1122	2616	0.30016	0.69984	**3738**	0.083086855
chr3R	dme-mir-92a	254	579	0.30477	0.69523	**833**	0.018525136
chrX	dme-mir-283	577	1245	0.31676	0.68324	**1822**	0.040489204
chrX	dme-mir-13b-2	92	189	0.32790	0.67210	**281**	0.006236436

chr2L	dme-mir-87	908	1834	0.33111	0.66889	**2742**	0.060954495

At least 10 normalized reads in the summed normalized reads were required.
A ratio (F/M+F) >=0.66 is female biased. A ratio (M/M+F) >=0.66 is male biased. F: female; M: male.

TABLE S6: Testis and Ovary biased miRNAs

Testis biased

chrom	miRNA	Testes reads	Ovary reads	T/Ov+T	Ov/T+Ov	Sum Reads	% miRNA
chr2L	dme-mir-1004	144	0	1	0	**144**	0.01472903
chr2R	dme-mir-137	38	0	1	0	**38**	0.003886827
chrX	dme-mir-210	10	0	1	0	**10**	0.001022849
chr3L	dme-mir-263b	13	0	1	0	**13**	0.001329704
chr3L	dme-mir-315	12	0	1	0	**12**	0.001227419
chr2L	dme-mir-375	1491	0	1	0	**1491**	0.152506835
chrX	dme-mir-971	33	0	1	0	**33**	0.003375403
chrX	dme-mir-972	961	0	1	0	**961**	0.098295821
chrX	dme-mir-973	51	0	1	0	**51**	0.005216532
chrX	dme-mir-974	82	0	1	0	**82**	0.008387364
chrX	dme-mir-975	2134	0	1	0	**2134**	0.218276047
chrX	dme-mir-976	7525	0	1	0	**7525**	0.76969412
chrX	dme-mir-977	8100	0	1	0	**8100**	0.828507956
chrX	dme-mir-978	8457	0	1	0	**8457**	0.865023677
chrX	dme-mir-979	497	0	1	0	**497**	0.050835612
chrX	dme-mir-981	16	0	1	0	**16**	0.001636559
chr2R	dme-mir-992	395	0	1	0	**395**	0.040402548
chr3R	dme-mir-997	59	0	1	0	**59**	0.006034811
chr3R	dme-mir-iab-4as	16	0	1	0	**16**	0.001636559
chr2L	dme-mir-959	17252	10	0.99943	0.00057	**17262**	1.765620246
chr2L	dme-mir-964	10115	12	0.99879	0.00121	**10127**	1.035862826
chr3L	dme-mir-274	7928	12	0.99846	0.00154	**7940**	0.812165678
chr2L	dme-mir-963	926	2	0.99737	0.00263	**928**	0.094965994
chr2L	dme-mir-960	5436	27	0.99508	0.00492	**5463**	0.558772501
chrX	dme-mir-985	321	2	0.99244	0.00756	**323**	0.033083609
chr3L	dme-mir-9a	6846	98	0.98591	0.01409	**6944**	0.710248489
chr2L	dme-mir-124	151	2	0.98406	0.01594	**153**	0.015695171
chr3R	dme-mir-277	9542	213	0.97819	0.02181	**9755**	0.997765528
chr2L	dme-mir-961	477	12	0.97501	0.02499	**489**	0.050040643
chr3R	dme-mir-1013	54	2	0.95667	0.04333	**56**	0.005773532
chr3R	dme-mir-252	990	51	0.95068	0.04932	**1041**	0.106515149
chr2L	dme-mir-133	38	2	0.93953	0.06047	**40**	0.004136973
chr2R	dme-mir-991	127	10	0.92848	0.07152	**137**	0.01399077
chr2R	dme-mir-988	6587	523	0.92640	0.07360	**7110**	0.727282088
chr2R	dme-mir-310	3356	289	0.92082	0.07918	**3645**	0.372785458
chrX	dme-mir-12	62228	5576	0.91776	0.08224	**67804**	6.935319591
chr2L	dme-mir-932	45	5	0.90196	0.09804	**50**	0.005103114
chr3R	dme-mir-1010	168	20	0.89569	0.10431	**188**	0.019185036
chr2R	dme-mir-278	2426	286	0.89450	0.10550	**2712**	0.277410324
chr3R	dme-mir-2c	19	2	0.88596	0.11404	**21**	0.00219356
chrX	dme-mir-983	6732	1010	0.86954	0.13046	**7742**	0.791892449
chr2R	dme-mir-311	3582	582	0.86022	0.13978	**4164**	0.425919368
chr2L	dme-mir-962	471	81	0.85372	0.14628	**552**	0.05643102
chr2L	dme-mir-125	3331	614	0.84439	0.15561	**3945**	0.403497747

chr3L	dme-mir-316	4417	814	0.84433	0.15567	**5231**	0.535091153
chr2L	dme-let-7	11559	2179	0.84139	0.15861	**13738**	1.405191589
chr2R	dme-mir-1008	11	2	0.81811	0.18189	**13**	0.00137528
chr3R	dme-mir-999	673	179	0.79034	0.20966	**852**	0.087098415
chr3R	dme-mir-317	4489	1294	0.77628	0.22372	**5783**	0.591484276
chr2L	dme-mir-305	18583	6588	0.73826	0.26174	**25171**	2.574654122
chr3L	dme-mir-956	54	22	0.71043	0.28957	**76**	0.0077747
chr2L	dme-mir-100	226	93	0.70861	0.29139	**319**	0.032621941
chr3R	dme-mir-13a	29	12	0.70341	0.29659	**41**	0.004216993
chrX	dme-mir-31b	875	416	0.67790	0.32210	**1291**	0.132024129

Ovary biased

chrom	miRNA	Testes reads	Ovary reads	T/Ov+T	Ov/T+Ov	Sum Reads	% miRNA
chr2R	dme-mir-989	6	111853	0.00005	0.99995	**111859**	11.44153945
chr3R	dme-mir-318	20	44135	0.00045	0.99955	**44155**	4.516429825
chr3R	dme-mir-994	19	18298	0.00104	0.99896	**18317**	1.873535481
chr2L	dme-mir-2b-1	2	460	0.00433	0.99567	**462**	0.04723201
chrX	dme-mir-13b-2	1	218	0.00457	0.99543	**219**	0.022365275
chr3R	dme-mir-996	348	36033	0.00957	0.99043	**36381**	3.72124572
chr3L	dme-bantam	687	69609	0.00977	0.99023	**70296**	7.190174187
chr2R	dme-mir-184	540	38992	0.01366	0.98634	**39532**	4.043561038
chr2R	dme-mir-1009	5	220	0.02221	0.97779	**225**	0.023024561
chr2L	dme-mir-965	9	355	0.02475	0.97525	**364**	0.037191728
chr2L	dme-mir-79	219	8506	0.02510	0.97490	**8725**	0.892408047
chr2L	dme-mir-263a	245	8899	0.02679	0.97321	**9144**	0.935340954
chr3L	dme-mir-33	166	5092	0.03157	0.96843	**5258**	0.537783186
chr2L	dme-mir-2b-2	40	1091	0.03538	0.96462	**1131**	0.115656495
chr2R	dme-mir-308	30	790	0.03659	0.96341	**820**	0.083865693
chr2L	dme-mir-275	605	15923	0.03660	0.96340	**16528**	1.690582725
chr3L	dme-mir-276	123	3194	0.03708	0.96292	**3317**	0.33927167
chr2R	dme-mir-281-2	21	430	0.04652	0.95348	**451**	0.046173672
chr3R	dme-mir-995	228	4654	0.04670	0.95330	**4882**	0.499348725
chr2L	dme-mir-1	241	3788	0.05981	0.94019	**4029**	0.41212676
chr2R	dme-mir-307	42	599	0.06551	0.93449	**641**	0.065581727
chr3R	dme-mir-998	84	986	0.07854	0.92146	**1070**	0.109400756
chr2L	dme-mir-87	12	139	0.07926	0.92074	**151**	0.015485739
chr2L	dme-mir-2a-1	13	149	0.08016	0.91984	**162**	0.016588608
chr2L	dme-mir-1005	3	34	0.08056	0.91944	**37**	0.003808898
chr2R	dme-mir-281-1	143	1277	0.10073	0.89927	**1420**	0.145202936
chr2L	dme-mir-966	6	51	0.10461	0.89539	**57**	0.005866775
chr2L	dme-mir-2a-2	112	829	0.11902	0.88098	**941**	0.096255393
chr3R	dme-mir-929	4	29	0.11995	0.88005	**33**	0.003410891
chr2R	dme-mir-313	370	1538	0.19389	0.80611	**1908**	0.195187234
chrX	dme-mir-1007	6	24	0.19701	0.80299	**30**	0.003115169
chr3R	dme-mir-284	16	56	0.22146	0.77854	**72**	0.007389916
chr2R	dme-mir-7	863	2981	0.22450	0.77550	**3844**	0.393199821
chr3L	dme-mir-190	13	44	0.22799	0.77201	**57**	0.005832331
chr2L	dme-mir-2b	6058	20095	0.23163	0.76837	**26153**	2.675091471

chr2L	dme-mir-2a	14216	47031	0.23211	0.76789	**61247**	6.264639548
chrX	dme-mir-304	556	1817	0.23430	0.76570	**2373**	0.24272887
chr2L	dme-mir-9c	2050	5715	0.26399	0.73601	**7765**	0.794275219
chr2L	dme-mir-306	951	2472	0.27779	0.72221	**3423**	0.350170536
chr3R	dme-mir-13b	5212	13392	0.28015	0.71985	**18604**	1.902908343
chr2R	dme-mir-986	309	736	0.29566	0.70434	**1045**	0.106899978
chr3R	dme-mir-1012	46	98	0.31984	0.68016	**144**	0.014710945
chr2R	dme-mir-312	1704	3546	0.32457	0.67543	**5250**	0.537005167
chr2L	dme-mir-9b	6727	13372	0.33469	0.66531	**20099**	2.055868849

At least 10 normalized reads in the summed normalized reads in male and female gonads are required.
A ratio (Testis/Ovary+Testis) >=0.66 is Testis biased. A ratio(Ovary/Ovary +Testis) >=0.66 is Ovary biased
T: Testis; Ov: Ovaries

TABLE S7: miRNAs with testis vs. male body biases

Male Body (male somatic tissues) biased miRNAs

chrom	miRNA	Male Body reads	Testis reads	BM/BM+T	Testis/BM+T	Sum reads	% miRNA
chr3R	dme-mir-1014	248	0	1	0	**248**	0.007666282
chr3L	dme-mir-285	76	0	1	0	**76**	0.002349344
chr2R	dme-mir-5	14	0	1	0	**14**	0.000432774
chrX	dme-mir-927	41	0	1	0	**41**	0.001267409
chr3L	dme-mir-957	839	0	1	0	**839**	0.025935526
chrX	dme-mir-969	27	0	1	0	**27**	0.000834636
chr2L	dme-mir-1	496888	844	0.99831	0.00169	**497732**	15.38608851
chr3R	dme-mir-993	1448	4	0.99759	0.00241	**1452**	0.044869387
chr3R	dme-mir-1000	875	4	0.99602	0.00398	**879**	0.027156567
chr3L	dme-mir-958	7379	32	0.99575	0.00425	**7411**	0.229076539
chr3R	dme-mir-929	1810	14	0.99232	0.00768	**1824**	0.056384267
chr3L	dme-mir-314	11627	102	0.99135	0.00865	**11729**	0.362556399
chr3L	dme-mir-276	47955	431	0.99110	0.00890	**48386**	1.495713233
chr3L	dme-bantam	244113	2405	0.99025	0.00975	**246518**	7.620454209
chr2L	dme-mir-2b-1	623	7	0.98889	0.01111	**630**	0.019474829
chr2R	dme-mir-987	803	11	0.98709	0.01291	**814**	0.025147259
chr2R	dme-mir-281-2	5100	74	0.98579	0.01421	**5174**	0.159925441
chr3L	dme-mir-276b	530	11	0.98057	0.01943	**541**	0.016708167
chr2L	dme-mir-965	1129	32	0.97286	0.02714	**1161**	0.035873872
chr2R	dme-mir-281-1	17602	501	0.97235	0.02765	**18103**	0.559592219
chr3R	dme-mir-10	19132	599	0.96967	0.03033	**19731**	0.609917652
chrX	dme-mir-13b-2	92	4	0.96335	0.03665	**96**	0.002952137
chr3L	dme-mir-263b	1144	46	0.96175	0.03825	**1190**	0.036770333
chr3R	dme-mir-996	29997	1218	0.96098	0.03902	**31215**	0.964931435
chr3L	dme-mir-219	84	4	0.96000	0.04000	**88**	0.002704837
chr3L	dme-mir-956	4342	189	0.95829	0.04171	**4531**	0.140064211
chr2L	dme-mir-87	908	42	0.95579	0.04421	**950**	0.029366807
chr2R	dme-mir-308	1864	105	0.94667	0.05333	**1969**	0.060866571
chr3L	dme-mir-33	9633	581	0.94312	0.05688	**10214**	0.315739544
chr2L	dme-mir-79	12143	767	0.94063	0.05937	**12910**	0.399063995
chr3R	dme-mir-1001	106	7	0.93805	0.06195	**113**	0.003493104
chr2R	dme-mir-307	2063	147	0.93348	0.06652	**2210**	0.068316467
chr2L	dme-mir-263a	11829	858	0.93241	0.06759	**12687**	0.392170527
chrX	dme-mir-210	409	35	0.92117	0.07883	**444**	0.013725119
chr2L	dme-mir-1005	122	11	0.92075	0.07925	**133**	0.004095897
chr3L	dme-mir-276a	90583	7868	0.92008	0.07992	**98451**	3.043359558
chr3R	dme-mir-284	523	56	0.90328	0.09672	**579**	0.017898297
chr3R	dme-mir-1015	62	7	0.89855	0.10145	**69**	0.002132958
chrX	dme-mir-304	17186	1946	0.89829	0.10171	**19132**	0.591416607
chr2R	dme-mir-184	15336	1890	0.89028	0.10972	**17226**	0.53249752
chr2L	dme-mir-133	1065	133	0.88898	0.11102	**1198**	0.037033091
chr2L	dme-mir-1006	415	53	0.88770	0.11230	**468**	0.014451561
chr3R	dme-mir-13a	797	102	0.88703	0.11297	**899**	0.027774818
chr3R	dme-mir-1017	25	4	0.87719	0.12281	**29**	0.000881004

chr2R	dme-mir-31a	24842	3969	0.86224	0.13776	**28811**	0.890618047
chrX	dme-mir-980	2995	539	0.84748	0.15252	**3534**	0.109244532
chr2L	dme-mir-124	2863	529	0.84417	0.15583	**3392**	0.104839511
chr2L	dme-mir-2b-2	615	140	0.81457	0.18543	**755**	0.023338886
chr3R	dme-mir-iab-4	94	25	0.79325	0.20675	**119**	0.003663123
chr3R	dme-mir-998	1074	294	0.78509	0.21491	**1368**	0.042288209
chr3L	dme-mir-190	162	46	0.78072	0.21928	**208**	0.00641433
chr2R	dme-mir-1008	106	39	0.73356	0.26644	**145**	0.004466847
chr3R	dme-mir-279	14571	5439	0.72819	0.27181	**20010**	0.618557825
chr2L	dme-mir-2a-2	1047	392	0.72759	0.27241	**1439**	0.044482994
chr3R	dme-mir-iab-4as	144	56	0.72000	0.28000	**200**	0.006182487
chr2R	dme-mir-137	341	133	0.71941	0.28059	**474**	0.014652494
chr3L	dme-mir-955	59	25	0.70659	0.29341	**84**	0.002581188
chr3R	dme-mir-277	76053	33397	0.69487	0.30513	**109450**	3.383366128
chr2R	dme-mir-8	447346	198170	0.69301	0.30699	**645516**	19.95447212
chrX	dme-mir-1007	47	21	0.69118	0.30882	**68**	0.002102046
chr2R	dme-mir-1009	38	18	0.68468	0.31532	**56**	0.00171564
chr2R	dme-mir-989	44	21	0.67692	0.32308	**65**	0.002009308

Testis enriched miRNAs

chrom	miRNA	Male Body reads	Testis reads	BM/BM+T	Testis/BM+T	Sum Reads	% miRNA
chrX	dme-mir-975	33	7469	0.00440	0.99560	**7502**	0.231905256
chr2R	dme-mir-310	55	11746	0.00466	0.99534	**11801**	0.36479791
chr2R	dme-mir-311	68	12537	0.00539	0.99461	**12605**	0.389651525
chr2L	dme-mir-959	478	60382	0.00785	0.99215	**60860**	1.881332152
chrX	dme-mir-978	241	29600	0.00808	0.99192	**29841**	0.922443182
chrX	dme-mir-979	21	1740	0.01193	0.98807	**1761**	0.054421381
chr2L	dme-mir-964	437	35403	0.01219	0.98781	**35840**	1.107887009
chrX	dme-mir-976	380	26338	0.01422	0.98578	**26718**	0.825903573
chr2R	dme-mir-312	95	5964	0.01568	0.98432	**6059**	0.187298577
chr3R	dme-mir-92b	42	2615	0.01581	0.98419	**2657**	0.082118942
chrX	dme-mir-972	61	3364	0.01781	0.98219	**3425**	0.105859709
chrX	dme-mir-977	680	28350	0.02342	0.97658	**29030**	0.897388622
chrX	dme-mir-983	724	23562	0.02981	0.97019	**24286**	0.750739922
chr2R	dme-mir-992	45	1383	0.03152	0.96848	**1428**	0.044127532
chrX	dme-mir-971	4	116	0.03347	0.96653	**120**	0.003694039
chr2R	dme-mir-988	876	23055	0.03661	0.96339	**23931**	0.739750538
chr2R	dme-mir-313	59	1295	0.04357	0.95643	**1354**	0.041855466
chr3R	dme-mir-92a	254	4984	0.04849	0.95151	**5238**	0.161919445
chr3R	dme-mir-318	4	70	0.05405	0.94595	**74**	0.002287522
chr3R	dme-mir-994	4	67	0.05674	0.94326	**71**	0.002179328
chr2R	dme-mir-3	2	28	0.06667	0.93333	**30**	0.000927374
chrX	dme-mir-984	551	7704	0.06675	0.93325	**8255**	0.255166864
chr2L	dme-mir-1004	44	504	0.08029	0.91971	**548**	0.016940025
chr2L	dme-mir-960	1717	19026	0.08277	0.91723	**20743**	0.641217054
chr3R	dme-mir-1011	1	11	0.08696	0.91304	**12**	0.000355493
chrX	dme-mir-12	21306	217798	0.08911	0.91089	**239104**	7.391291592
chr2L	dme-mir-961	177	1670	0.09586	0.90414	**1847**	0.057079847

chr2L	dme-mir-963	368	3241	0.10197	0.89803	**3609**	0.111563048
chr3L	dme-mir-274	3593	27748	0.11464	0.88536	**31341**	0.968827221
chr3R	dme-mir-317	2370	15712	0.13107	0.86893	**18082**	0.558943528
chr2L	dme-mir-9b	4263	23545	0.15330	0.84670	**27808**	0.859598032
chrX	dme-mir-985	214	1124	0.16000	0.84000	**1338**	0.041345405
chr2L	dme-mir-305	13965	65041	0.17676	0.82324	**79006**	2.442253734
chr4	dme-mir-954	50	217	0.18727	0.81273	**267**	0.008253625
chr3R	dme-mir-34	9383	40124	0.18953	0.81047	**49507**	1.530382746
chr2L	dme-mir-966	5	21	0.19231	0.80769	**26**	0.000803724
chr2L	dme-mir-962	401	1649	0.19566	0.80434	**2050**	0.063355069
chr2R	dme-mir-991	120	445	0.21258	0.78742	**565**	0.017450079
chr3R	dme-mir-1013	52	189	0.21577	0.78423	**241**	0.007449901
chrX	dme-mir-982	118	420	0.21933	0.78067	**538**	0.016630899
chr2L	dme-mir-306	1152	3329	0.25711	0.74289	**4481**	0.13850323
chr3L	dme-mir-316	5546	15460	0.26403	0.73597	**21006**	0.649331456
chrX	dme-mir-303	142	396	0.26419	0.73581	**538**	0.016615442
chr3R	dme-mir-2c	27	67	0.28877	0.71123	**94**	0.002890314
chrX	dme-mir-973	76	179	0.29862	0.70138	**255**	0.007867218
chr3R	dme-mir-11	14438	32372	0.30844	0.69156	**46810**	1.446996236
chr2L	dme-mir-125	5238	11659	0.31000	0.69000	**16897**	0.522312177
chrX	dme-mir-283	577	1257	0.31470	0.68530	**1834**	0.056677973
chr2L	dme-mir-2a-1	21	46	0.31579	0.68421	**67**	0.002055678
chr3L	dme-mir-193	12	25	0.32877	0.67123	**37**	0.001128304

At least 10 normalized reads in the summed normalized reads were required. A ratio (BodyM/BodyM+Testis) >=0.66 is male body biased. A ratio (Testis/Body M+Testis) >=0.66 is testis biased. BM: Body Male; T: testis

TABLE S8: Adult Female Body vs. Ovary biased miRNAs

Female Body (female somatic tissues) biased:

chrom	miRNA	Female Body reads	Ovary reads	BF/BF+Ov	BF/BF+Ov	Sum Reads	% miRNA
chr3R	dme-mir-1000	206	0	1	0	**206**	0.016796842
chr3R	dme-mir-1001	29	0	1	0	**29**	0.002364604
chr2L	dme-mir-1004	13	0	1	0	**13**	0.001059995
chr3R	dme-mir-1014	66	0	1	0	**66**	0.005381513
chr3R	dme-mir-1015	15	0	1	0	**15**	0.001223071
chr2R	dme-mir-137	80	0	1	0	**80**	0.006523046
chrX	dme-mir-210	121	0	1	0	**121**	0.009866106
chr3L	dme-mir-219	21	0	1	0	**21**	0.001712299
chr3L	dme-mir-263b	263	0	1	0	**263**	0.021444512
chr3L	dme-mir-276b	112	0	1	0	**112**	0.009132264
chr2L	dme-mir-375	811	0	1	0	**811**	0.066127374
chr3L	dme-mir-957	307	0	1	0	**307**	0.025032187
chr3L	dme-mir-958	2103	0	1	0	**2103**	0.171474559
chrX	dme-mir-981	19	0	1	0	**19**	0.001549223
chr2R	dme-mir-987	308	0	1	0	**308**	0.025113725
chr3R	dme-mir-993	314	0	1	0	**314**	0.025602954
chr3R	dme-mir-iab-4as	28	0	1	0	**28**	0.002283066
chr2L	dme-mir-124	470	2	0.99590	0.00410	**472**	0.038480513
chr2L	dme-mir-133	300	2	0.99360	0.00640	**302**	0.024619041
chr3L	dme-mir-314	4449	31	0.99310	0.00690	**4480**	0.365284793
chr3L	dme-mir-274	1179	10	0.99187	0.00813	**1189**	0.096921485
chr3R	dme-mir-277	19989	168	0.99166	0.00834	**20157**	1.643577423
chr3L	dme-mir-9a	8813	77	0.99130	0.00870	**8890**	0.724899812
chr3L	dme-mir-956	1393	17	0.98766	0.01234	**1410**	0.115001112
chr3R	dme-mir-10	6256	79	0.98749	0.01251	**6335**	0.51656459
chr2L	dme-mir-1	199357	2994	0.98520	0.01480	**202351**	16.4993386
chr3R	dme-mir-929	819	23	0.97246	0.02754	**842**	0.068671122
chr3R	dme-mir-252	1420	41	0.97221	0.02779	**1461**	0.119094084
chr3R	dme-mir-13a	202	10	0.95434	0.04566	**212**	0.017258791
chr2R	dme-mir-1008	36	2	0.94904	0.05096	**38**	0.003092991
chr2L	dme-mir-932	70	4	0.94766	0.05234	**74**	0.006022905
chr3R	dme-mir-iab-4	35	2	0.94766	0.05234	**37**	0.003011453
chr3L	dme-mir-276	37412	2525	0.93678	0.06322	**39937**	3.256354306
chr3L	dme-mir-955	26	2	0.93080	0.06920	**28**	0.00227761
chr2L	dme-mir-1006	101	8	0.92889	0.07111	**109**	0.008865826
chr3R	dme-mir-1013	24	2	0.92546	0.07454	**26**	0.002114534
chr3L	dme-mir-276a	31855	2710	0.92159	0.07841	**34565**	2.818378803
chr2R	dme-mir-278	2040	226	0.90020	0.09980	**2266**	0.184779232
chrX	dme-mir-980	908	106	0.89518	0.10482	**1014**	0.082705681
chr2R	dme-mir-31a	11038	1703	0.86633	0.13367	**12741**	1.038880662
chr3R	dme-mir-1010	92	15	0.85610	0.14390	**107**	0.008762464
chr3R	dme-mir-999	771	141	0.84529	0.15471	**912**	0.074372131
chr2R	dme-mir-281-1	5351	1009	0.84134	0.15866	**6360**	0.518587988
chr3R	dme-mir-2c	10	2	0.83801	0.16199	**12**	0.000973001

chr2R	dme-mir-281-2	1730	340	0.83566	0.16434	**2070**	0.168802027
chr2L	dme-mir-100	366	73	0.83285	0.16715	**439**	0.035832503
chr3L	dme-mir-190	169	35	0.82926	0.17074	**204**	0.016617099
chr2L	dme-mir-87	535	110	0.82922	0.17078	**645**	0.052607222
chr2L	dme-let-7	8023	1722	0.82326	0.17674	**9745**	0.794619587
chr2R	dme-mir-8	191101	44755	0.81024	0.18976	**235856**	19.23123099
chr2L	dme-mir-125	1718	485	0.77977	0.22023	**2203**	0.17964509
chr3R	dme-mir-279	4143	1208	0.77422	0.22578	**5351**	0.436324888
chr3L	dme-mir-316	1713	644	0.72686	0.27314	**2357**	0.192162262
chr3R	dme-mir-284	116	44	0.72292	0.27708	**160**	0.013083682

Ovary enriched miRNAs:

chrom	miRNA	Female Body reads	Ovary reads	BF/BF+Ov	Ov/BF+Ov	Sum Reads	% miRNA
chr3R	dme-mir-318	76	34886	0.00217	0.99783	**34962**	2.850769902
chrX	dme-mir-984	7	1378	0.00505	0.99495	**1385**	0.112954019
chr3R	dme-mir-994	76	14463	0.00523	0.99477	**14539**	1.185511752
chr2R	dme-mir-313	8	1216	0.00654	0.99346	**1224**	0.099795454
chrX	dme-mir-303	1	128	0.00778	0.99222	**129**	0.010484476
chrX	dme-mir-983	7	798	0.00869	0.99131	**805**	0.065667938
chr2R	dme-mir-312	40	2803	0.01407	0.98593	**2843**	0.231810914
chr2R	dme-mir-1009	3	174	0.01695	0.98305	**177**	0.014430438
chr2R	dme-mir-311	13	460	0.02748	0.97252	**473**	0.038573619
chrX	dme-mir-982	3	89	0.03264	0.96736	**92**	0.007495147
chr2R	dme-mir-310	9	228	0.03796	0.96204	**237**	0.019333034
chr2L	dme-mir-275	763	12586	0.05716	0.94284	**13349**	1.088479123
chr3R	dme-mir-92b	68	990	0.06429	0.93571	**1058**	0.086246167
chr3R	dme-mir-92a	169	1514	0.10044	0.89956	**1683**	0.137196605
chr3R	dme-mir-995	459	3679	0.11093	0.88907	**4138**	0.337377347
chr2L	dme-mir-966	6	41	0.12877	0.87123	**47**	0.003799254
chr2R	dme-mir-989	13128	88414	0.12929	0.87071	**101542**	8.279510048
chr2L	dme-mir-9b	1608	10570	0.13204	0.86796	**12178**	0.99298085
chr2L	dme-mir-2a-1	22	118	0.15723	0.84277	**140**	0.011408674
chr2L	dme-mir-306	499	1954	0.20340	0.79660	**2453**	0.200041589
chr2R	dme-mir-184	7879	30821	0.20359	0.79641	**38700**	3.155536026
chr4	dme-mir-954	11	43	0.20550	0.79450	**54**	0.004364565
chr3R	dme-mir-996	8051	28482	0.22038	0.77962	**36533**	2.978840048
chrX	dme-mir-13b-2	55	172	0.24224	0.75776	**227**	0.018512798
chr2L	dme-mir-79	2196	6723	0.24621	0.75379	**8919**	0.727260898
chr2L	dme-mir-2b-2	319	862	0.27007	0.72993	**1181**	0.096309284
chr2L	dme-mir-959	3	8	0.27953	0.72047	**11**	0.000875095
chr2R	dme-mir-7	928	2356	0.28254	0.71746	**3284**	0.267806437
chr3L	dme-mir-33	1974	4025	0.32907	0.67093	**5999**	0.48912155
chr3R	dme-mir-34	3245	6344	0.33839	0.66161	**9589**	0.781900759

At least 10 normalized reads in summed normalized reads were required. A ratio (BodyF/BodyF+Ovary) >=0.66 is female body biased and a ratio (Ovary/Body M+Ovary) >=0.66 is ovary biased. BF: Body Female; Ov: Ovary.

TABLE S9: Raw Counts miRNA-Seq

		Late Embryo Lymphoid Cells		L3 Larvae Salivary Glands		Adult Head		Adult Body		Adult Gonads	
Chrom	miRNA	S2 (M)	Kc (F)	S. Glands M	S. Glands F	Head M	Head F	Body M	Body F	Testis	Ovary
chr3L	dme-bantam	35460	18240	12348	24423	103920	152727	244113	72941	28463	687
chr2L	dme-let-7	5	5	30	219	20606	51163	28931	8023	891	11559
chr2L	dme-let-7-as	0	0	0	0	0	0	0	0	0	0
chr2L	dme-mir-1	23	55	679	1503	126814	175008	496888	199357	1549	241
chr3R	dme-mir-10	1	18	199	395	3730	4794	19132	6256	41	171
chr2L	dme-mir-100	0	0	1	10	1004	1527	1103	366	38	226
chr3R	dme-mir-1000	1	867	13	27	18668	25776	875	206	0	1
chr3R	dme-mir-1001	0	0	0	0	162	208	106	29	0	2
chr2L	dme-mir-1002	0	0	0	0	0	0	0	0	0	0
chr3R	dme-mir-1003	1487	902	34	30	107	228	124	34	16	63
chr2L	dme-mir-1004	0	0	0	1	157	253	44	13	0	144
chr2L	dme-mir-1004-as	0	0	0	0	1	0	0	0	0	0
chr2L	dme-mir-1005	1	0	16	11	101	332	122	44	14	3
chr2L	dme-mir-1006	58	97	71	107	315	519	415	101	4	15
chr2L	dme-mir-1006-as	0	0	0	0	0	0	0	0	0	0
chrX	dme-mir-1007	13	5	0	4	109	125	47	19	10	6
chr2R	dme-mir-1008	94	175	8	9	119	104	106	36	1	11
chr2R	dme-mir-1009	4	6	5	2	30	85	38	3	90	5
chr3R	dme-mir-1010	1	71	1	0	851	1677	319	92	8	168
chr3R	dme-mir-1011	0	0	0	0	8	19	1	0	0	3
chr3R	dme-mir-1012	164	42	230	346	374	623	215	79	40	46
chr3R	dme-mir-1013	1	4	3	4	90	131	52	24	1	54
chr3R	dme-mir-1014	0	0	0	0	0	0	248	66	0	0
chr3R	dme-mir-1015	0	0	0	0	0	1	62	15	0	2
chr2R	dme-mir-1016	5	4	3	4	35	76	18	8	0	6
chr3R	dme-mir-1017	0	0	0	0	183	278	25	6	0	1
chr3R	dme-mir-11	15690	9328	5007	12439	6209	21450	14438	5606	3338	9249
chrX	dme-mir-12	415	7053	16391	43021	1117	2682	21306	2801	2280	62228
chr2L	dme-mir-124	8	63	10	16	29849	48896	2863	470	1	151
chr2L	dme-mir-124-as	0	0	0	0	0	0	0	0	0	0
chr2L	dme-mir-125	10	3	23	63	7175	20670	5238	1718	251	3331
chrX	dme-mir-12-as	0	0	0	0	0	0	0	0	0	0
chr2L	dme-mir-133	5	3	6	4	4836	16473	1065	300	1	38
chr2R	dme-mir-137	0	2	0	1	701	1301	341	80	0	38
chr3R	dme-mir-13a	25	57	11	17	5608	9074	797	202	5	29
chr3R	dme-mir-13b	11557	9820	5207	12399	27953	34823	21017	7131	5476	5212
chr3R	dme-mir-13b-1	0	0	7	9	14	22	4	1	0	0
chrX	dme-mir-13b-2	299	300	62	70	27	101	92	55	89	1
chr2R	dme-mir-14	182756	130160	2602	2658	31243	68581	26146	5504	1571	6722
chr2R	dme-mir-14-as	0	0	0	0	2	1	0	0	0	0
chr2R	dme-mir-184	54062	73256	810	1085	51441	89330	15336	7879	15944	540
chr3L	dme-mir-190	171	308	130	168	1250	634	162	169	18	13
chr3L	dme-mir-193	3	64	0	4	1978	4491	12	1	1	7
chr2L	dme-mir-1-as	0	0	0	0	0	0	0	0	0	0
chrX	dme-mir-210	1	1	31	29	30904	106957	409	121	0	10
chr3L	dme-mir-219	0	0	1	0	259	437	84	21	0	1
chr2RHet	dme-mir-2279	8	9	2	5	7	16	12	3	0	3
chr2RHet	dme-mir-2279-as	0	1	0	1	0	0	0	0	0	0
chr2L	dme-mir-2280	0	0	0	0	0	0	1	0	0	0
chr3R	dme-mir-2281	0	0	0	0	0	1	4	1	0	0
chr3L	dme-mir-2282	1	3	0	0	0	0	0	0	0	0
chr3R	dme-mir-2283	0	0	0	0	3	3	4	0	0	1
chr3R	dme-mir-252	13294	137	831	644	14416	37717	4036	1420	21	990
chr2L	dme-mir-263a	66	3	27399	39275	17316	25950	11829	3892	3639	245
chr2L	dme-mir-263a-as	0	0	0	0	0	0	0	0	0	0
chr3L	dme-mir-263b	1	2	2	6	3141	6005	1144	263	0	13
chr3L	dme-mir-274	1	0	12	16	13878	55708	3593	1179	5	7928
chr2L	dme-mir-275	461	832	13608	2588	668	2503	1122	763	6511	605
chr2L	dme-mir-275-as	0	0	0	1	1	1	0	0	0	0
chr3L	dme-mir-276	4524	10288	1946	5840	68388	58112	47955	37412	1306	123
chr3L	dme-mir-276a	9143	7257	1158	3728	73713	163232	90583	31855	1402	2248
chr3L	dme-mir-276b	5	125	1	8	7324	16746	530	112	0	3
chr3R	dme-mir-277	3703	1688	807	1660	59156	104947	76053	19989	87	9542
chr2R	dme-mir-278	47	1099	797	526	2829	9122	4966	2040	117	2426
chr3R	dme-mir-279	16526	10095	321	1492	8345	13021	14571	4143	625	1554
chr3R	dme-mir-279-as	0	0	0	0	0	0	0	0	0	0
chr2R	dme-mir-281-1	179	132	55	118	260	557	17602	5351	522	143
chr2R	dme-mir-281-2	34	23	53	84	277	439	5100	1730	176	21
chr3L	dme-mir-282	13543	3084	4147	31936	6842	6760	23325	12554	3427	11072
chr3L	dme-mir-282-as	0	0	0	0	0	0	0	0	0	0
chrX	dme-mir-283	48	930	4683	7791	370	448	577	363	133	359
chr3R	dme-mir-284	0	5	2	1	518	2009	523	116	23	16
chr3L	dme-mir-285	0	0	12	38	40821	63213	76	4	0	0
chr2R	dme-mir-286	43	14	23	31	4	15	5	1	0	0
chr2L	dme-mir-287	0	0	0	0	0	0	0	1	0	0
chr3L	dme-mir-289	0	0	0	0	0	0	0	1	0	0
chr2L	dme-mir-2a	7839	19872	7976	9677	40963	62518	42678	21855	19231	14216
chr2L	dme-mir-2a-1	173	259	16	27	34	64	21	22	61	13
chr2L	dme-mir-2a-2	2015	6472	112	164	1780	4486	1047	363	339	112
chr2L	dme-mir-2b	9981	13905	6378	7854	43346	58488	18220	8986	8217	6058
chr2L	dme-mir-2b-1	498	138	461	465	1684	1927	623	328	188	2
chr2L	dme-mir-2b-2	431	1100	189	177	714	1184	615	319	446	40
chr3R	dme-mir-2c	9	13	3	0	163	287	27	10	1	19
chr2R	dme-mir-3	15	8	1	1	3	5	2	1	3	8
chrX	dme-mir-303	7	8	0	0	1	3	142	1	66	113
chrX	dme-mir-304	34	841	15014	30430	1286	2492	17186	2108	743	556
chrX	dme-mir-304-as	0	0	0	0	0	0	0	0	0	0
chr2L	dme-mir-305	3321	6880	7165	9763	11336	20428	13965	3692	2694	18583
chr2L	dme-mir-305-as	0	3	2	7	12	8	0	1	1	0
chr2L	dme-mir-306	2500	4089	1067	1144	752	2067	1152	499	1011	951
chr2R	dme-mir-307	932	22	1	0	5587	15933	2063	482	245	42
chr2R	dme-mir-307-as	1	0	5	17	0	3	6	1	0	0

chr2R	dme-mir-308	1483	1685	2781	5046	1048	1674	1864	684	323	30
chr2R	dme-mir-309	4	3	1	0	0	1	0	0	0	0
chr2R	dme-mir-310	8	4	1	0	2	2	55	9	118	3356
chr2R	dme-mir-311	8	2	0	0	1	2	68	13	238	3582
chr2R	dme-mir-312	3	6	0	0	8	9	95	40	1450	1704
chr2R	dme-mir-313	2	2	0	0	4	4	59	8	629	370
chr3L	dme-mir-314	0	2	2	3	18	72	11627	4449	16	29
chr3L	dme-mir-314-as	0	0	0	0	0	0	0	1	0	0
chr3L	dme-mir-315	0	0	0	0	1204	2424	24	7	0	12
chr3L	dme-mir-316	0	0	8	14	1119	3236	5546	1713	333	4417
chr3L	dme-mir-316-as	0	0	0	0	0	0	1	0	0	0
chr3R	dme-mir-317	9157	14069	718	1536	8974	14533	2370	561	529	4489
chr3R	dme-mir-317-as	0	0	0	0	0	0	0	1	0	0
chr3R	dme-mir-318	13	60	0	1	1	6	4	76	18047	20
chr2R	dme-mir-31a	5	12	521	763	11606	22138	24842	11038	881	1134
chrX	dme-mir-31b	3	3	0	0	7	44	2068	447	170	875
chr3L	dme-mir-33	1927	2696	1239	2256	1864	3555	9633	1974	2082	166
chr3R	dme-mir-34	13980	15190	1643	2983	45375	77345	9383	3245	3282	11464
chr2L	dme-mir-375	1	0	18745	34030	57	182	4698	811	0	1491
chr2R	dme-mir-4	6	2	1	6	3	5	2	0	0	0
chr2R	dme-mir-5	14	9	18	26	7	22	14	4	4	0
chr2R	dme-mir-6-1	7	1	0	0	0	0	0	0	0	0
chr2R	dme-mir-6-2	1	1	0	0	0	0	0	0	0	0
chr2R	dme-mir-6-3	2	1	0	0	0	0	0	0	0	0
chr2R	dme-mir-6-3-as	0	0	0	0	0	0	0	0	0	0
chr2R	dme-mir-7	332	243	176	270	13849	20729	3010	928	1219	863
chr2L	dme-mir-79	2043	3617	1604	3518	7700	13318	12143	2196	3478	219
chr2R	dme-mir-8	4003	18559	84972	180692	184826	244757	447346	191101	23152	56620
chr2L	dme-mir-87	0	2	2	4	2344	4107	908	535	57	12
chrX	dme-mir-927	0	1	0	0	662	994	41	9	0	0
chr3R	dme-mir-929	1	2	20	39	12012	13343	1810	819	12	4
chr3R	dme-mir-929-as	0	0	0	0	0	0	2	0	0	0
chr3R	dme-mir-92a	13	1478	2	7	1421	2484	254	169	783	1424
chr3R	dme-mir-92a-as	0	0	0	0	0	0	0	0	0	0
chr3R	dme-mir-92b	20	447	31	64	54	68	42	68	512	747
chr2L	dme-mir-932	5	118	4	2	3614	8766	276	70	2	45
chr4	dme-mir-954	11	61	1	1	59	124	50	11	22	62
chr3L	dme-mir-955	0	0	0	0	54	84	59	26	1	7
chr3L	dme-mir-956	0	1	0	1	4	20	4342	1393	9	54
chr3L	dme-mir-957	0	0	2	7	6154	12255	839	307	0	0
chr3L	dme-mir-958	1	19	0	1	3	29	7379	2103	0	9
chr2L	dme-mir-959	0	0	0	0	7	18	478	3	4	17252
chr2L	dme-mir-960	0	1	0	2	30	103	1717	34	11	5436
chr2L	dme-mir-961	0	0	0	0	5	20	177	5	5	477
chr2L	dme-mir-962	0	0	1	0	28	55	401	39	33	471
chr2L	dme-mir-963	0	1	0	0	5	20	368	6	1	926
chr2L	dme-mir-964	0	0	0	0	7	41	437	10	5	10115
chr2L	dme-mir-965	559	608	131	567	361	613	1129	201	145	9
chr2L	dme-mir-966	15	39	1	4	8	12	5	6	21	6
chr2L	dme-mir-967	10	7	0	1	4	2	3	0	0	0
chr2L	dme-mir-967-as	0	0	0	0	0	0	0	1	0	0
chr2L	dme-mir-968	0	0	0	0	2	3	0	0	0	0
chrX	dme-mir-969	0	0	0	2	194	192	27	6	0	0
chrX	dme-mir-970	1140	1185	177	198	1442	3119	656	205	59	100
chrX	dme-mir-971	0	35	0	1	40	70	4	0	0	33
chrX	dme-mir-972	0	0	0	0	0	1	61	0	0	961
chrX	dme-mir-973	0	8	0	0	0	0	76	1	0	51
chrX	dme-mir-974	0	2	0	0	5	2	236	1	0	82
chrX	dme-mir-975	0	3	0	0	0	0	33	0	0	2134
chrX	dme-mir-976	0	1	0	0	0	2	380	2	0	7525
chrX	dme-mir-977	1	44	0	0	3	4	680	0	0	8100
chrX	dme-mir-978	1	4	0	0	2	3	241	1	0	8457
chrX	dme-mir-979	0	0	0	0	0	0	21	0	0	497
chrX	dme-mir-980	1534	302	3	3	349	1464	2995	908	55	154
chrX	dme-mir-981	1	952	0	3	231	968	56	19	0	16
chrX	dme-mir-981-as	1	4	0	0	1	1	0	0	0	0
chrX	dme-mir-982	0	11	0	0	1	3	118	3	46	120
chrX	dme-mir-983	6	9	0	0	9	16	724	7	413	6732
chrX	dme-mir-983-1	0	0	0	0	0	0	1	0	2	1
chrX	dme-mir-984	25	68	0	0	10	11	551	7	713	2201
chrX	dme-mir-985	0	0	0	0	1	0	214	2	1	321
chr2R	dme-mir-986	3	29	211	226	271	1006	1880	510	301	309
chr2R	dme-mir-987	0	3	9	36	14710	16043	803	308	0	3
chr2R	dme-mir-988	13800	15082	558	539	620	1460	876	280	214	6587
chr2R	dme-mir-988-as	1	0	0	0	0	0	0	0	0	0
chr2R	dme-mir-989	3	158	14	30	1	6	44	13128	45737	6
chr2R	dme-mir-990	0	0	0	0	382	430	8	2	0	0
chr2R	dme-mir-991	0	0	0	0	0	1	120	2	4	127
chr2R	dme-mir-992	2	4	0	0	0	1	45	1	0	395
chr3R	dme-mir-993	0	1	0	2	982	1433	1448	314	0	1
chr3R	dme-mir-994	5	27	0	2	2	3	4	76	7482	19
chr3R	dme-mir-995	3761	3754	1631	3220	2255	3287	909	459	1903	228
chr3R	dme-mir-995-as	0	0	0	0	0	0	1	0	0	0
chr3R	dme-mir-996	23117	10275	2982	6077	10447	27396	29997	8051	14734	348
chr3R	dme-mir-997	0	0	0	0	0	0	184	0	0	59
chr3R	dme-mir-998	3118	3965	2123	5021	4751	5610	1074	459	403	84
chr3R	dme-mir-999	247	374	27	35	7193	10562	1464	771	73	673
chr3L	dme-mir-9a	49	83	1540	2193	12061	32808	28787	8813	40	6846
chr2L	dme-mir-9b	2463	7931	1257	1648	1557	3726	4263	1608	5468	6727
chr2L	dme-mir-9c	1896	3769	737	920	2615	5475	5508	2430	2337	2050
chr3R	dme-mir-iab-4	0	1	0	0	2	2	94	35	1	7
chr3R	dme-mir-iab-4as	0	0	0	0	0	1	144	28	0	16

S. Glands: Salivary Glands; M: Male; F: Female

TABLE S10: Normalized read counts in libraries

Chrom	miRNA	S2	Kc	S. Glands M	S. Glands F	Head M	Head F	Body M	Body F	Testis	Ovary	SUM
chr3L	dme-bantam	35460	27334	19757	24423	181971	152727	244113	250083	2405	55022	**993293**
chr2L	dme-let-7	5	7	48	219	36082	51163	28931	27507	40457	1722	**186142**
chr2L	dme-let-7-as	0	0	0	0	0	0	0	0	0	0	**0**
chr2L	dme-mir-1	23	82	1086	1503	222060	175008	496888	683509	844	2994	**1583998**
chr2L	dme-mir-1-as	0	0	0	0	0	0	0	0	0	0	**0**
chr3R	dme-mir-10	1	27	318	395	6531	4794	19132	21449	599	79	**53326**
chr2L	dme-mir-100	0	0	2	10	1758	1527	1103	1255	791	73	**6519**
chr3R	dme-mir-1000	1	1299	21	27	32689	25776	875	706	4	0	**61398**
chr3R	dme-mir-1001	0	0	0	0	284	208	106	99	7	0	**704**
chr2L	dme-mir-1002	0	0	0	0	0	0	0	0	0	0	**0**
chr3R	dme-mir-1003	1487	1352	54	30	187	228	124	117	221	31	**3830**
chr2L	dme-mir-1004	0	0	0	1	275	253	44	45	504	0	**1121**
chr2L	dme-mir-1004-as	0	0	0	0	2	0	0	0	0	0	**2**
chr2L	dme-mir-1005	1	0	26	11	177	332	122	151	11	27	**857**
chr2L	dme-mir-1006	58	145	114	107	552	519	415	346	53	8	**2316**
chrX	dme-mir-1007	13	7	0	4	191	125	47	65	21	19	**493**
chr2R	dme-mir-1008	94	262	13	9	208	104	106	123	39	2	**960**
chr2R	dme-mir-1009	4	9	8	2	53	85	38	10	18	174	**400**
chr3R	dme-mir-1010	1	106	2	0	1490	1677	319	315	588	15	**4514**
chr3R	dme-mir-1011	0	0	0	0	14	19	1	0	11	0	**45**
chr3R	dme-mir-1012	164	63	368	346	655	623	215	271	161	77	**2943**
chr3R	dme-mir-1013	1	6	5	4	158	131	52	82	189	2	**630**
chr3R	dme-mir-1014	0	0	0	0	0	0	248	226	0	0	**474**
chr3R	dme-mir-1015	0	0	0	0	0	1	62	51	7	0	**121**
chr2R	dme-mir-1016	5	6	5	4	61	76	18	27	21	0	**224**
chr3R	dme-mir-1017	0	0	0	0	320	278	25	21	4	0	**648**
chr3R	dme-mir-11	15690	13979	8011	12439	10872	21450	14438	19221	32372	6453	**154924**
chrX	dme-mir-12	415	10569	26226	43021	1956	2682	21306	9603	217798	4407	**337984**
chr2L	dme-mir-124	8	94	16	16	52268	48896	2863	1611	529	2	**106303**
chr2L	dme-mir-125	10	4	37	63	12564	20670	5238	5890	11659	485	**56620**
chr2L	dme-mir-133	5	4	10	4	8468	16473	1065	1029	133	2	**27193**
chr2R	dme-mir-137	0	3	0	1	1228	1301	341	274	133	0	**3281**
chr3R	dme-mir-13a	25	85	18	17	9820	9074	797	693	102	10	**20640**
chr3R	dme-mir-13b	11557	14716	8331	12399	48948	34823	21017	24449	18242	10586	**205067**
chr3R	dme-mir-13b-1	0	0	11	9	25	22	4	3	0	0	**74**
chrX	dme-mir-13b-2	299	450	99	70	47	101	92	189	4	172	**1522**
chr2R	dme-mir-14	182756	195051	4163	2658	54709	68581	26146	18871	23527	3037	**579498**
chr2R	dme-mir-184	54062	109778	1296	1085	90077	89330	15336	27014	1890	30821	**420688**
chr3L	dme-mir-190	171	462	208	168	2189	634	162	579	46	35	**4653**
chr3L	dme-mir-193	3	96	0	4	3464	4491	12	3	25	2	**8099**
chrX	dme-mir-210	1	1	50	29	54115	106957	409	415	35	0	**162012**
chr3L	dme-mir-219	0	0	2	0	454	437	84	72	4	0	**1052**
chr2RHet	dme-mir-2279	8	13	3	5	12	16	12	10	11	0	**91**
chr2RHet	dme-mir-2279-as	0	1	0	1	0	0	0	0	0	0	**2**
chr2L	dme-mir-2280	0	0	0	0	0	0	1	0	0	0	**1**
chr3R	dme-mir-2281	0	0	0	0	0	1	4	3	0	0	**8**
chr3L	dme-mir-2282	1	4	0	0	0	0	0	0	0	0	**5**
chr3R	dme-mir-2283	0	0	0	0	5	3	4	0	4	0	**16**
chr3R	dme-mir-252	13294	205	1330	644	25243	37717	4036	4869	3465	41	**90843**
chr2L	dme-mir-263a	66	4	43838	39275	30321	25950	11829	13344	858	7035	**172520**
chr3L	dme-mir-263b	1	3	3	6	5500	6005	1144	902	46	0	**13610**
chr3L	dme-mir-274	1	0	19	16	24301	55708	3593	4042	27748	10	**115438**
chr2L	dme-mir-275	461	1247	21773	2588	1170	2503	1122	2616	2118	12586	**48183**
chr2L	dme-mir-275-as	0	0	0	1	2	1	0	0	0	0	**4**
chr3L	dme-mir-276	4524	15417	3114	5840	119752	58112	47955	128270	431	2525	**385939**
chr3L	dme-mir-276a	9143	10875	1853	3728	129076	163232	90583	109217	7868	2710	**528285**
chr3L	dme-mir-276b	5	187	2	8	12825	16746	530	384	11	0	**30697**
chr3R	dme-mir-277	3703	2530	1291	1660	103586	104947	76053	68534	33397	168	**395869**
chr2R	dme-mir-278	47	1647	1275	526	4954	9122	4966	6994	8491	226	**38248**

chr3R	dme-mir-279	16526	15128	514	1492	14613	13021	14571	14205	5439	1208	**96716**
chr2R	dme-mir-281-1	179	198	88	118	455	557	17602	18346	501	1009	**39053**
chr2R	dme-mir-281-2	34	34	85	84	485	439	5100	5931	74	340	**12606**
chr3L	dme-mir-282	13543	4622	6635	31936	11981	6760	23325	43042	38752	6625	**187220**
chrX	dme-mir-283	48	1394	7493	7791	648	448	577	1245	1257	257	**21157**
chr3R	dme-mir-284	0	7	3	1	907	2009	523	398	56	44	**3949**
chr3L	dme-mir-285	0	0	19	38	71480	63213	76	14	0	0	**134840**
chr2R	dme-mir-286	43	21	37	31	7	15	5	3	0	0	**162**
chr2L	dme-mir-287	0	0	0	0	0	0	0	3	0	0	**3**
chr3L	dme-mir-289	0	0	0	0	0	0	0	3	0	0	**3**
chr2L	dme-mir-2a	7839	29779	12762	9677	71729	62518	42678	74931	49756	37175	**398844**
chr2L	dme-mir-2a-1	173	388	26	27	60	64	21	75	46	118	**997**
chr2L	dme-mir-2a-2	2015	9699	179	164	3117	4486	1047	1245	392	655	**22999**
chr2L	dme-mir-2b	9981	20837	10205	7854	75902	58488	18220	30809	21203	15884	**269383**
chr2L	dme-mir-2b-1	498	207	738	465	2949	1927	623	1125	7	363	**8901**
chr2L	dme-mir-2b-2	431	1648	302	177	1250	1184	615	1094	140	862	**7704**
chr3R	dme-mir-2c	9	19	5	0	285	287	27	34	67	2	**735**
chr2R	dme-mir-3	15	12	2	1	5	5	2	3	28	6	**79**
chrX	dme-mir-303	7	12	0	0	2	3	142	3	396	128	**692**
chrX	dme-mir-304	34	1260	24022	30430	2252	2492	17186	7227	1946	1436	**88286**
chr2L	dme-mir-305	3321	10310	11464	9763	19850	20428	13965	12658	65041	5208	**172008**
chr2L	dme-mir-305-as	0	4	3	7	21	8	0	3	0	2	**49**
chr2L	dme-mir-306	2500	6128	1707	1144	1317	2067	1152	1711	3329	1954	**23008**
chr2R	dme-mir-307	932	33	2	0	9783	15933	2063	1653	147	474	**31019**
chr2R	dme-mir-307-as	1	0	8	17	0	3	6	3	0	0	**38**
chr2R	dme-mir-308	1483	2525	4450	5046	1835	1674	1864	2345	105	624	**21951**
chr2R	dme-mir-309	4	4	2	0	0	1	0	0	0	0	**11**
chr2R	dme-mir-310	8	6	2	0	4	2	55	31	11746	228	**12081**
chr2R	dme-mir-311	8	3	0	0	2	2	68	45	12537	460	**13124**
chr2R	dme-mir-312	3	9	0	0	14	9	95	137	5964	2803	**9034**
chr2R	dme-mir-313	2	3	0	0	7	4	59	27	1295	1216	**2613**
chr3L	dme-mir-314	0	3	3	3	32	72	11627	15254	102	31	**27126**
chr3L	dme-mir-315	0	0	0	0	2108	2424	24	24	42	0	**4622**
chr3L	dme-mir-316	0	0	13	14	1959	3236	5546	5873	15460	644	**32745**
chr3R	dme-mir-317	9157	21083	1149	1536	15714	14533	2370	1923	15712	1023	**84200**
chr3R	dme-mir-318	13	90	0	1	2	6	4	261	70	34886	**35333**
chr2R	dme-mir-31a	5	18	834	763	20323	22138	24842	37845	3969	1703	**112439**
chrX	dme-mir-31b	3	4	0	0	12	44	2068	1533	3063	329	**7055**
chr3L	dme-mir-33	1927	4040	1982	2256	3264	3555	9633	6768	581	4025	**38031**
chr3R	dme-mir-34	13980	22763	2629	2983	79455	77345	9383	11126	40124	6344	**266132**
chr2L	dme-mir-375	1	0	29992	34030	100	182	4698	2781	5219	0	**77002**
chr2R	dme-mir-4	6	3	2	6	5	5	2	0	0	0	**29**
chr2R	dme-mir-5	14	13	29	26	12	22	14	14	0	8	**152**
chr2R	dme-mir-6	10	4	0	0	0	0	0	0	0	0	**14**
chr2R	dme-mir-7	332	364	282	270	24251	20729	3010	3182	3021	2356	**57796**
chr2L	dme-mir-79	2043	5420	2566	3518	13483	13318	12143	7529	767	6723	**67511**
chr2R	dme-mir-8	4003	27812	135955	180692	323642	244757	447346	655203	198170	44755	**2262335**
chr2L	dme-mir-87	0	3	3	4	4105	4107	908	1834	42	110	**11116**
chrX	dme-mir-927	0	1	0	0	1159	994	41	31	0	0	**2227**
chr3R	dme-mir-929	1	3	32	39	21034	13343	1810	2808	14	23	**39107**
chr3R	dme-mir-92a	13	2215	3	7	2488	2484	254	579	4984	1514	**14541**
chr3R	dme-mir-92b	20	670	50	64	95	68	42	233	2615	990	**4845**
chr2L	dme-mir-932	5	177	6	2	6328	8766	276	240	158	4	**15962**
chr4	dme-mir-954	11	91	2	1	103	124	50	38	217	43	**680**
chr3L	dme-mir-955	0	0	0	0	95	84	59	89	25	2	**353**
chr3L	dme-mir-956	0	1	0	1	7	20	4342	4776	189	17	**9354**
chr3L	dme-mir-957	0	0	3	7	10776	12255	839	1053	0	0	**24933**
chr3L	dme-mir-958	1	28	0	1	5	29	7379	7210	32	0	**14686**
chr2L	dme-mir-959	0	0	0	0	12	18	478	10	60382	8	**60908**
chr2L	dme-mir-960	0	1	0	2	53	103	1717	117	19026	21	**21040**
chr2L	dme-mir-961	0	0	0	0	9	20	177	17	1670	10	**1902**
chr2L	dme-mir-962	0	0	2	0	49	55	401	134	1649	64	**2353**

chr2L	dme-mir-963	0	1	0	0	9	20	368	21	3241	2	**3662**
chr2L	dme-mir-964	0	0	0	0	12	41	437	34	35403	10	**35937**
chr2L	dme-mir-965	559	911	210	567	632	613	1129	689	32	280	**5622**
chr2L	dme-mir-966	15	58	2	4	14	12	5	21	21	41	**192**
chr2L	dme-mir-967	10	10	0	1	7	2	3	0	0	0	**33**
chr2L	dme-mir-968	0	0	0	0	4	3	0	0	0	0	**7**
chrX	dme-mir-969	0	0	0	2	340	192	27	21	0	0	**581**
chrX	dme-mir-970	1140	1776	283	198	2525	3119	656	703	350	114	**10864**
chrX	dme-mir-971	0	52	0	1	70	70	4	0	116	0	**313**
chrX	dme-mir-972	0	0	0	0	0	1	61	0	3364	0	**3426**
chrX	dme-mir-973	0	12	0	0	0	0	76	3	179	0	**270**
chrX	dme-mir-974	0	3	0	0	9	2	236	3	287	0	**540**
chrX	dme-mir-975	0	4	0	0	0	0	33	0	7469	0	**7507**
chrX	dme-mir-976	0	1	0	0	0	2	380	7	26338	0	**26728**
chrX	dme-mir-977	1	66	0	0	5	4	680	0	28350	0	**29106**
chrX	dme-mir-978	1	6	0	0	4	3	241	3	29600	0	**29857**
chrX	dme-mir-979	0	0	0	0	0	0	21	0	1740	0	**1761**
chrX	dme-mir-980	1534	453	5	3	611	1464	2995	3113	539	106	**10823**
chrX	dme-mir-981	1	1427	0	3	404	968	56	65	56	0	**2980**
chrX	dme-mir-982	0	16	0	0	2	3	118	10	420	89	**658**
chrX	dme-mir-983	6	13	0	0	16	16	724	24	23562	798	**25160**
chrX	dme-mir-983-1	0	0	0	0	0	0	1	0	4	4	**8**
chrX	dme-mir-984	25	102	0	0	18	11	551	24	7704	1378	**9812**
chrX	dme-mir-985	0	0	0	0	2	0	214	7	1124	2	**1348**
chr2R	dme-mir-986	3	43	338	226	475	1006	1880	1749	1082	582	**7383**
chr2R	dme-mir-987	0	4	14	36	25758	16043	803	1056	11	0	**43726**
chr2R	dme-mir-988	13800	22601	893	539	1086	1460	876	960	23055	414	**65683**
chr2R	dme-mir-989	3	237	22	30	2	6	44	45010	21	88414	**133789**
chr2R	dme-mir-990	0	0	0	0	669	430	8	7	0	0	**1114**
chr2R	dme-mir-991	0	0	0	0	0	1	120	7	445	8	**580**
chr2R	dme-mir-992	2	6	0	0	0	1	45	3	1383	0	**1440**
chr3R	dme-mir-993	0	1	0	2	1720	1433	1448	1077	4	0	**5684**
chr3R	dme-mir-994	5	40	0	2	4	3	4	261	67	14463	**14848**
chr3R	dme-mir-995	3761	5626	2610	3220	3949	3287	909	1574	798	3679	**29411**
chr3R	dme-mir-996	23117	15398	4771	6077	18293	27396	29997	27603	1218	28482	**182353**
chr3R	dme-mir-997	0	0	0	0	0	0	184	0	207	0	**391**
chr3R	dme-mir-998	3118	5942	3397	5021	8319	5610	1074	1574	294	779	**35128**
chr3R	dme-mir-999	247	560	43	35	12595	10562	1464	2643	2356	141	**30647**
chr3L	dme-mir-9a	49	124	2464	2193	21120	32808	28787	30216	23961	77	**141799**
chr2L	dme-mir-9b	2463	11885	2011	1648	2726	3726	4263	5513	23545	10570	**68350**
chr2L	dme-mir-9c	1896	5648	1179	920	4579	5475	5508	8331	7175	4518	**45229**
chr3R	dme-mir-iab-4	0	1	0	0	4	2	94	120	25	2	**247**
chr3R	dme-mir-iab-4as	0	0	0	0	0	1	144	96	56	0	**297**
SUM_Norm_Reads_in_libr		**476512**	**670269**	**419331**	**506593**	**2221284**	**2140318**	**1943944**	**2554945**	**1290996**	**481225**	

TABLE S11: Abundance of miRNAs in *msl3* mutant salivary glands

	Genotype	Exp.	Average Ct [a]	Corrected amount [b]	Fold Difference (FD)[c]	log2 (FD)	Average log2(FD)	SD [d]	p value [e]
Dspt4	msl3-/msl3+	1	23.5091	95.762	1.000	0.000	0.000	0.000	
		2	23.7935	200.048	1.000	0.000			
	msl3-/msl3-	1	23.2659	106.222					
		2	23.2766	250.610					
mir-283	msl3-/msl3+	1	24.9728	89.769	0.514	-0.961	-0.901	0.086	0.00045
		2	24.7449	185.152	0.559	-0.840			
	msl3-/msl3-	1	26.4340	57.172					
		2	26.1674	129.580					
mir-304	msl3-/msl3+	1	29.9743	100.663	0.338	-1.564	-1.631	0.095	0.00070
		2	30.2644	203.835	0.308	-1.698			
	msl3-/msl3-	1	32.2164	37.754					
		2	32.3252	78.686					
mir-12	msl3-/msl3+	1	21.5294	88.515	0.406	-1.300	-1.284	0.022	0.00006
		2	21.8149	182.599	0.415	-1.269			
	msl3-/msl3-	1	23.8153	39.885					
		2	24.1442	94.941					
mir-979	msl3-/msl3+	1	36.2751	149.915	0.833	-0.263	-0.749	0.687	0.24047
		2	35.4645	209.309	0.425	-1.235			
	msl3-/msl3-	1	36.5484	138.570					
		2	37.5508	111.399					
mir-210	msl3-/msl3+	1	28.5830	100.340	1.425	0.511	0.384	0.180	0.07654
		2	29.1231	202.647	1.195	0.257			
	msl3-/msl3-	1	27.8037	158.625					
		2	28.3154	303.278					
U6	msl3-/msl3+	1	17.1883	100.088	0.611	-0.710	-0.627	0.117	0.01472
		2	17.7507	184.333	0.686	-0.544			
	msl3-/msl3-	1	18.0034	67.880					
		2	18.2684	158.374					

a. Dilution series were prepared in the control sample to construct standard curves for the Dspt4 autosomal gene reference and for each miRNA. C_T values measured in replicates for the target miRNA and Dspt4 reference in mutant and heterozygous mutant control samples respectively are averaged in individual experiments (Exp.1 and 2) and the corrected amount of target miRNA and Dspt4 reference inferred from the standard curve in b.

c. The amounts of miRNA are normalized in the mutant sample and in the heterozygous mutant control sample by dividing the calculated amount of miRNA by the amount of the Dspt4 reference. The fold difference (FD) or relative expression level of a miRNA corresponds to the

ratio of the normalized abundance of the miRNA in the mutant relative to the heterozygous mutant control sample, that is the ratio [miRNA/Dspt4] Mutant / [miRNA/Dspt4] Control; the average of the base 2 logarithm of the fold difference is plotted in Figure 2B,C.
d. SD is the standard deviation of the difference.
e. p-values are established in a two tailed Students t-test comparing the means of the normalized amounts of target miRNA in the mutant and in the heterozygous mutant control samples. *p<0.05, **p<0.005. ***p<0.0005

TABLE S12: Abundance of miRNAs in *msl3* mutant L3 larvae

	Genotype	Exp.	Average Ct [a]	Corrected amount [b]	Fold Difference (FD) [c]	log2 (FD)	Average log2(FD)	SD [d]	p value [e]
Dspt4	msl3-/msl3+	1	25.9974	34.628	1.000	0.000			
		2	25.6265	92.801	1.000	0.000			
	msl3-/msl3-	1	24.8854	54.398					
		2	24.7720	132.066					
mir-283	msl3-/msl3+	1	26.9201	49.324	0.756	-0.403	-0.253	0.213	0.18885
		2	27.2713	98.504	0.932	-0.102			
	msl3-/msl3-	1	26.3534	58.590					
		2	26.1358	130.596					
mir-304	msl3-/msl3+	1	31.2445	57.627	0.356	-1.488	-1.475	0.019	0.03552
		2	31.5988	109.348	0.363	-1.462			
	msl3-/msl3-	1	32.5782	32.271					
		2	33.0699	56.492					
mir-12	msl3-/msl3+	1	22.7659	57.656	0.455	-1.136	-1.040	0.136	0.00881
		2	22.9153	134.505	0.520	-0.943			
	msl3-/msl3-	1	23.7208	41.214					
		2	23.9739	99.544					
mir-979	msl3-/msl3+	1	31.1498	1044.716	0.760	-0.396	-0.259	0.193	0.38647
		2	31.4659	927.357	0.918	-0.123			
	msl3-/msl3-	1	30.6831	1247.539					
		2	30.7420	1211.981					
mir-210	msl3-/msl3+	1	27.5383	185.744	1.197	0.259	0.065	0.275	0.38641
		2	27.5514	461.878	0.914	-0.129			
	msl3-/msl3-	1	26.4166	349.245					
		2	26.9873	600.996					
U6	msl3-/msl3+	1	17.1512	101.819	0.694	-0.526	-0.444	0.117	0.14280
		2	17.5728	194.135	0.778	-0.362			
	msl3-/msl3-	1	16.9733	111.054					
		2	17.2156	215.036					

a-e as in Table S11.

TABLE S13: Abundance of miRNAs in *msl3* mutant salivary glands

	Genotype	Exp.	Average Ct [a]	Corrected amount [b]	Fold Difference (FD)[c]	log2 (FD)	Average log2(FD)	SD [d]	p value [e]
Dspt4	msl3-/msl3+	1	24.216	100.872	1.000	0.000	0.000	0.000	
		2	24.262	99.102	1.000	0.000			
	msl3-/msl3-	1	23.663	124.744					
		2	24.150	103.457					
mir-314	msl3-/msl3+	1	31.225	100.048	2.258	1.175	1.149	0.037	0.0667
		2	30.498	152.880	2.178	1.123			
	msl3-/msl3-	1	29.463	279.422					
		2	29.089	347.564					
mir-981	msl3-/msl3+	1	32.920	117.805	0.958	-0.061	0.197	0.366	0.2414
		2	33.704	84.927	1.372	0.456			
	msl3-/msl3-	1	32.513	139.636					
		2	32.844	121.608					
mir-13b	msl3-/msl3+	1	23.450	122.437	0.411	-1.282	-0.884	0.564	0.0703
		2	24.218	81.676	0.714	-0.485			
	msl3-/msl3-	1	24.733	62.257					
		2	24.774	60.919					
mir-100	msl3-/msl3+	1	29.324	99.987	1.185	0.245	0.545	0.425	0.0596
		2	29.977	75.275	1.796	0.845			
	msl3-/msl3-	1	28.447	146.492					
		2	28.532	141.148					
mir-1013	msl3-/msl3+	1	31.660	84.010	1.176	0.234	-0.137	0.524	0.3233
		2	31.010	119.016	0.704	-0.507			
	msl3-/msl3-	1	30.962	122.159					
		2	31.585	87.439					
U6	msl3-/msl3+	1	18.097	100.004	0.726	-0.462	-0.418	0.061	0.0046
		2	18.127	98.736	0.771	-0.375			
	msl3-/msl3-	1	18.352	89.811					
		2	18.643	79.476					

a-e as in Table S11.

TABLE S14: Abundance of miRNAs in *msl3* mutant L3 larvae

	Genotype	Exp.	Average Ct [a]	Corrected amount [b]	Fold Difference (FD) [c]	log2 (FD)	Average log2(FD)	SD [d]	p value [e]
Dspt4	msl3-/msl3+	1	26.1455	48.078	1.000	0.000			
		2	26.1633	47.750	1.000	0.000			
	msl3-/msl3-	1	24.995	74.796					
		2	25.335	65.635					
mir-314	msl3-/msl3+	1	21.1699	35123.558	0.350	-1.514	-1.441	0.104	0.0003
		2	21.2272	33969.861	0.388	-1.367			
	msl3-/msl3-	1	22.213	19128.386					
		2	22.307	18104.321					
mir-981	msl3-/msl3+	1	29.5758	476.005	0.655	-0.609	-0.290	0.452	0.1481
		2	30.2449	359.989	1.021	0.030			
	msl3-/msl3-	1	29.529	485.377					
		2	29.433	505.205					
mir-13b	msl3-/msl3+	1	21.4858	344.693	0.540	-0.889	-0.905	0.022	0.0079
		2	21.5918	325.964	0.528	-0.921			
	msl3-/msl3-	1	21.817	289.481					
		2	22.199	236.640					
mir-100	msl3-/msl3+	1	26.8667	291.331	0.208	-2.262	-2.062	0.284	0.0032
		2	27.1654	255.822	0.275	-1.861			
	msl3-/msl3-	1	29.455	94.471					
		2	29.398	96.819					
mir-1013	msl3-/msl3+	1	29.240	142.324	0.573	-0.803	-0.610	0.273	0.0861
		2	28.286	126.568	0.749	-0.417			
	msl3-/msl3-	1	29.365	126.899					
		2	29.391	130.301					
U6	msl3-/msl3+	1	17.259	307.518	0.601	-0.734	-1.024	0.410	0.0125
		2	17.538	512.989	0.402	-1.314			
	msl3-/msl3-	1	17.532	287.625					
		2	17.469	283.612					

a-e as in Table S11.

TABLE S15: Abundance of miRNAs in *mle* mutant salivary glands

	Genotype	Exp.	Average Ct [a]	Corrected amount [b]	Fold Difference (FD)[c]	log2 (FD)	Average log2(FD)	SD [d]	p value [e]
Dspt4	mle-/mle+	1	24.693	102.093	1.000	0.000			
		2	24.533	100.668	1.000	0.000			
	mle-/mle-	1	23.901	170.434					
		2	23.827	158.044					
mir-283	mle-/mle+	1	25.142	100.816	0.740	-0.435	-0.430	0.008	0.0040
		2	24.812	102.914	0.745	-0.425			
	mle-/mle-	1	24.788	124.474					
		2	24.510	120.380					
mir-304	mle-/mle+	1	30.746	96.522	0.636	-0.652	-0.739	0.123	0.0031
		2	31.004	99.139	0.564	-0.826			
	mle-/mle-	1	30.568	102.559					
		2	31.168	87.778					
mir-12	mle-/mle+	1	21.652	101.133	0.532	-0.910	-0.946	0.051	0.0003
		2	21.533	100.745	0.506	-0.983			
	mle-/mle-	1	21.869	89.833					
		2	21.882	80.045					
mir-979	mle-/mle+	1	36.290	101.068	0.730	-0.454	-0.635	0.257	0.0203
		2	35.292	102.616	0.568	-0.817			
	mle-/mle-	1	36.064	123.209					
		2	35.753	91.460					
mir-210	mle-/mle+	1	29.642	107.507	0.782	-0.355	-0.182	0.244	0.2301
		2	29.573	109.561	0.994	-0.009			
	mle-/mle-	1	29.288	140.360					
		2	29.094	170.943					
U6	mle-/mle+	1	18.185	99.069	0.883	-0.180	0.098	0.393	0.3556
		2	18.095	99.106	1.298	0.376			
	mle-/mle-	1	17.555	146.012					
		2	17.022	201.962					

a-e as in Table S11.

TABLE S16: Abundance of miRNAs in *mle* mutant L3 larvae

	Genotype	Exp.	Average Ct [a]	Corrected amount [b]	Fold Difference (FD) [c]	log2 (FD)	Average log2(FD)	SD [d]	p value [e]
Dspt4	mle-/mle+	1	25.034	81.970	1.000	0.000			
		2	24.991	76.150	1.000	0.000			
	mle-/mle-	1	25.047	81.265					
		2	24.697	90.724					
mir-283	mle-/mle+	1	26.352	48.723	0.807	-0.309	-0.165	0.204	0.2143
		2	26.170	46.630	0.986	-0.021			
	mle-/mle-	1	26.717	38.996					
		2	25.887	54.769					
mir-304	mle-/mle+	1	33.859	16.253	1.264	0.338	0.117	0.313	0.2913
		2	33.412	15.797	0.930	-0.104			
	mle-/mle-	1	33.445	20.368					
		2	33.277	17.510					
mir-12	mle-/mle+	1	24.132	19.072	0.892	-0.165	-0.164	0.002	0.0126
		2	24.135	18.169	0.894	-0.162			
	mle-/mle-	1	24.311	16.868					
		2	24.037	19.341					
mir-979	mle-/mle+	1	32.007	1533.669	1.972	0.980	0.550	0.607	0.3187
		2	31.470	404.038	1.088	0.121			
	mle-/mle-	1	30.972	2998.693					
		2	30.760	523.538					
mir-210	mle-/mle+	1	26.990	1098.538	1.579	0.659	0.484	0.247	0.3002
		2	26.722	2357.685	1.239	0.309			
	mle-/mle-	1	26.467	1719.262					
		2	26.347	3479.985					
U6	mle-/mle+	1	16.909	227.810	1.506	0.591	0.559	0.046	0.3274
		2	16.978	208.576	1.440	0.526			
	mle-/mle-	1	16.296	340.231					
		2	16.160	357.836					

a-e as in Table S11.

Table S17: Levels of let-7 miRNA in adult females and males

Tissue		C_T *let±7* ± StDev	C_T *2SrRNA* ± StDev	ΔC_T (ΔC_T *let-7* - ΔC_T *2SrRNA*) [a]	$\Delta\Delta C_T$ (ΔC_T - ΔC_T ^{control}) [b]	Average $\Delta\Delta C_T$ ± StDev	Fold Difference [c]
Female carcasses	Exp 1	25.33±0.30	6.14±0.24	19.19±0.39	0.00±0.39	0.00±0.28	1.00 (0.82 - 1.22)
	Exp 2	26.35±0.30	8.29±0.36	18.06±0.47	0.00±0.47		
Germaria	Exp 1	22.18±0.18	6.29±0.09	15.90±0.20	3.29±0.20	-2.24±0.11	4.72 (4.38 - 5.09) $p=7.76x10^{-6***}$
	Exp 2	22.35±0.05	7.72±0.11	14.63±0.12	3.43±0.12		
Male carcasses	Exp 1	22.71±0.11	7.10±0.03	15.61±0.12	3.58±0.12	-1.92±0.09	3.79 (3.57 – 4.02) $p=1.55x10^{-6***}$
	Exp 2	23.68±0.08	7.80±0.12	15.88±0.14	2.18±0.14		
Testes	Exp 1	21.14±0.26	6.56±0.03	14.58±0.26	4.61±0.26	-2.89±0.12	7.43 (6.84 - 8.07) $p=7.73x10^{-8***}$
	Exp 2	22.40±0.05	8.41±0.09	13.99±0.10	4.07±0.10		

a: ΔC_T was determined by subtracting the average *2SrRNA* C_T value from the average Experimental C_T value. The standard deviation of the difference is calculated from the standard deviation of the Experimental and *2SrRNA* values using the formula $s = \sqrt{(s_1^2 + s_2^2)}$ where s = standard deviation

b: $\Delta\Delta C_T$ is calculated by subtracting the ΔC_T control value (ΔC_T of female carcasses). The standard deviation is the same as for ΔC_T

c: the fold difference between the Experimental Sample and the control is calculated by: $2^{\pm\Delta\Delta CT}$ with $\Delta\Delta C_T$ -s and $\Delta\Delta C_T$ –s where s is the standard deviation of $\Delta\Delta C_T$ value The fold difference of the experimental values was compared to the respective control. P-value was calculated using the two tailed Students t-test. *p<0.05. **p<0.005. ***p<0.0005

Table S18: Levels of sex specific mRNAs in *Δlet-7* females and males

Genotype		C_T *SxlF* ± StDev	C_T *RpL32* ± StDev	ΔC_T (ΔC_T *SxlF*- ΔC_T *RpL32*) [a]	$\Delta\Delta C_T$ (ΔC_T- ΔC_T ^{control}) [b]	Fold Difference [c]
Females	**Control:** *let-7-C* Rescue	16.15±0.22	11.32±0.12	4.83±0.25	0.00±0.25	1.00 (0.840-1.190)
	Δ let-7	15.95±0.03	11.16±0.09	4.78±0.25	-0.05±0.09	1.033 (0.969-1.102) p=0.70
Males	**Control:** *let-7-C* Rescue	21.48±0.12	12.28±0.16	9.21±0.20	0.00±0.20	1.00 (0.872-1.147)
	Δ let-7	18.89±0.09	12.20±0.22	6.69±0.23	-2.51±0.23	5.704 (4.853-6.705) $1.73x10^{-4}$***
Genotype		C_T *tra1* ± StDev	C_T *RpL32* ± StDev	ΔC_T (ΔC_T *tra1*- ΔC_T *RpL32*) [a]	$\Delta\Delta C_T$ (ΔC_T- ΔC_T ^{control}) [b]	Fold Difference [c]
Females	**Control:** *let-7-C* Rescue	21.30±0.13	11.32±0.12	9.98±0.17	0.00±0.17	1.00 (0.886-1.129)
	Δ let-7	20.72±0.14	11.16±0.09	9.56±0.16	-0.42±0.16	1.334 (1.190-1.495) p=0.06
Males	**Control:** *let-7-C* Rescue	29.84±0.03	12.28±0.16	17.57±0.16	0.00±0.16	1.00 (0.896-1.116)
	Δ let-7	29.66±0.09	12.20±0.22	17.46±0.23	-0.11±0.23	1.079 (0.917-1.270) p=0.40
Genotype		C_T *DsxM* ± StDev	C_T *RpL32* ± StDev	ΔC_T (ΔC_T *DsxM*- ΔC_T *RpL32*) [a]	$\Delta\Delta C_T$ (ΔC_T- ΔC_T ^{control}) [b]	Fold Difference [c]
Females	**Control:** *let-7-C* Rescue	25.23±0.09	11.32±0.12	13.90±0.15	0.00±0.15	1.00 (0.900-1.111)
	Δ let-7	25.69±0.05	11.16±0.09	14.52±0.10	0.62±0.10	0.649 (0.605-0.697) $p=1.83x10^{-3}$**
Males	**Control:** *let-7-C* Rescue	17.89±0.33	12.28±0.16	5.61±0.37	0.00±0.37	1.00 (0.950-1.052)
	Δ let-7	17.94±0.03	12.20±0.22	5.74±0.22	0.30±0.17	0.914 (0.786-1.062) 0.75

Genotype		C_T *Yp1* ± StDev	C_T *RpL32* ± StDev	ΔC_T (ΔC_T *Yp1*- ΔC_T *RpL32*) [a]	$\Delta\Delta C_T$ (ΔC_T- ΔC_T control) [b]	Fold Difference [c]
Females	**Control:** *let-7-C* Rescue	10.33±0.07	11.32±0.12	-1.00±0.14	0.00±0.14	1.00 (0.908-1.101)
	Δ let-7	12.93±0.10	11.16±0.09	1.77±0.13	2.76±0.13	0.147 (0.134-0.162) $p=3.29x10^{-6}$***
Males	**Control:** *let-7-C* Rescue	25.99±0.05	12.28±0.16	13.71±0.16	0.00±0.16	1.00 (0.894-1.119)
	Δ let-7	25.01±0.13	12.20±0.22	12.81±0.25	-0.90±0.25	1.867 (1.568-2.223) $p=9.85x10^{-4}$**

a: ΔC_T was determined by subtracting the average *RpL32* C_T value from the average Experimental C_T value. The standard deviation of the difference is calculated from the standard deviation of the Experimental and *RpL32* values using the formula $s = \sqrt{(s_1^2 + s_2^2)}$ where s = standard deviation

b: $\Delta\Delta C_T$ is calculated by subtracting the ΔC_T control. The standard deviation is the same as for ΔC_T

c: the fold difference between the Experimental Sample and the control is calculated by: $2^{-\Delta\Delta CT}$ with $\Delta\Delta C_T$ +s and $\Delta\Delta C_T$ –s where s is the standard deviation of $\Delta\Delta C_T$ value. The fold difference of the experimental values was compared to the respective control. P-value was calculated using the two tailed Students t-test. *p<0.05, **p<0.005. ***p<0.0005

Table S19: let-7 expression depends on ecdysone signaling in adult ovaries and testes

	Genotype, conditions	C_T *let-7* ± StDev[a]	C_T *RpL32* ± StDev	ΔC_T (ΔC_T *let-7* - ΔC_T *RpL32*)[a]	$\Delta\Delta C_T$ (ΔC_T-$\Delta C_T^{control}$)[b]	Fold Difference[c]	Relative change of *let-7* levels[d]
Females	*OregonR*, 4d at 18°C	25.88±0.16	14.13±0.21	11.74±0.06	0.00±0.06	1.00 (0.96-1.04)	1.00 (0.88-1.13)
	OregonR, 4d at 29°C	25.00±0.04	14.39±0.17	10.58±0.18	-1.16±0.18	2.24 (1.98-2.54) $p=2.01x10^{-5}$***	
	$ecd1^{ts\,4210}$, 4d at 18°C	24.07±0.04	13.42±0.28	10.65±0.05	0.00±0.05	1.00 (0-97-1.03)	0.38 (0.37.0.38) $p=2.44x10^{-4}$***
	$ecd1^{ts\,4210}$, 4d at 29°C	24.80±0.15	13.96±0.45	10.92±0.001	0.27±0.001	0.84 (0.84-0.84) p=0.14	
	Genotype, conditions	**C_T *let-7* ± StDev**	**C_T *S2rRNA* ± StDev**	**ΔC_T (ΔC_T *let-7* - ΔC_T *S2rRNA*)[a]**	**$\Delta\Delta C_T$ (ΔC_T-$\Delta C_T^{control}$)[b]**	**Fold Difference[c]**	**Relative change of *let-7* levels[d]**
Males	*OregonR*, 4d at 18°C	22.90±0.03	8.41±0.11	14.49±0.13	0.00±0.13	1.00 (0.91-1.09)	1.00 (0.92-1.08)
	OregonR, 4d at 29°C	22.55±0.03	8.35±0.12	14.20±0.12	-0.29±0.12	1.23 (1.14-1.33) p=0.02*	
	$ecd1^{ts\,4210}$, 4d at 18°C	22.13±0.55	8.33±0.09	13.80±0.15	0.00±0.15	1.00 (0.90-1.11)	0.24 (0.23-0.25) $p=1.77x10^{-4}$***
	$ecd1^{ts\,4210}$, 4d at 29°C	23.49±0.02	7.87±0.11	15.64±0.08	1.85±0.08	0.29 (0.28-0.31) $p=3.59x10^{-4}$***	

a: ΔC_T values were determined by subtracting the average *RpL32* or *2SrRNA* C_T value from the average Experimental C_T value. The standard deviation of the difference is calculated from the standard deviation of the Experimental and *RpL32* or *2SrRNA* values using the formula $s = \sqrt{(s_1^2 + s_2^2)}$ where s = standard deviation

b: $\Delta\Delta C_T$ is calculated by subtracting the ΔC_T control value (ΔC_T of the respective genotype at 18°C). The standard deviation is the same as for ΔC_T

c: the fold difference between the Experimental Sample and the control is calculated by: $2^{-\Delta\Delta CT}$ with $\Delta\Delta C_T$ +s and $\Delta\Delta C_T$ –s where s is the standard deviation of $\Delta\Delta C_T$ value. The fold difference of the experimental values was compared to the respective control. P-value between ΔC_T values of the experiments was calculated using the two tailed Students t-test

d: The relative changes of *let-7* levels were calculated by dividing the fold difference ranges of $ecd1^{ts}$ and *OrR*. Students T-test was used to compare the relative changes *p<0.05, **p<0.005

Table S20: Levels of sex specific mRNAs are misregulated upon ecdysone deficit

Genotype, conditions			C_T *DsxM* ± StDev	C_T *Rpl32* ± StDev	ΔC_T (ΔC_T *DsxM*- ΔC_T *Rpl32*) [a]	$\Delta\Delta C_T$ (ΔC_T-ΔC_T $_{control}$) [b]	Fold Difference [c]
Females	**Control**: *OrR*	18°C	26.20±0.07	15.40±0.20	10.80±0.21	0.00±0.21	1.00 (0.866-1.155)
	OrR	29°C	26.34±0.01	13.95±0.03	12.39±0.03	1.58±0.03	0.334 (0.326-0.341) p=3.73x10^{-3}**
	Control: *ecd1^{ts}*	18°C	26.41±0.07	13.69±0.07	12.72±0.10	0.00±0.10	1.00 (0.935-1.070)
	ecd1^{ts}	29°C	25.88±0.12	14.36±0.07	11.52±0.14	-1.20±0.14	2.299 (2.081-2.539) 2.59x10^{-4}***
Males	**Control**: OrR	18°C	17.84±0.04	15.67±0.15	2.17±0.16	0.00±0.16	1.00 (0.896-1.116)
	OrR	29°C	18.17±0.06	15.45±0.29	2.72±0.30	0.55±0.30	0.681 (0.553-0.838) p=0.06
	Control: *ecd1^{ts}*	18°C	18.40±0.02	15.77±0.20	2.63±0.20	0.00±0.20	1.00 (0.868-1.152)
	ecd1^{ts}	29°C	18.04±0.05	14.60±0.14	3.45±0.25	0.81±0.15	0.569 (0.511-0.633) p=7.97x10^{-3}*

Genotype, conditions			C_T *Esg* ± StDev	C_T *Rpl32* ± StDev	ΔC_T (ΔC_T *Esg*- ΔC_T *Rpl32*) [a]	$\Delta\Delta C_T$ (ΔC_T-ΔC_T $_{control}$) [b]	Fold Difference [c]
Females	**Control**: *OrR*	18°C	29.30±0.09	15.40±0.20	13.90±0.22	0.00±0.22	1.00 (0.862-1.161)
	OrR	29°C	27.90±0.08	13.95±0.03	13.94±0.09	0.04±0.09	0.970 (0.912-1.032) p=0.81
	Control: *ecd1^{ts}*	18°C	24.39±0.28	13.69±0.07	10.70±0.28	0.00±0.28	1.00 (0.821-1.218)
	ecd1^{ts}	29°C	24.69±0.22	14.36±0.07	10.33±0.24	-0,37±0.24	1.293 (1.097-1.523) p=0.07
Males	**Control**: OrR	18°C	26.86±0.05	15.67±0.15	11.19±0.16	0.00±0.16	1.00 (0.894-1.119)
	OrR	29°C	27.48±0.003	15.45±0.29	12.03±0.29	0.84±0.29	0.559 (0.456-0.685) p=0.55
	Control: *ecd1^{ts}*	18°C	25.89±0.02	15.77±0.20	10.12±0.20	0.00±0.20	1.00 (0.868-1.152)
	ecd1^{ts}	29°C	25.34±0.13	14.60±0.14	10.75±0.20	0.63±0.20	0.648 (0.566-0.742) p=8.77x10^{-3}*

Genotype, conditions			C_T *SxlFl1* ± StDev	C_T *Rpl32* ± StDev	ΔC_T (ΔC_T *SxlFl1*- ΔC_T *Rpl32*) [a]	$\Delta\Delta C_T$ (ΔC_T-ΔC_T $_{control}$) [b]	Fold Difference [c]
Females	**Control**: *OrR*	18°C	17.81±0.08	15.40±0.20	2.41±0.21	0.00±0.21	1.00 (0.864-1.158)
	OrR	29°C	15.96±0.16	13.95±0.03	2.00±0.16	-0.41±0.16	1.330 (1.189-1.487) p=5.00x10^{-2}*
	Control: *ecd1^{ts}*	18°C	16.02±0.04	13.69±0.07	2.33±0.08	0.00±0.08	1.00 (0.947-1.056)
	ecd1^{ts}	29°C	16.18±0.16	14.36±0.07	1.82±0.17	-0.51±0.17	1.424 (1.262-1.607) p=1.64x10^{-3}**
Males	**Control**: OrR	18°C	21.05±0.12	15.67±0.15	5.38±0.20	0.00±	1.00 (0.873-1.146)
	OrR	29°C	21.44±0.07	15.45±0.29	5.99±0.30	0.61±	0.653 (0.530-0.805) p=0.15
	Control: *ecd1^{ts}*	18°C	22.24±0.12	15.77±0.20	6.47±0.24	0.00±	1.00 (0.848-1.179)
	ecd1^{ts}	29°C	19.38±0.07	14.60±0.14	4.78±0.16	-1.69±	3.222 (2.883-3.600) p=9.13x10^{-3}**

Genotype, conditions			C_T *tra1* ± StDev	C_T *Rpl32* ± StDev	ΔC_T (ΔC_T *tra1*- ΔC_T *Rpl32*) [a]	$\Delta\Delta C_T$ (ΔC_T-ΔC_T $_{control}$) [b]	Fold Difference [c]
Females	**Control**: *OrR*	18°C	21.04±0.05	15.40±0.20	5.64±0.20	0.00±0.20	1.00 (0.868-1.152)
	OrR	29°C	19.87±0.11	13.95±0.03	5.92±0.11	0.28±0.11	0.826 (0.765-0.891) p=0.14
	Control: *ecd1^{ts}*	18°C	20.01±0.08	13.69±0.07	6.32±0.11	0.00±0.11	1.00 (0.927-1.079)
	ecd1^{ts}	29°C	20.69±0.11	14.36±0.07	6.33±0.13	0.008±0.13	0.994 (0.909-1.088) p=0.93
Males	**Control**: OrR	18°C	28.84±0.09	15.67±0.15	13.18±0.18	0.00±0.18	1.00 (0.885-1.129)
	OrR	29°C	28.67±0.05	15.45±0.29	13.22±0.30	0.05±0.30	0.969 (0.789-1.190) p=0.73
	Control: *ecd1^{ts}*	18°C	28.69±0.12	15.77±0.20	12.92±0.23	0.00±0.23	1.00 (0.850-1.176)
	ecd1^{ts}	29°C	23.68±0.06	14.60±0.14	9.08±0.16	-3.84±0.16	14.277 (12.801-15.924) p=1.76x10^{-5}***

Genotype, conditions			C_T *Yp1* ± StDev	C_T *Rpl32* ± StDev	ΔC_T (ΔC_T *Yp1*- ΔC_T *Rpl32*) [a]	$\Delta\Delta C_T$ (ΔC_T-ΔC_T $_{control}$) [b]	Fold Difference [c]
Females	**Control**: *OrR*	18°C	12.33±0.14	15.40±0.20	-3.07±0.24	0.00±0.24	1.00 (0.846-1.182)
	OrR	29°C	11.21±0.23	13.95±0.03	-2.74±0.23	0.33±0.23	0.794 (0.678-0.930) p=0.12
	Control: *ecd1^{ts}*	18°C	10.86±0.31	13.69±0.07	-2.82±0.32	0.00±0.32	1.00 (0.800-1.249)
	ecd1^{ts}	29°C	11.24±0.20	14.36±0.07	-3.12±0.21	-0.30±0.21	1.231 (1.061-1.428) p=0.15
Males	**Control**: OrR	18°C	26.15±0.11	15.67±0.15	10.48±0.19	0.00±0.19	1.00 (0.876-1.142)
	OrR	29°C	25.57±0.03	15.45±0.29	10.12±0.29	-0.36±0.29	1.285 (1.048-1.576) p=0.14
	Control: *ecd1^{ts}*	18°C	24.63±0.08	15.77±0.20	8.86±0.22	0.00±0.22	1.00 (0.86-1.163)
	ecd1^{ts}	29°C	16.76±0.06	14.60±0.14	2.16±0.16	-6.702±0.16	104.080 (93.395-115.987) p=3.22x10^{-6}***

a: ΔC_T was determined by subtracting the average *RpL32* C_T value from the average Experimental C_T value. Since the same set of samples was used for all PCRs, the same *RpL32* C_T values are used as internal control. The standard deviation of the difference is calculated from the standard deviation of the Experimental and *RpL32* values using the formula $s = \sqrt{(s_1^2 + s_2^2)}$ where s = standard deviation.
b: $\Delta\Delta C_T$ is calculated by subtracting the ΔC_T control value (ΔC_T of the sample of the respective sex and genotype at 18°C). The standard deviation is the same as for ΔC_T.
c: the fold difference between the Experimental Sample and the control is calculated by: $2^{-\Delta\Delta CT}$ with $\Delta\Delta C_T$ +s and $\Delta\Delta C_T$ –s where s is the standard deviation of $\Delta\Delta C_T$ value. The fold difference of the experimental values was compared to the respective control. P-value was calculated using the two tailed Students t-test. *p<0.05, **p<0.005. ***p<0.0005.

Table S21. Ecdysteroid deficit leads to differentiation defects in the CySC lineage cells in adult testes

Genotype, conditions	Clustering of somatic cyst cells				Appearance of epithelium-like clusters			
	< 5 cells	≥ 5 cells	> 10 cells	P value	None	Apical	Lateral	P value
Control: *ecd*^{1ts,} 5 days, 18°	40%	60%	0%		100%	0%	0%	
ecd^{1ts,} 5 days, 29°	7%	57%	36%	0.0368*	43%	43%	14%	0.0137*
Control: *ecd*^{1ts,} 11 days, 18°	50%	50%	0%		83%	17%	0%	
ecd^{1ts,} 11 days, 29°	17%	8%	75%	0.0113*	0%	50%	50%	0.0001***

To calculate the significance two-way tables and chi-squared test with 2 degrees of freedom were used. The frequencies of the testes with the somatic cell clustering phenotype (<5, ≥ 5 or >10 somatic cell in the cluster) and the frequencies of the testes with epithelial sheets (none, apical or lateral) acquired by induction of ecdysone deficit for 5d or 11d at the restrictive temperature (29°) were compared to the frequencies of the same phenotypes in flies with the same genotype but kept for the same periods of time (5d or 11d) at the permissive temperature (18°). N=10-20 testes for each genotype. *p<0.05, **p<0.005. ***p<0.0005.

TABLE S22: Ranked abundance of miRNAs in each sexed library (Complete list)

	Late embryo Lymphoid Cells				L3 Larvae Salivary Glands				Adult Head				Adult Body				Adult Gonads			
					S. Gland M		S. Gland F										Testis			
Chrom	miRNA	S2 M (%)	miRNA	Kc F (%)	miRNA	(%)	miRNA	(%)	miRNA	Head M (%)	miRNA	Head F (%)	miRNA	Body M (%)	miRNA	Body F (%)	miRNA	(%)	miRNA	Ovary (%)
chr2R	mir-14	38.35286	mir-14	29.10042	mir-8	32.42188	mir-8	35.66808	mir-8	14.57004	mir-8	11.43554	mir-1	25.56082	mir-1	26.75240	mir-12	16.87054	mir-989	18.37262
chr2R	mir-184	11.34536	mir-184	16.37821	mir-263a	10.45437	mir-12	8.49222	mir-1	9.99692	mir-1	8.17673	mir-8	23.01229	mir-8	25.64450	mir-8	15.35016	bantam	11.43364
chr3L	bantam	7.44158	mir-2a	4.44288	mir-375	7.15235	mir-263a	7.75277	bantam	8.19215	mir-276a	7.62653	bantam	12.55761	bantam	9.78819	mir-305	5.03802	mir-8	9.30021
chr3R	mir-996	4.85129	mir-8	4.14932	mir-12	6.25415	mir-375	6.71742	mir-276a	5.81087	bantam	7.13572	mir-276a	4.65975	mir-276	5.02046	mir-959	4.67717	mir-2a	7.72512
chr3R	mir-279	3.46812	bantam	4.07801	mir-304	5.72874	mir-282	6.30407	mir-276	5.39112	mir-210	4.99725	mir-277	3.91230	mir-276a	4.27473	mir-2a	3.85408	mir-318	7.24950
chr3R	mir-11	3.29268	mir-34	3.39610	mir-275	5.19227	mir-304	6.00679	mir-277	4.66334	mir-277	4.90334	mir-276	2.46689	mir-2a	2.93279	let-7	3.13374	mir-184	6.40474
chr3R	mir-34	2.93382	mir-988	3.37195	bantam	4.71150	bantam	4.82103	mir-184	4.05515	mir-184	4.17368	mir-2a	2.19543	mir-277	2.68239	mir-34	3.10799	mir-996	5.91867
chr2R	mir-988	2.89604	mir-317	3.14547	mir-2a	3.04332	mir-11	2.45542	mir-34	3.57697	mir-34	3.61372	mir-996	1.54310	mir-989	1.76169	mir-282	3.00171	mir-2b	3.30079
chr3L	mir-282	2.84211	mir-2b	3.10880	mir-305	2.73388	mir-13b	2.44753	mir-2b	3.41702	mir-14	3.20424	let-7	1.48826	mir-282	1.68466	mir-964	2.74226	mir-994	3.00554
chr3R	mir-252	2.78986	mir-276	2.30014	mir-2b	2.43359	mir-305	1.92719	mir-2a	3.22916	mir-285	2.95344	mir-9a	1.48086	mir-31a	1.48123	mir-277	2.58692	mir-275	2.61547
chr3R	mir-13b	2.42533	mir-996	2.29723	mir-13b	1.98678	mir-2a	1.91021	mir-285	3.21797	mir-2a	2.92097	mir-14	1.34500	mir-2b	1.20586	mir-11	2.50748	mir-13b	2.19972
chr2L	mir-2b	2.09460	mir-279	2.25699	mir-11	1.91047	mir-2b	1.55036	mir-14	2.46292	mir-2b	2.73268	mir-31a	1.27792	mir-9a	1.18265	mir-978	2.29276	mir-9b	2.19650
chr3R	mir-317	1.92167	mir-13b	2.19551	mir-283	1.78685	mir-283	1.53792	mir-210	2.43620	mir-276	2.71511	mir-282	1.19988	mir-996	1.08039	mir-977	2.19598	mir-263a	1.46179
chr3L	mir-276a	1.91873	mir-11	2.08551	mir-282	1.58233	mir-996	1.19958	mir-124	2.35303	mir-274	2.60279	mir-12	1.09602	let-7	1.07663	mir-274	2.14935	mir-79	1.39712
chr2L	mir-2a	1.64508	mir-9b	1.77317	mir-996	1.13781	mir-276	1.15280	mir-13b	2.20357	let-7	2.39044	mir-13b	1.08115	mir-184	1.05731	mir-976	2.04009	mir-282	1.37663
chr3L	mir-276	0.94940	mir-276a	1.62248	mir-308	1.06112	mir-308	0.99607	let-7	1.62439	mir-124	2.28452	mir-10	0.98418	mir-13b	0.95693	mir-9a	1.85601	mir-11	1.34088
chr2R	mir-8	0.84006	mir-12	1.57688	mir-14	0.99282	mir-998	0.99113	mir-1000	1.47162	mir-252	1.76221	mir-2b	0.93727	mir-10	0.83951	mir-983	1.82510	mir-34	1.31839
chr3R	mir-995	0.78928	mir-305	1.53819	mir-998	0.81005	mir-276a	0.73590	mir-263a	1.36504	mir-13b	1.62700	mir-281-1	0.90548	mir-11	0.75229	mir-9b	1.82375	mir-305	1.08218
chr3R	mir-277	0.77711	mir-2a-2	1.44698	mir-276	0.74252	mir-79	0.69444	mir-987	1.15961	mir-9a	1.53286	mir-304	0.88408	mir-14	0.73860	mir-14	1.82239	mir-9c	0.93878
chr2L	mir-305	0.69694	mir-306	0.91420	mir-34	0.62690	mir-995	0.63562	mir-252	1.13643	mir-996	1.28000	mir-184	0.78891	mir-281-1	0.71807	mir-988	1.78579	mir-12	0.91588
chr3R	mir-998	0.65434	mir-998	0.88647	mir-995	0.62232	mir-34	0.58884	mir-274	1.09402	mir-263a	1.21244	mir-279	0.74956	mir-314	0.59703	mir-2b	1.64237	mir-33	0.83634
chr2L	mir-306	0.52465	mir-9c	0.84265	mir-79	0.61202	mir-14	0.52468	mir-7	1.09173	mir-1000	1.20431	mir-11	0.74272	mir-279	0.55596	mir-960	1.47375	mir-995	0.76444
chr2L	mir-9b	0.51688	mir-995	0.83930	mir-9a	0.58760	mir-275	0.51086	mir-9a	0.95078	mir-31a	1.03433	mir-305	0.71838	mir-263a	0.52228	mir-13b	1.41302	mir-14	0.63107
chr2L	mir-79	0.42874	mir-79	0.80867	mir-9b	0.47962	mir-33	0.44533	mir-929	0.94692	mir-11	1.00219	mir-79	0.62466	mir-305	0.49544	mir-317	1.21701	mir-1	0.62224
chr2L	mir-2a-2	0.42286	mir-282	0.68950	mir-33	0.47275	mir-9a	0.43289	mir-31a	0.91492	mir-7	0.96850	mir-263a	0.60851	mir-34	0.43546	mir-316	1.19749	mir-312	0.58247
chr3L	mir-33	0.40440	mir-33	0.60276	mir-276a	0.44185	mir-277	0.32768	mir-305	0.89363	mir-125	0.96574	mir-314	0.59811	mir-12	0.37588	mir-311	0.97111	mir-276a	0.56319
chr2L	mir-9c	0.39789	mir-277	0.37739	mir-306	0.40712	mir-9b	0.32531	mir-996	0.82355	mir-305	0.95444	mir-33	0.49554	mir-9c	0.32609	mir-310	0.90984	mir-276	0.52462
chrX	mir-980	0.32192	mir-308	0.37672	mir-252	0.31708	mir-317	0.30320	mir-317	0.70743	mir-276b	0.78241	mir-34	0.48268	mir-79	0.29469	mir-125	0.90306	mir-7	0.48967
chr3R	mir-1003	0.31206	mir-92a	0.33044	mir-184	0.30906	mir-1	0.29669	mir-279	0.65784	mir-133	0.76965	mir-958	0.37959	mir-304	0.28288	mir-278	0.65771	mir-306	0.40612
chr2R	mir-308	0.31122	mir-970	0.26494	mir-277	0.30792	mir-279	0.29452	mir-79	0.60700	mir-987	0.74956	mir-316	0.28530	mir-958	0.28221	mir-276a	0.60945	let-7	0.35792
chrX	mir-970	0.23924	mir-2b-2	0.24593	mir-278	0.30410	mir-306	0.22582	mir-276b	0.57736	mir-307	0.74442	mir-9c	0.28334	mir-278	0.27375	mir-984	0.59671	mir-31a	0.35390
chr2R	mir-307	0.19559	mir-278	0.24571	mir-9c	0.28121	mir-184	0.21418	mir-999	0.56703	mir-317	0.67901	mir-125	0.26945	mir-33	0.26490	mir-975	0.57855	mir-92a	0.31453
chr2L	mir-965	0.11731	mir-981	0.21284	mir-317	0.27396	mir-9c	0.18161	mir-125	0.56561	mir-929	0.62341	mir-281-2	0.26235	mir-281-2	0.23215	mir-9c	0.55577	mir-304	0.29846
chr2L	mir-2b-1	0.10451	mir-283	0.20792	mir-1	0.25908	mir-31a	0.15061	mir-282	0.53936	mir-79	0.62224	mir-278	0.25546	mir-125	0.23054	mir-312	0.46197	mir-984	0.28641
chr2L	mir-275	0.09674	mir-1003	0.20166	mir-988	0.21291	mir-252	0.12712	mir-11	0.48946	mir-279	0.60837	mir-375	0.24167	mir-316	0.22987	mir-279	0.42130	mir-313	0.25267
chr2L	mir-2b-2	0.09045	mir-1000	0.19384	mir-31a	0.19879	mir-965	0.11192	mir-957	0.48513	mir-957	0.57258	mir-956	0.22336	mir-9b	0.21578	mir-375	0.40422	mir-279	0.25106
chrX	mir-12	0.08709	mir-304	0.18803	mir-2b-1	0.17590	mir-988	0.10640	mir-13a	0.44209	mir-999	0.49348	mir-9b	0.21930	mir-252	0.19055	mir-92a	0.38606	mir-317	0.21250
chr2R	mir-7	0.06967	mir-275	0.18601	mir-279	0.12248	mir-278	0.10383	mir-307	0.44043	mir-278	0.42620	mir-252	0.20762	mir-956	0.18693	mir-31a	0.30744	mir-281-1	0.20969
chrX	mir-13b-2	0.06275	mir-965	0.13593	mir-1012	0.08776	mir-2b-1	0.09179	mir-133	0.38123	mir-13a	0.42396	mir-274	0.18483	mir-274	0.15821	mir-252	0.26840	mir-92b	0.20567
chr3R	mir-999	0.05184	mir-92b	0.09994	mir-986	0.08051	mir-10	0.07797	mir-998	0.37453	mir-932	0.40957	mir-7	0.15484	mir-7	0.12453	mir-972	0.26054	mir-2b-2	0.17916
chr2R	mir-281-1	0.03756	mir-999	0.08362	mir-10	0.07593	mir-1012	0.06830	mir-10	0.29404	mir-282	0.31584	mir-980	0.15407	mir-980	0.12185	mir-306	0.25782	mir-983	0.16590
chr2L	mir-2a-1	0.03631	mir-190	0.06886	mir-2b-2	0.07211	mir-7	0.05330	mir-932	0.28490	mir-263b	0.28057	mir-124	0.14728	mir-929	0.10990	mir-963	0.25105	mir-998	0.16189
chr3L	mir-190	0.03589	mir-980	0.06752	mir-970	0.06754	mir-986	0.04461	mir-263b	0.24761	mir-998	0.26211	mir-317	0.12192	mir-375	0.10883	mir-31b	0.23722	mir-2a-2	0.13618
chr3R	mir-1012	0.03442	mir-13b-2	0.06707	mir-7	0.06715	let-7	0.04323	mir-278	0.22301	mir-9c	0.25580	mir-31b	0.10638	mir-999	0.10346	mir-7	0.23397	mir-316	0.13377
chr2R	mir-1008	0.01973	mir-2a-1	0.05791	mir-965	0.04998	mir-970	0.03908	mir-9c	0.20614	mir-10	0.22399	mir-307	0.10612	mir-275	0.10239	mir-92b	0.20252	mir-308	0.12975
chr2L	mir-263a	0.01385	mir-7	0.05433	mir-190	0.04960	mir-2b-2	0.03494	mir-87	0.18478	mir-193	0.20983	mir-986	0.09671	mir-308	0.09179	bantam	0.18625	mir-986	0.12091
chr2L	mir-1006	0.01217	mir-1008	0.03913	mir-2a-2	0.04273	mir-190	0.03316	mir-995	0.17776	mir-2a-2	0.20960	mir-308	0.09589	mir-317	0.07528	mir-999	0.18246	mir-125	0.10083
chr3L	mir-9a	0.01028	mir-989	0.03532	mir-1006	0.02709	mir-2a-2	0.03237	mir-193	0.15593	mir-87	0.19189	mir-929	0.09311	mir-87	0.07179	mir-275	0.16402	mir-307	0.09842
chrX	mir-283	0.01007	mir-2b-1	0.03085	mir-13b-2	0.02366	mir-281-1	0.02329	mir-33	0.14694	mir-9b	0.17409	mir-960	0.08833	mir-986	0.06844	mir-304	0.15074	mir-311	0.09560
chr2R	mir-278	0.00986	mir-252	0.03063	mir-281-1	0.02099	mir-1006	0.02112	mir-2a-2	0.14032	mir-33	0.16610	mir-999	0.07531	mir-306	0.06696	mir-184	0.14640	mir-988	0.08596
chr2R	mir-286	0.00902	mir-281-1	0.02951	mir-281-2	0.02022	mir-281-2	0.01658	mir-2b-1	0.13275	mir-995	0.15358	mir-993	0.07449	mir-307	0.06468	mir-979	0.13474	mir-2b-1	0.07552
chr2R	mir-281-2	0.00714	mir-276b	0.02795	mir-1003	0.01297	mir-13b-2	0.01382	mir-9b	0.12274	mir-316	0.15119	mir-306	0.05926	mir-124	0.06307	mir-961	0.12932	mir-281-2	0.07070
chrX	mir-304	0.00714	mir-932	0.02638	mir-210	0.01183	mir-92b	0.01263	mir-970	0.11367	mir-970	0.14573	mir-263b	0.05885	mir-995	0.06159	mir-962	0.12769	mir-31b	0.06829
chr3R	mir-13a	0.00525	mir-1006	0.02169	mir-92b	0.01183	mir-125	0.01244	mir-92a	0.11202	mir-12	0.12531	mir-965	0.05808	mir-998	0.06159	mir-992	0.10709	mir-965	0.05825
chrX	mir-984	0.00525	mir-9a	0.01856	let-7	0.01145	mir-929	0.00770	mir-304	0.10138	mir-275	0.11695	mir-275	0.05772	mir-31b	0.05998	mir-313	0.10031	mir-283	0.05343
chr2L	mir-1	0.00483	mir-1010	0.01587	mir-999	0.01030	mir-285	0.00750	mir-190	0.09854	mir-304	0.11643	mir-100	0.05674	mir-100	0.04911	mir-283	0.09733	mir-310	0.04740
chr3R	mir-92b	0.00420	mir-984	0.01520	mir-125	0.00878	mir-987	0.00711	mir-315	0.09491	mir-92a	0.11606	mir-998	0.05525	mir-283	0.04871	mir-996	0.09435	mir-278	0.04700
chr2R	mir-3	0.00315	mir-193	0.01431	mir-286	0.00878	mir-999	0.00691	mir-316	0.08821	mir-315	0.11325	mir-133	0.05479	mir-2a-2	0.04871	mir-985	0.08703	mir-1009	0.03615
chr2L	mir-966	0.00315	mir-124	0.01409	mir-929	0.00763	mir-286	0.00612	mir-12	0.08805	mir-306	0.09657	mir-2a-2	0.05386	mir-2b-1	0.04402	mir-986	0.08377	mir-13b-2	0.03575
chr2R	mir-5	0.00294	mir-954	0.01364	mir-5	0.00687	mir-1003	0.00592	mir-308	0.08262	mir-284	0.09386	mir-995	0.04676	mir-2b-2	0.04281	mir-263a	0.06642	mir-277	0.03495
chrX	mir-1007	0.00273	mir-318	0.01341	mir-1005	0.00610	mir-989	0.00592	mir-100	0.07915	mir-2b-1	0.09003	mir-87	0.04671	mir-993	0.04214	mir-1	0.06534	mir-999	0.02932
chr3R	mir-318	0.00273	mir-13a	0.01274	mir-2a-1	0.00610	mir-210	0.00572	mir-993	0.07741	mir-1010	0.07835	mir-988	0.04506	mir-987	0.04133	mir-995	0.06181	mir-303	0.02651
chr3R	mir-92a	0.00273	mir-1	0.01230	mir-989	0.00534	mir-1000	0.00533	mir-1010	0.06709	mir-308	0.07821	mir-1000	0.04501	mir-957	0.04120	mir-100	0.06127	mir-2a-1	0.02450
chr4	mir-954	0.00231	mir-977	0.00984	mir-1000	0.00496	mir-2a-1	0.00533	mir-306	0.05928	mir-100	0.07134	mir-957	0.04316	mir-133	0.04026	mir-79	0.05937	mir-970	0.02370
chr2L	mir-125	0.00210	mir-1012	0.00939	mir-274	0.00458	mir-5	0.00513	mir-2b-2	0.05629	mir-980	0.06840	mir-987	0.04131	mir-988	0.03757	mir-10	0.04636	mir-87	0.02290
chr2R	mir-6	0.00210	mir-966	0.00872	mir-285	0.00458	mir-13a	0.00336	mir-137	0.05526	mir-988	0.06821	mir-13a	0.04100	mir-263b	0.03529	mir-1010	0.04555	mir-980	0.02209
chr2L	mir-967	0.00210	mir-971	0.00783	mir-13a	0.00420	mir-307-as	0.00336	mir-275	0.05266	mir-993	0.06695	mir-983	0.03724	mir-1000	0.02764	mir-33	0.04500	mir-982	0.01848
chr3R	mir-2c	0.00189	mir-986	0.00648	mir-124	0.00382	mir-124	0.00316	mir-927	0.05219	mir-137	0.06079	mir-977	0.03498	mir-970	0.02751	mir-980	0.04175	mir-10	0.01647
chr2L	mir-124	0.00168	mir-994	0.00604	mir-987	0.00343	mir-274	0.00316	mir-988	0.04888	mir-2b-2	0.05532	mir-970	0.03375	mir-13a	0.02711	mir-124	0.04094	mir-1012	0.01607
chr2RHet	mir-2279	0.00168	mir-281-2	0.00514	mir-1008	0.00305	mir-316	0.00276	mir-284	0.04083	mir-986	0.04700	mir-2b-1	0.03205	mir-965	0.02697	mir-1004	0.03904	mir-9a	0.01607
chr2R	mir-310	0.00168	mir-307	0.00492	mir-316	0.00305	mir-1005	0.00217	mir-990	0.03011	mir-927	0.04644	mir-2b-2	0.03164	mir-190	0.02268	mir-281-1	0.03877	mir-100	0.01526
chr2R	mir-311	0.00168	mir-958	0.00425	mir-13b-1	0.00267	mir-100	0.00197	mir-1012	0.02948	mir-981	0.04523	mir-283	0.02968	mir-92a	0.02268	mir-991	0.03443	mir-962	0.01326
chrX	mir-303	0.00147	mir-10	0.00402	mir-133	0.00229	mir-1008	0.00178	mir-283	0.02917	mir-190	0.02962	mir-984	0.02834	mir-210	0.01624	mir-276	0.03335	mir-284	0.00924
chr2R	mir-4	0.00126	mir-286	0.00313	mir-1009	0.00191	mir-13b-1	0.00178	mir-965	0.02846	mir-1012	0.02911	mir-276b	0.02726	mir-284	0.01557	mir-982	0.03253	mir-954	0.00884
chrX	mir-983	0.00126	mir-2c	0.00291	mir-307-as	0.00191	mir-276b	0.00158	mir-980	0.02751	mir-965	0.02864	mir-284	0.02690	mir-276b	0.01503	mir-303	0.03064	mir-252	0.00844
chr2L	let-7	0.00105	mir-31a	0.00268	mir-932	0.00153	mir-305-as	0.00138	mir-1006	0.02483	mir-281-1	0.02602	mir-959	0.02459	mir-1006	0.01355	mir-2a-2	0.03036	mir-966	0.00844
chr2R	mir-1016	0.00105	mir-982	0.00246	mir-1013	0.00114	mir-92a	0.00138	mir-281-2	0.02184	mir-1006	0.02425	mir-964	0.02248	mir-1010	0.01235	mir-970	0.02711	mir-190	0.00723
chr2L	mir-133	0.00105	mir-2279	0.00201	mir-1016	0.00114	mir-957	0.00138	mir-986	0.02136	mir-283	0.02093	mir-1006	0.02135	mir-137	0.01074	mir-998	0.02277	mir-1003	0.00643
chr3L	mir-276b	0.00105	mir-5	0.00201	mir-2c	0.00114	mir-263b	0.00118	mir-281-1	0.02050	mir-281-2	0.02051	mir-210	0.02104	mir-1012	0.01060	mir-974	0.02223	mir-314	0.00643
chr2R	mir-31a	0.00105	mir-983	0.00201	mir-980	0.00114	mir-4	0.00118	mir-219	0.02042	mir-219	0.02042	mir-962	0.02063	mir-318	0.01020	mir-1003	0.01708	mir-1005	0.00562
chr2L	mir-932	0.00105	mir-3	0.00179	mir-2279	0.00076	mir-2279	0.00099	mir-981	0.01821	mir-990	0.02009	mir-976	0.01955	mir-994	0.01020	mir-954	0.01681	mir-929	0.00482
chr3R	mir-994	0.00105	mir-303	0.00179	mir-263b	0.00076	mir-1007	0.00079	mir-969	0.01529	mir-1005	0.01551	mir-963	0.01893	mir-932	0.00939	mir-997	0.01600	mir-960	0.00442
chr2R	mir-1009	0.00084	mir-973	0.00179	mir-284	0.00076	mir-1013	0.00079	mir-1017	0.01443	mir-2c	0.01341	mir-137	0.01754	mir-92b	0.00913	mir-1013	0.01464	mir-1007	0.00402
chr2R	mir-309	0.00084	mir-967	0.00157	mir-305-as	0.00076	mir-1016	0.00079	mir-2c	0.01285	mir-1017	0.01299	mir-1010	0.01641	mir-1014	0.00886	mir-956	0.01464	mir-956	0.00362
chr3L	mir-193	0.00063	mir-1009	0.00134	mir-314	0.00076	mir-133	0.00079	mir-1001	0.01277	mir-1004	0.01182	mir-932	0.01420	mir-13b-2	0.00738	mir-973	0.01383	mir-1010	0.00321
chr2R	mir-312	0.00063	mir-312	0.00134	mir-87	0.00076	mir-193	0.00079	mir-1004	0.01238	mir-1003	0.01065	mir-92a	0.01307	mir-1005	0.00590	mir-1012	0.01247	mir-13a	0.00201
chrX	mir-31b	0.00063	let-7	0.00112	mir-92a	0.00076	mir-87	0.00079	mir-1008	0.00938	mir-1001	0.00972	mir-1014	0.01276	mir-312	0.00537	mir-932	0.01220	mir-274	0.00201
chr2R	mir-986	0.00063	mir-1007	0.00112	mir-957	0.00076	mir-966	0.00079	mir-1007	0.00859	mir-969	0.00897	mir-978	0.01240	mir-962	0.00523	mir-307	0.01139	mir-961	0.00201

chr2R	mir-989	0.00063 mir-284	0.00112 mir-100	0.00038 mir-314	0.00059 mir-1003	0.00843 mir-375	0.00850 mir-974	0.01214 mir-1008	0.00483 mir-2b-2	0.01084 mir-964	0.00201
chr2R	mir-313	0.00042 mir-1013	0.00089 mir-1010	0.00038 mir-980	0.00059 mir-1005	0.00796 mir-1013	0.00612 mir-1012	0.01106 mir-iab-4	0.00470 mir-133	0.01030 mir-1006	0.00161
chr2R	mir-992	0.00042 mir-1016	0.00089 mir-219	0.00038 mir-981	0.00059 mir-1013	0.00709 mir-1007	0.00584 mir-985	0.01101 mir-1003	0.00456 mir-137	0.01030 mir-5	0.00161
chr3R	mir-10	0.00021 mir-310	0.00089 mir-276b	0.00038 mir-1009	0.00039 mir-954	0.00465 mir-954	0.00579 mir-997	0.00947 mir-960	0.00456 mir-971	0.00895 mir-959	0.00161
chr3R	mir-1000	0.00021 mir-978	0.00089 mir-3	0.00038 mir-932	0.00039 mir-375	0.00449 mir-1008	0.00486 mir-961	0.00911 mir-1001	0.00389 mir-308	0.00813 mir-991	0.00161
chr2L	mir-1005	0.00021 mir-992	0.00089 mir-307	0.00038 mir-960	0.00039 mir-92b	0.00426 mir-960	0.00481 mir-190	0.00833 mir-iab-4as	0.00376 mir-13a	0.00786 mir-3	0.00121
chr3R	mir-1010	0.00021 mir-125	0.00067 mir-309	0.00038 mir-969	0.00039 mir-955	0.00426 mir-13b-2	0.00472 mir-iab-4as	0.00741 mir-955	0.00349 mir-314	0.00786 mir-932	0.00080
chr3R	mir-1013	0.00021 mir-133	0.00067 mir-310	0.00038 mir-993	0.00039 mir-971	0.00315 mir-1009	0.00397 mir-303	0.00730 mir-1013	0.00322 mir-281-2	0.00569 mir-983-1	0.00080
chrX	mir-210	0.00021 mir-2282	0.00067 mir-4	0.00038 mir-994	0.00039 mir-1016	0.00276 mir-955	0.00392 mir-1003	0.00638 mir-2a-1	0.00295 mir-318	0.00542 mir-1008	0.00040
chr3L	mir-2282	0.00021 mir-263a	0.00067 mir-954	0.00038 mir-1004	0.00020 mir-2a-1	0.00268 mir-1016	0.00355 mir-1005	0.00628 mir-219	0.00282 mir-2c	0.00515 mir-1013	0.00040
chr3L	mir-263b	0.00021 mir-305-as	0.00067 mir-962	0.00038 mir-137	0.00020 mir-1009	0.00236 mir-314	0.00336 mir-991	0.00617 mir-1007	0.00255 mir-994	0.00515 mir-124	0.00040
chr3L	mir-274	0.00021 mir-309	0.00067 mir-966	0.00038 mir-2279-as	0.00020 mir-960	0.00236 mir-971	0.00327 mir-982	0.00607 mir-981	0.00255 mir-284	0.00434 mir-133	0.00040
chr2R	mir-307-as	0.00021 mir-31b	0.00067 let-7-as	0.00000 mir-275-as	0.00020 mir-962	0.00221 mir-92b	0.00318 mir-1001	0.00545 mir-1015	0.00201 mir-981	0.00434 mir-193	0.00040
chr2L	mir-375	0.00021 mir-6	0.00067 mir-1-as	0.00000 mir-284	0.00020 mir-13b-2	0.00213 mir-2a-1	0.00299 mir-1008	0.00545 mir-1004	0.00174 mir-iab-4as	0.00434 mir-2c	0.00040
chr3R	mir-929	0.00021 mir-975	0.00067 mir-1001	0.00000 mir-3	0.00020 mir-314	0.00142 mir-962	0.00257 mir-312	0.00489 mir-311	0.00174 mir-1006	0.00407 mir-305-as	0.00040
chr3L	mir-958	0.00021 mir-987	0.00067 mir-1002	0.00000 mir-318	0.00020 mir-13b-1	0.00110 mir-31b	0.00206 mir-iab-4	0.00484 mir-954	0.00148 mir-190	0.00352 mir-955	0.00040
chrX	mir-977	0.00021 mir-137	0.00045 mir-1004	0.00000 mir-954	0.00020 mir-305-as	0.00095 mir-964	0.00192 mir-13b-2	0.00473 mir-2c	0.00134 mir-263b	0.00352 mir-963	0.00040
chrX	mir-978	0.00021 mir-263b	0.00045 mir-1004-as	0.00000 mir-956	0.00020 mir-984	0.00079 mir-958	0.00135 mir-219	0.00432 mir-964	0.00134 mir-2a-1	0.00352 mir-985	0.00040
chrX	mir-981	0.00021 mir-311	0.00045 mir-1007	0.00000 mir-958	0.00020 mir-983	0.00071 mir-13b-1	0.00103 mir-285	0.00391 mir-310	0.00121 mir-315	0.00325 mir-iab-4	0.00040
chr2L	let-7-as	0.00000 mir-313	0.00045 mir-1011	0.00000 mir-967	0.00020 mir-1011	0.00063 mir-5	0.00103 mir-973	0.00391 mir-927	0.00121 mir-87	0.00325 let-7-as	0.00000
chr2L	mir-1-as	0.00000 mir-314	0.00045 mir-1014	0.00000 mir-971	0.00020 mir-312	0.00063 mir-956	0.00093 mir-311	0.00350 mir-1016	0.00107 mir-1008	0.00298 mir-1-as	0.00000
chr2L	mir-100	0.00000 mir-4	0.00045 mir-1015	0.00000 let-7-as	0.00000 mir-966	0.00063 mir-961	0.00093 mir-1015	0.00319 mir-313	0.00107 mir-210	0.00271 mir-1000	0.00000
chr3R	mir-1001	0.00000 mir-87	0.00045 mir-1017	0.00000 mir-1-as	0.00000 mir-2279	0.00055 mir-963	0.00093 mir-972	0.00314 mir-315	0.00094 mir-958	0.00244 mir-1001	0.00000
chr2L	mir-1002	0.00000 mir-929	0.00045 mir-137	0.00000 mir-1001	0.00000 mir-31b	0.00055 mir-1011	0.00089 mir-313	0.00304 mir-983	0.00094 mir-965	0.00244 mir-1002	0.00000
chr2L	mir-1004	0.00000 mir-974	0.00045 mir-193	0.00000 mir-1002	0.00000 mir-5	0.00055 mir-959	0.00084 mir-955	0.00304 mir-984	0.00094 mir-3	0.00217 mir-1004	0.00000
chr2L	mir-1004-as	0.00000 mir-210	0.00022 mir-2279-as	0.00000 mir-1004-as	0.00000 mir-959	0.00055 mir-2279	0.00075 mir-981	0.00288 mir-1017	0.00081 mir-193	0.00190 mir-1004-as	0.00000
chr3R	mir-1011	0.00000 mir-2279-as	0.00022 mir-2280	0.00000 mir-1010	0.00000 mir-964	0.00055 mir-983	0.00075 mir-310	0.00283 mir-963	0.00081 mir-955	0.00190 mir-1011	0.00000
chr3R	mir-1014	0.00000 mir-927	0.00022 mir-2281	0.00000 mir-1011	0.00000 mir-961	0.00039 mir-286	0.00070 mir-1013	0.00267 mir-966	0.00081 mir-iab-4	0.00190 mir-1014	0.00000
chr3R	mir-1015	0.00000 mir-956	0.00022 mir-2282	0.00000 mir-1014	0.00000 mir-963	0.00039 mir-966	0.00056 mir-954	0.00257 mir-969	0.00081 mir-1007	0.00163 mir-1015	0.00000
chr3R	mir-1017	0.00000 mir-960	0.00022 mir-2283	0.00000 mir-1015	0.00000 mir-974	0.00039 mir-984	0.00051 mir-1007	0.00242 mir-961	0.00067 mir-1016	0.00163 mir-1016	0.00000
chr2R	mir-137	0.00000 mir-963	0.00022 mir-275-as	0.00000 mir-1017	0.00000 mir-286	0.00032 mir-312	0.00042 mir-992	0.00231 mir-285	0.00054 mir-966	0.00163 mir-1017	0.00000
chr3R	mir-13b-1	0.00000 mir-976	0.00022 mir-287	0.00000 mir-219	0.00000 mir-313	0.00032 mir-305-as	0.00037 mir-1004	0.00226 mir-5	0.00054 mir-989	0.00163 mir-137	0.00000
chr3L	mir-219	0.00000 mir-993	0.00022 mir-289	0.00000 mir-2280	0.00000 mir-956	0.00032 mir-318	0.00028 mir-989	0.00226 mir-1009	0.00040 mir-1009	0.00136 mir-13b-1	0.00000
chr2RHet	mir-2279-as	0.00000 mir-iab-4	0.00022 mir-303	0.00000 mir-2281	0.00000 mir-967	0.00032 mir-989	0.00028 mir-92b	0.00216 mir-2279	0.00040 mir-929	0.00108 mir-210	0.00000
chr2L	mir-2280	0.00000 let-7-as	0.00000 mir-311	0.00000 mir-2282	0.00000 mir-2283	0.00024 mir-3	0.00023 mir-927	0.00211 mir-959	0.00040 mir-1005	0.00081 mir-219	0.00000
chr3R	mir-2281	0.00000 mir-1-as	0.00000 mir-312	0.00000 mir-2283	0.00000 mir-3	0.00024 mir-4	0.00023 mir-1009	0.00195 mir-982	0.00040 mir-1011	0.00081 mir-2279	0.00000
chr3R	mir-2283	0.00000 mir-100	0.00000 mir-313	0.00000 mir-287	0.00000 mir-4	0.00024 mir-313	0.00019 mir-975	0.00170 mir-976	0.00027 mir-2279	0.00081 mir-2279-as	0.00000
chr2L	mir-275-as	0.00000 mir-1001	0.00000 mir-315	0.00000 mir-289	0.00000 mir-958	0.00024 mir-977	0.00019 mir-2c	0.00139 mir-985	0.00027 mir-276b	0.00081 mir-2280	0.00000
chr3R	mir-284	0.00000 mir-1002	0.00000 mir-318	0.00000 mir-2c	0.00000 mir-977	0.00024 mir-2283	0.00014 mir-969	0.00139 mir-990	0.00027 mir-987	0.00081 mir-2281	0.00000
chr3L	mir-285	0.00000 mir-1004	0.00000 mir-31b	0.00000 mir-303	0.00000 mir-310	0.00016 mir-303	0.00014 mir-1017	0.00129 mir-991	0.00027 mir-1001	0.00054 mir-2282	0.00000
chr2L	mir-287	0.00000 mir-1004-as	0.00000 mir-6	0.00000 mir-307	0.00000 mir-968	0.00016 mir-307-as	0.00014 mir-315	0.00123 mir-13b-1	0.00013 mir-1015	0.00054 mir-2283	0.00000
chr3L	mir-289	0.00000 mir-1005	0.00000 mir-927	0.00000 mir-309	0.00000 mir-978	0.00016 mir-968	0.00014 mir-2a-1	0.00108 mir-193	0.00013 mir-2b-1	0.00054 mir-263b	0.00000
chr2L	mir-305-as	0.00000 mir-1011	0.00000 mir-955	0.00000 mir-310	0.00000 mir-994	0.00016 mir-978	0.00014 mir-979	0.00108 mir-2281	0.00013 mir-1000	0.00027 mir-275-as	0.00000
chr3L	mir-314	0.00000 mir-1014	0.00000 mir-956	0.00000 mir-311	0.00000 mir-iab-4	0.00016 mir-982	0.00014 mir-1016	0.00093 mir-286	0.00013 mir-1017	0.00027 mir-276b	0.00000
chr3L	mir-315	0.00000 mir-1015	0.00000 mir-958	0.00000 mir-312	0.00000 mir-1004-as	0.00008 mir-994	0.00014 mir-5	0.00072 mir-287	0.00013 mir-13b-2	0.00027 mir-285	0.00000
chr3L	mir-316	0.00000 mir-1017	0.00000 mir-959	0.00000 mir-313	0.00000 mir-275-as	0.00008 mir-310	0.00009 mir-193	0.00062 mir-289	0.00013 mir-219	0.00027 mir-286	0.00000
chr2L	mir-87	0.00000 mir-13b-1	0.00000 mir-960	0.00000 mir-315	0.00000 mir-303	0.00008 mir-311	0.00009 mir-2279	0.00062 mir-3	0.00013 mir-2283	0.00027 mir-287	0.00000
chrX	mir-927	0.00000 mir-219	0.00000 mir-961	0.00000 mir-31b	0.00000 mir-311	0.00008 mir-967	0.00009 mir-990	0.00041 mir-303	0.00013 mir-983-1	0.00027 mir-289	0.00000
chr3L	mir-955	0.00000 mir-2280	0.00000 mir-963	0.00000 mir-6	0.00000 mir-318	0.00008 mir-974	0.00009 mir-307-as	0.00031 mir-305-as	0.00013 mir-993	0.00027 mir-307-as	0.00000
chr3L	mir-956	0.00000 mir-2281	0.00000 mir-964	0.00000 mir-927	0.00000 mir-982	0.00008 mir-976	0.00009 mir-286	0.00026 mir-307-as	0.00013 let-7-as	0.00000 mir-309	0.00000
chr3L	mir-957	0.00000 mir-2283	0.00000 mir-967	0.00000 mir-955	0.00000 mir-985	0.00008 mir-iab-4	0.00009 mir-966	0.00026 mir-973	0.00013 mir-1-as	0.00000 mir-315	0.00000
chr2L	mir-959	0.00000 mir-274	0.00000 mir-968	0.00000 mir-959	0.00000 mir-989	0.00008 mir-1015	0.00005 mir-13b-1	0.00021 mir-974	0.00013 mir-1002	0.00000 mir-375	0.00000
chr2L	mir-960	0.00000 mir-275-as	0.00000 mir-969	0.00000 mir-961	0.00000 let-7-as	0.00000 mir-2281	0.00005 mir-2281	0.00021 mir-978	0.00013 mir-1004-as	0.00000 mir-4	0.00000
chr2L	mir-961	0.00000 mir-285	0.00000 mir-971	0.00000 mir-962	0.00000 mir-1-as	0.00000 mir-275-as	0.00005 mir-2283	0.00021 mir-992	0.00013 mir-1014	0.00000 mir-6	0.00000
chr2L	mir-962	0.00000 mir-287	0.00000 mir-972	0.00000 mir-963	0.00000 mir-1002	0.00000 mir-309	0.00005 mir-318	0.00021 let-7-as	0.00000 mir-13b-1	0.00000 mir-927	0.00000
chr2L	mir-963	0.00000 mir-289	0.00000 mir-973	0.00000 mir-964	0.00000 mir-1014	0.00000 mir-972	0.00005 mir-971	0.00021 mir-1-as	0.00000 mir-2279-as	0.00000 mir-957	0.00000
chr2L	mir-964	0.00000 mir-307-as	0.00000 mir-974	0.00000 mir-968	0.00000 mir-1015	0.00000 mir-991	0.00005 mir-994	0.00021 mir-1002	0.00000 mir-2280	0.00000 mir-958	0.00000
chr2L	mir-968	0.00000 mir-315	0.00000 mir-975	0.00000 mir-972	0.00000 mir-2279-as	0.00000 mir-992	0.00005 mir-967	0.00015 mir-1004-as	0.00000 mir-2281	0.00000 mir-967	0.00000
chrX	mir-969	0.00000 mir-316	0.00000 mir-976	0.00000 mir-973	0.00000 mir-2280	0.00000 mir-iab-4as	0.00005 mir-3	0.00010 mir-1011	0.00000 mir-2282	0.00000 mir-968	0.00000
chrX	mir-971	0.00000 mir-375	0.00000 mir-977	0.00000 mir-974	0.00000 mir-2281	0.00000 let-7-as	0.00000 mir-4	0.00010 mir-2279-as	0.00000 mir-275-as	0.00000 mir-969	0.00000
chrX	mir-972	0.00000 mir-955	0.00000 mir-978	0.00000 mir-975	0.00000 mir-2282	0.00000 mir-1-as	0.00000 mir-1011	0.00005 mir-2280	0.00000 mir-285	0.00000 mir-971	0.00000
chrX	mir-973	0.00000 mir-957	0.00000 mir-979	0.00000 mir-976	0.00000 mir-287	0.00000 mir-1002	0.00000 mir-2280	0.00005 mir-2282	0.00000 mir-286	0.00000 mir-972	0.00000
chrX	mir-974	0.00000 mir-959	0.00000 mir-981	0.00000 mir-977	0.00000 mir-289	0.00000 mir-1004-as	0.00000 mir-983-1	0.00005 mir-2283	0.00000 mir-287	0.00000 mir-973	0.00000
chrX	mir-975	0.00000 mir-961	0.00000 mir-982	0.00000 mir-978	0.00000 mir-307-as	0.00000 mir-1014	0.00000 let-7-as	0.00000 mir-275-as	0.00000 mir-289	0.00000 mir-974	0.00000
chrX	mir-976	0.00000 mir-962	0.00000 mir-983	0.00000 mir-979	0.00000 mir-309	0.00000 mir-2279-as	0.00000 mir-1-as	0.00000 mir-309	0.00000 mir-305-as	0.00000 mir-975	0.00000
chrX	mir-979	0.00000 mir-964	0.00000 mir-983-1	0.00000 mir-982	0.00000 mir-6	0.00000 mir-2280	0.00000 mir-1002	0.00000 mir-4	0.00000 mir-307-as	0.00000 mir-976	0.00000
chrX	mir-982	0.00000 mir-968	0.00000 mir-984	0.00000 mir-983	0.00000 mir-972	0.00000 mir-2282	0.00000 mir-1004-as	0.00000 mir-6	0.00000 mir-309	0.00000 mir-977	0.00000
chrX	mir-983-1	0.00000 mir-969	0.00000 mir-985	0.00000 mir-983-1	0.00000 mir-973	0.00000 mir-287	0.00000 mir-2279-as	0.00000 mir-967	0.00000 mir-4	0.00000 mir-978	0.00000
chrX	mir-985	0.00000 mir-972	0.00000 mir-990	0.00000 mir-984	0.00000 mir-975	0.00000 mir-289	0.00000 mir-2282	0.00000 mir-968	0.00000 mir-5	0.00000 mir-979	0.00000
chr2R	mir-987	0.00000 mir-979	0.00000 mir-991	0.00000 mir-985	0.00000 mir-976	0.00000 mir-6	0.00000 mir-275-as	0.00000 mir-971	0.00000 mir-6	0.00000 mir-981	0.00000
chr2R	mir-990	0.00000 mir-983-1	0.00000 mir-992	0.00000 mir-990	0.00000 mir-979	0.00000 mir-973	0.00000 mir-287	0.00000 mir-972	0.00000 mir-927	0.00000 mir-987	0.00000
chr2R	mir-991	0.00000 mir-985	0.00000 mir-993	0.00000 mir-991	0.00000 mir-983-1	0.00000 mir-975	0.00000 mir-289	0.00000 mir-975	0.00000 mir-957	0.00000 mir-990	0.00000
chr3R	mir-993	0.00000 mir-990	0.00000 mir-994	0.00000 mir-992	0.00000 mir-991	0.00000 mir-979	0.00000 mir-305-as	0.00000 mir-977	0.00000 mir-967	0.00000 mir-992	0.00000
chr3R	mir-997	0.00000 mir-991	0.00000 mir-997	0.00000 mir-997	0.00000 mir-992	0.00000 mir-983-1	0.00000 mir-309	0.00000 mir-979	0.00000 mir-968	0.00000 mir-993	0.00000
chr3R	mir-iab-4	0.00000 mir-997	0.00000 mir-iab-4	0.00000 mir-iab-4	0.00000 mir-997	0.00000 mir-985	0.00000 mir-6	0.00000 mir-983-1	0.00000 mir-969	0.00000 mir-997	0.00000
chr3R	mir-iab-4as	0.00000 mir-iab-4as	0.00000 mir-iab-4as	0.00000 mir-iab-4as	0.00000 mir-iab-4as	0.00000 mir-997	0.00000 mir-968	0.00000 mir-997	0.00000 mir-990	0.00000 mir-iab-4as	0.00000
SUM_Norm_Reads_in_lib		**476512.00**	**670268.57**	**419331.00**	**506593.00**	**2221284.28**	**2140318.00**	**1943944.00**	**2554945.07**	**1290996.29**	**481224.84**

The number of reads matching each miRNA in a given library is given in decreasing order as a percentage of all reads in that library. miRNAs representing less than 0.01% of each library are shaded in grey. S. Glands: Salivary glands; M: Male; F: Female.